Design of a Wireless Underground Sensor Network for Precision Agriculture

Damien Wohwe Sambo

UNIVERSITÉ DE NGAOUNDERE THE UNIVERSITY OF NGAOUNDERE

Faculté des Sciences Faculty of Science

Order N^o: _ _ _ _ _ _ _ _ _

DÉPARTEMENT DE MATHÉMATIQUES ET INFORMATIQUE
DEPARTMENT OF MATHEMATICS AND COMPUTER SCIENCE

Unité de Formations Doctorale de Mathématiques, Informatique et Applications
Doctoral Training unit of Mathematics, Computer Science and Applications

Design of a Wireless Underground Sensor Network for Precision Agriculture

THESIS

Submitted in partial fulfillment of the requirements for the award of

Doctor of Phylosophy (Ph.D.)

Speciality: System and Software in Distributed Environments

By

Damien WOHWE SAMBO
Master of Science in Computer Engineering
Speciality: System and Software in Distributed Environments
Registration number: 09A062FS

Thesis defended on 23^{rd} July 2021 in the presence of the jury:

Joseph Yves EFFA	**Professor**	**The University of Ngaoundéré**	**President**
Georges KOUAMOU	**Associate Professor**	**The University of Yaounde I**	**Reporter**
Jean Claude KAMGANG	**Professor**	**The University of Ngaoundéré**	**Reporter**
Duplex Elvis HOUPA DANGA	**Associate Professor**	**The University of Ngaoundéré**	**Member**
Anna FÖRSTER	**Professor**	**The University of Bremen**	**Advisor**
Blaise Omer YENKE	**Associate Professor**	**The University of Ngaoundéré**	**Advisor**
Paul DAYANG	**Senior Lecturer**	**The University of Ngaoundéré**	**Co-advisor**

Year 2021

Author's declaration

I declare that the work in this dissertation was carried out in accordance with the requirements of the University's Regulations and Code of Practice for Research Degree Programmes and that it has not been submitted for any other academic award. Except where indicated by specific reference in the text, the work is the candidate's own work. Work done in collaboration with, or with the assistance of, others, is indicated as such. Any views expressed in the dissertation are those of the author.

SIGNED: ..... DATE: .....

Dedication

To

My late mother NANASO DODO

My father SAMBO GAROUA

Acknowledgements

Glory be to Almighty GOD for all the graces received, the courage and persistence that allowed me to present this work.

I would like to express my deepest gratitude to my supervisors, Prof. Dr. Anna FÖRSTER, who has been kind enough to honour me with her guidance during these years of research. Her constant support, expertise, advice and orientation are the key factors enabling me to present this work. To Prof. Blaise Omer YENKE, my second father, I would not cease to express my gratitude; his very good mood, his advice and his simplicity of life inspired me to overcome the difficulties encountered during this research. To Dr. Paul DAYANG for his kindness and constant encouragement.

I would like to thank all the actors of the Faculty of Sciences of the University of Ngaoundéré, especially those of the Department of Mathematics and Computer Science who have spared no effort for our formation. I am thinking of Prof. Joseph Yves EFFA, Dr. Franklin TCHAKOUNTE, Dr Vivient Corneille KAMLA, Dr. Arouna NDAM NJOYA, Dr. Jean Louis FENDJI EBONGUE and to all the members of the Doctoral training unit of Mathematics, Computer Science and Applications.

A big thanks to Prof. Idrissa SARR who honoured me in the follow-up and practical orientation of my work during my doctoral internship obtained through the ERMIT scholarship program at the University Cheikh Anta Diop (UCAD) of Dakar in Senegal. I am thinking of Prof. Karim KONATÉ head of the Computer Science Section, Prof. Bamba GUEYE and Mr. Bassirou KASSÉ of the Computer Science Section for their comments, advices and guidances. Thanks to Prof. Nalla MBAYE for his advice in botany, he enabled me to carry out tests in the Botanical Garden of UCAD. .

My stay in the Computer Science Section of UCAD gave me the opportunity to meet great people with whom it is pleasant to work, I think of Bakary DIARRA SOUMBIÉ, Gildas TÉEG-WENDÉ ZOUGMORE and Félicité GAMGNE.

A special thank to all the members of my family: Adèle NASER, Koué MBESSO SAMBO, Marie-José MAÏTAO-YANG SAMBO, Gaëtan DOBA SAMBO, Hermann DANGWANG SAMBO, Jean-Jacques NENBA SAMBO, Verra MAÏLAÏSSO SAMBO and Habib Ulrich WANGNAMOU AKASSOU who always believed in me and never stopped encouraging me from near and far.

My thanks also go to my friends and persons who have always supported me during difficult moments, I speak among others of Nicole-Noël MADAMA TCHINDEBE, Joël Paulin TANZOUAK VAUMI, Samuel MOULOUOM NDAM, Christian TOTOUM FOTSING, Rodrigue NGUENANG TOUKAP, Eric Carel MVONDO MEBO and Jaures Casimir KOUONG.

A strong thought to all those whose names I forgot to mention above.

Abstract

During the past few years, Wireless Underground Sensor Networks (WUSNs) become widely used due to their large amount of applications. These applications are classified into mine detection, landslide activities, ecology monitoring or precision agriculture. in this latter, the buried nodes have to check the good growth of plants by verifying the water content, the temperature and the presence of nutriment. Thus, the user is able to decide to water or to add fertilizers in a particular area, therefore, an efficient use of the resources is performed. However, since the ground which is more denser than the air is the communication channel, the electromagnetic (EM) waves used for wireless communications are widely attenuated due to soil properties that may change along the time. Thus, a sensor node must waste its energy by sending its sensed data to a destination node without being received by this latter due to signal loss in soil. A WUSN requires beforehand to allow a reliable communication between buried sensor nodes. This thesis aims at allowing a reliable and energy efficient communication in WUSN for real time application of precision agriculture. Ta achieve it, we proposed the Wireless Underground Sensor Network Path Loss Model called WUSN-PLM for the prediction of the signal loss in precision agriculture. In order to validate the proposed WUSN-PLM, intensive measurements have been conducted in real agricultural field of onions culture at the Botanic Garden of the University Cheikh Anta Diop of Dakar. Over the 140 measurements, WUSN-PLM outperforms the existing models with 87.13% precision. Furthermore, for a real time prediction of the packet loss, we proposed a link channel optimization for reliable communications in WUSNs based on the Sugeno Fuzzy Inference System (FIS). The proposed FIS consists of 04 inputs, one output and 36 rules. The inputs give information related to the buried depth of transmitter and receiver nodes, the average value of the soil moisture proportion and the linear distance between nodes. The output of the FIS gives the reception probability of a packet sent by source node according the previous parameters. The evaluation of the proposed approach obtains a higher accuracy and precision than WUSN-PLM (91.429% and 87.129% respectively) The Fuzzy Logic based approach has been integrated within real sensor nodes made up of ARDUINO boards for practical use.

Keywords : Wireless Underground Sensor Network; Precision Agriculture; Path loss model; WUSN-PLM; Fuzzy Inference System.

Résumé

Au cours des derniéres années, les réseaux sans fil avec capteurs enfouis sous terre (WUSNs) sont devenus largement utilisés en raison de leur grand nombre d'applications. Ces applications sont classées en détection de mines, détection gde lissement de terrain, surveillance écologique ou agriculture de précision. Dans ce dernier, les noeuds enterrés vérifient la bonne croissance des plantes en contrôlant la teneur en eau, la température et la présence de nutriments. Ainsi, l'utilisateur du WUSN peut décider d'arroser ou d'ajouter des engrais dans une zone particuliére, ce qui permet une utilisation efficace des ressources. Cependant, comme le sol qui est plus dense que l'air, est le canal de communication pourles ondes électromagnétiques utilisées pour les communications sans fil sont largement atténuées en raison des propriétés du sol qui peuvent changer au fil du temps. Ainsi, un noeud capteur va gaspiller son énergie en envoyant ses données collectées à un autre noeud sans être reçu par ce dernier du fait de l'atténuation du signal dans le sol. Cette thése vise à permettre une communication fiable et énergie efficiente pour une application en temps réel en agriculture de précision. Pour y parvenir, nous proposons le modéle de perte de signaux dans les WUSNs en agriculture de précision appelé WUSN-PLM. Afin de valider cette approche, plusieurs mesures ont été effectuées dans un champ agricole dédié à a culture d'oignons à l'aide de capteurs réels au sein du jardin botanique de l'université Cheikh Anta Diop de Dakar. Sur les 140 mesures, WUSN-PLM surpasse les modéles existants avec une précision de $87,13\%$. En outre, pour une prédiction en temps réel de la perte de paquets, nous proposons une optimisation des communications dans les WUSNs à l'aide du Moteur d'Inférence Floue (MIF) Sugeno. Le MIF proposé se compose de 04 entrées, une sortie et 36 règles. Les entrées donnent des informations relatives à la profondeur d'enfouissement des noeuds d'émission et de réception, la valeur moyenne de la contenance en eau dans le sol et la distance entre les noeuds. La sortie du MIF donne la probabilité de réception d'un paquet envoyé par un noeud source selon les paramètres précédents. L'évaluation de l'approche proposée permet d'obtenir une exactitude et une précision supérieures à celles du WUSN-PLM ($91,429\%$ et $87,129\%$ respectivement). L'approche basée sur la logique floue a été intégrée dans des noeuds capteurs réels constitués de cartes ARDUINO pour une utilisation pratique.

Mots clés : Réseau Sans Fils de Capteurs enfouis sous terre; Agriculture de Précision; Modèle de prédiction d'atténuation du signal; WUSN-PLM; Moteur d'inférence Floue.

Table of Contents

List of Tables

Table **Page**

List of Figures

List of abbreviations

ACC: Accuracy
ACO: Ant Colony Optimization
ADC: Analog to Digital Converter
AG: Aboveground
AG2UG: Aboveground-To-Underground
AG2UG2AG: Aboveground-To-Underground-To-Aboveground
BP: Bad Prediction
bACC: Balanced Accuracy
BCO: Bee Colony Optimization
BS: Base Station
CI: Computational Intelligence
CDC: Complex Dielectric Constant
DC: Dielectric Constant
EM: ElectroMagnetic
EPROM: Erasable Programmable Read Only Memory
EEPROM: Electrically Erasable Programmable Read Only Memory
FN: False Negative
FP: False Positive
FSPL: Free Space Path Loss
FIS: Fuzzy Inference System
FL: Fuzzy Logic
GA: Genetic Algorithm
GP: Good Prediction
GPS: Global Positioning System
IOT: Internet of Things
IOUT: Internet of Underground Things
LF: Loss Factor
ML: Machine Learning
MI: Magnetic Induction

MAE: Mean Absolute Error
MAPE: Mean Absolute Percent Error
MCC: Matthews Correlation Coefficient
MEMS: Micro Electro Mechanical Systems
MBSDM: Mineralogy-Based Soil Dielectric Model
NN: Neural Network
NAC: Normalized Attenuation Coefficient
PSO: Particle Swarm Optimization
RF: Radio Frequency
RAM: Random Access Memory
RI: Refractive Index
RSSI: Received Signal Strength Indicator
RL: Reinforcement Learning
ROM: Read Only Memory
ROC: Receiver Operating Characteristic
RMSE: Root Mean Squared Error
SI: Swarm Intelligence
TMDM: Temperature and Mineralogy Dependable Soil Dielectric Model
TWSN: Terrestrial Wireless Sensor Network
TN: True Negative
TP: True Positive
UG: Underground
UG2AG: Underground-To-Aboveground
UG2UG: Underground-To-Underground
UWSN: UnderWater Wireless Sensor Network
WMSN: Wireless Multimedia Sensor Network
WSN: Wireless Sensor Network
WUC: Wireless Underground Communication
WUSN: Wireless Underground Sensor Network
WUSN-PLM: Wireless Underground Sensor Network Path Loss Model

Introduction

Context and Motivation

Smart technologies are widely used in fields like building, health, ecological monitoring, security, home, vehicles, planes and shipboard. However, smart environments rely first on sensory data from the real world like it is done by sentient organisms. Smart environments are possible due to the recent evolution of wireless communication technologies and Micro Electro Mechanical Systems (MEMS) which have seen the apparition of sensors. They are small in size and are able to collect information on its environment like temperature, pressure, humidity, water content, gas presence and luminosity [3]. In spite of the large amount of applications offered by sensor nodes, they are designed with limited resources such as a restricted computing capacity, reduced memory size and storage, weak range of communication, low bandwidth, and a limited amount of energy. To efficiently cover areas, a single sensor is not sufficient due to its limited communication range. In order to cover a more consequent space, several sensors are deployed and connected to each other, thereby forming a Wireless Sensor Network (WSN) [4].

A WSN consists of spatially distributed sensors, and one or more sink nodes (also called base stations). Sensors monitor, in real-time, physical conditions, such as temperature, vibration, or motion, and produce sensory data. A sensor node could behave both as data originator and data router. A sink, on the other hand, collects data from sensors. For example, in an event monitoring application, sensors are required to send data to the sink(s) when they detect the occurrence of events of interest. The sink may communicate with the end-user via direct connections, Internet, satellite, or any type of wireless links [5].

However, the recent developments on the Internet of Things (IoT) have resulted in the emergence of a sub-domain called Internet Of Underground Things (IOUT). The IOUT by the used of Wireless Underground Sensors Networks (WUSNs) have nowadays several applications like the monitoring of the landslide, detection of persons after disasters like earthquakes or floods, detection of mines, ecological monitoring and precision agriculture [6], [7], [8], [9], [10], [11]. For precision agriculture particularly, the sensors are buried under the ground in order to estimate the properties of soils and the water content necessary for the good growth of plants.

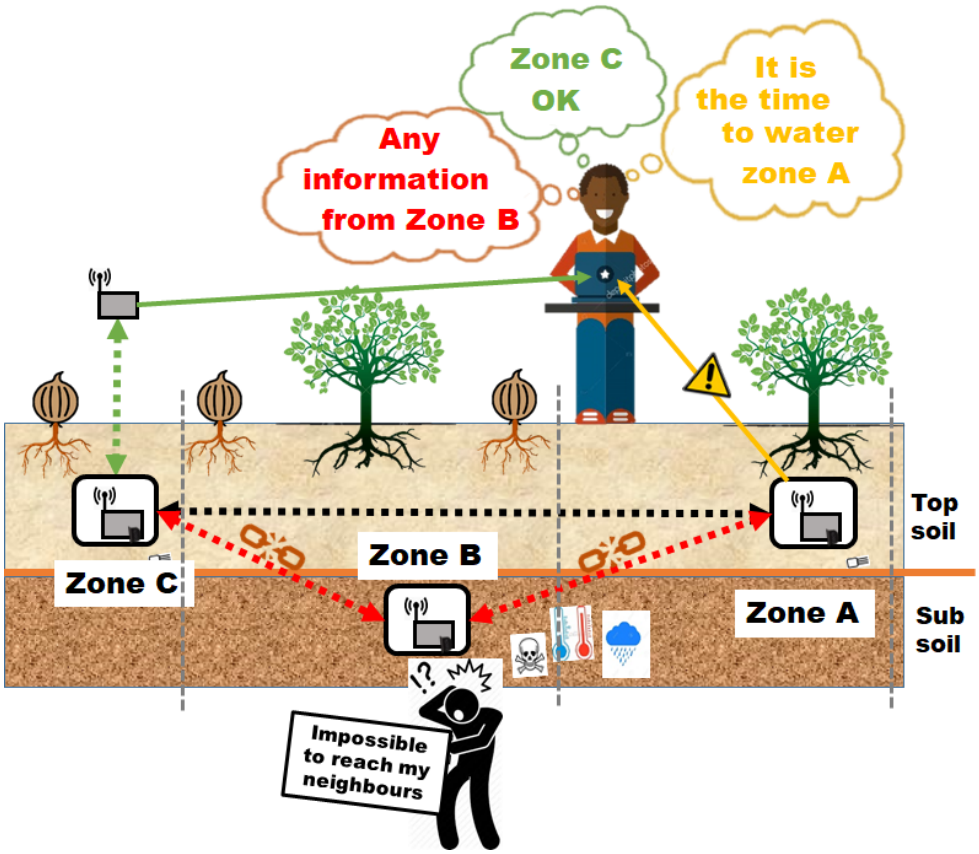

Figure 1: Intelligent watering system used in precision agriculture.

For this kind of application, the exact amount of water needed by the plant is supplied by an intelligent watering system for an efficient use of water resource. From Figure 1, an user can either decide to water a particular zone (Zone A) after receiving data from buried nodes of the same zone. The final user may either decide to not water a particular zone which has enough water (Zone C), thus, saves water resource.

Since the soil is denser than air, theoretical communication range of a terrestrial sensor node decreases drastically when the node is buried [12]. This is because the communication channel changes from the air to the soil which highly affect electromagnetic waves. When the wave loss in soil becomes higher than the sensibility of the receiver, the wireless underground link between the source and the destination nodes is broken. For this scenario, the data collected *in situ* by a sensor node nodes is therefore loss since it is not able to reach its neighbour or the BS. For example the sensor node of Zone B in Figure 1 is not able to send its sensed data to nodes of zones A and C, it will waste its energy by sending a data that will not reach its neighbours. The node of zone B will continue sending its collected data because it does not have the ability to verify is its sent data is received or not by the destination node.

Contrary to conventional terrestrial Wireless Sensor Networks (TWSNs) which can be confused to WSN in the literature, in WUSN, the communication between two nodes is directly

affected by the properties of the soil where the network is deployed. Routing in WUSN remains an important challenge as changing soil properties along time have directly an impact on the attenuation of radio waves under the ground [13]. Designing a path loss model for wireless underground communications becomes a necessity before any deployment WUSN because it helps at predicting the energy received *in situ* by a node according to the soil conditions [6]. Thus, these models are used in order to evaluate the link quality for an optimal communication between buried sensor nodes. A path loss model consists of predicting the signal strength received by a receiver node from a sender node. There are many existing path loss models adapted for WUSNs. The most useful and famous is the Modified Friis known as Conventional Modified Friis [14] which is based on the Free Space Path Loss (FSPL) initially proposed by H. Friis [15]. This modified version of FSPL adds the wave attenuation in soil. Another famous model in literature called CRIM-Fresnel [16] is a mixed model of the complex refractive index model and the Fresnel equations. Contrary to the Modified Friis, this model takes into account attenuation due to wave reflection on the ground. Others existing path loss models combine the characteristics of Modified Friis and CRIM-Fresnel. However, all these models have the particularity to use the Peplinski derivations in order to predict the value of the Complex Dielectric Constant (CDC) [17], [18].

A limit of the Peplinski model is that it considers only the presence of free water inside the soil. Furthermore, as it is said by Topp et *al.* [19], bound water seems to dominate over free water in moist soil. Thus, to increase the accuracy of path loss, we considered a powerful approach for predicting the CDC named Mineralogy-Based Soil Dielectric Model (MBSDM) [20]. This approach takes into account the presence of free and bound water in the soil for a better prediction. Contrary to the Peplinski, the MBSDM can operate on a wider frequency range between 45 MHz and 26.5 GHz. Due to the large set of soil types used to design MBSDM, only three inputs parameters (wave frequency, the clay portion and the volumetric water content VWC) are needed for the CDC prediction.

Despite the proposition of path loss models design to predict the signal attenuation in soil, the prediction *in situ* of the link channel quality by sensor nodes remains a challenge due to the limited resources of sensor nodes. Furthermore, in order to get soil properties (CDC), additional laboratory analyzes are required. Thus, the prediction *in situ* of the path loss remains highly challenging even for the best path loss model.

With the advancement of Computational Intelligence (CI) and Machine Learning (ML), recent solutions take into account the limited resources of sensor nodes that have been widely proposed [4], [21]. Between these CI and ML approaches, we can mention Neural Network, Genetic Algorithm, Swarm Intelligence or Fuzzy Logic (FL). The latter is widely used due to its performance and its lightness during implementation. Nowadays, Fuzzy Inference Systems (FIS) are widely used in several application domains such as in space fault detection [22],

evaluation of Hapto Audio Visual Environments [23], diagnostic of diseases [24], fault detection of PhotoVoltaic systems [25] and for precision agriculture [26]. Moreover, the FL has the capability to be lightweight and easy to integrate to mechanical engine such as a steam engine [27], [28], to satellite [22], to haptic [23] and to PhotoVoltaic systems [25] depending on their resources.

The design of a WUSN for a real time application as precision agriculture is a key challenge that the present work aims to address. In order to increase the lifetime of buried sensor nodes used in precision agriculture application, the following objectives are raised out:

- Proposition of a new model for increasing the accuracy of path loss models to better predict the EM signal loss in soil: this consist at firstly analyze the parameters needed by path loss models. Thereafter, a better approach for predicting the path loss should be proposed according a wide review of the existing path loss models;
- Proposition of a new path loss model models according the requirements of application such as prediction agriculture. The path loss model should predict with a high reliability the signal attenuation of EM according to the type of wireless underground communication. Thus, the proposed model should be able to evaluate the path loss according to the wireless underground communication types and soil condition such as the soil moisture, the temperature, etc. Since the data collected by the buried node must be reached an aboveground sink node or BS, the signal EM should be evaluated with a high accuracy in the different communication types.
- Integration of a lightweight model within a real sensor device for a reliable underground channel. This approach should be sufficient to be executed by a node without energy wastage and with a high reliability so that each sensor node should be able to predict if a sent data would be received or not by a destination node according to soil properties. The main idea of this approach is to allow a transmitter node to predict *in situ* if a sensed data should reach or not the destination node, thus in case of not reception of the data, the sensor node may save its energy by avoiding a transmission.

Contributions

In this section, we present briefly our contributions and thereafter the list of our contributions related to our contributions.

– We firstly analyze the existing path losses in literature. Secondly, we evaluated and compared the Complex Dielectric Constant (CDC) derivation schemes. Thirdly, we

proposed a new path loss model that uses a better CDC prediction than the existing path losses. To validate our approach, measurements in real experimental field were made and real sensor nodes are used. The conducted experimentations show that our proposed path loss is more accurate than the existing path loss models with the lowest errors. Furthermore, we show the efficiency of our approach by considering ±3% error of the soil moisture sensor.

– We proposed a WUSN path loss for precision agriculture called WUSN-PLM. To achieve it, the proposed model is based on an accurate prediction of the Complex Dielectric Constant (CDC). WUSN-PLM allows evaluating the path loss according to the different types of communication (Underground-to-Underground, Underground to Aboveground and Aboveground to Underground). On each communication type, WUSN-PLM takes into account reflective and refractive wave attenuation according to the sensor node burial depth. To evaluate WUSN-PLM, intensive measurements on real sensor nodes with two different pairs of transceivers have been conducted on the botanic garden of the University Cheikh Anta Diop in Senegal. The results show that the proposed model outperforms the existing path loss models in different communication types. The results show that our proposed approach can be used on real cheap sensor with 87.13% precision and 85% balanced accuracy.

– We proposed a link channel optimization for reliable communications in WUSNs based on Fuzzy Logic. To achieve it, we designed a Fuzzy Inference System (FIS) based on the famous Sugeno FIS. The proposed inference system consists of 04 inputs and one output. The inputs are made up of fuzzy sets that give information on a sensor node according to the previous study in which we proposed the path loss model called WUSN-PLM. These information are the burial depth of the transmitter and receiver nodes, the soil moisture portion in percent and the distance between nodes. The resulting output of the proposed approach gives the probability of a sent packet to be received or not by the receiver node. To evaluate the proposed approach, intensive experimentations (140 in dry and moist soil configurations) have been conducted with real sensor node devices deployed within a real agricultural field. To validate our approach, powerful metrics used in prediction models have been used. Moreover, comparisons of the proposed approach and the WUSN-PLM are done. The obtained results show that the proposed approach has a high accuracy for predicting the reception or loss of packets in WUSN applications with fewer computations.

Journal publications

- Damien Wohwe Sambo, Anna Förster, Blaise Omer Yenke, Idrissa Sarr, Bamba Gueye and Paul Dayang, "Wireless Underground Sensor Networks Path Loss Model for Precision

Agriculture (WUSN-PLM)", IEEE Sensors Journal, vol. 20, no. 10, pp. 5298 - 5313, 2020.

Impact factor: 3.071

- Damien Wohwe Sambo, Blaise Omer Yenke, Anna Förster, and Paul Dayang, "Optimized Clustering Algorithms for Large Wireless Sensor Networks: A Review", Sensors, vol. 19, no. 2, pp. 1 - 27, 2019.

  Impact factor: 3.031

Conference publications

- Damien Wohwe Sambo, Anna Förster, Blaise Omer Yenke, and Idrissa Sarr, "A new approach for path loss prediction in wireless underground sensor networks", in Proceedings - 2019 IEEE 44^{th} Local Computer Networks Symposium on Emerging Topics in Networking, (LCN Symposium 2019), Osnabrück, Germany, 14^{th} - 17^{th} October 2019.

  International conference: rank A

- Damien Wohwe Sambo, Blaise Omer Yenke and Idrissa Sarr, "Precision agriculture of onions and garlics through a large wireless underground sensor network", in the 9^{th} ConfereNce sur la Recherche en Informatique et ses Applications (CNRIA), Saint-Louis, Senegal, 24^{th} - 28^{th} April 2019.

  National Conference

Other publication

- Blaise Omer Yenke, Damien Wohwe Sambo, Ado Adamou Abba Ari, and Abdelhak Gueroui, "MMEDD : Multithreading Model for an Efficient Data Delivery in wireless sensor networks", International Journal of Communication Networks and information Security (IJCNIS), vol. 8, no. 3, pp. 179-186, 2016.

Thesis Organization

The rest of the thesis is organized as follows:

- Chapter 1 introduces background around WSN. This chapter starts by describing the architecture of sensor nodes and the general overview of a WSN for better understanding the rest of the thesis.

- Chapter 2 presents in details the WUSN. The chapter starts by discussing the architecture of a WUSN and the different types of communication that can occur in such sensor network due to the location of nodes (UG2UG, UG2AG and AG2UG). Thereafter, the existing path loss models for predicting this loss are classified and presented according to the target communication type.

- Chapter 3 gives the first contribution of our Ph.D. thesis. A new approach for path loss prediction in WUSN is presented in this chapter. Our proposal focused on a better way to predict the soil properties summarized by the Complex Dielectric Constant (CDC) needed by all the existing path loss models.

- Chapter 4 improves the approach presented in Chapter 3 by addressing its limits. Indeed, the previous approach was designed essentially for fully underground communications (UG2UG). The Wireless Underground Sensor Network Path Loss Model (WUSN-PLM) designed precision agriculture application is presented in this chapter.

- Chapter 5 aims at designing an approach to predict *in situ* the lost of packets sent by sensor nodes in order to allow a reliable underground channel. We proposed in this chapter, a powerful model for reliable communication based on fuzzy logic which lesser computation and resources similar to sensor node devices. The proposed approach consists of 36 rules and it is based on the famous Sugeno FIS which gives as output the probability of a packet loss according to several parameters.

- Thereafter, the PhD thesis is concluded and future works that deserve further investigation are discussed at the end of the document.

Chapter 1

Introduction to Wireless Sensor Networks

Rapid advances in the areas of sensor design, information technologies, and wireless networks have paved the way for the proliferation of smart Ad hoc networks [3], [29], [30]. These networks have the potential to interface the physical world with the virtual (computing) world on an unprecedented scale and provide practical usefulness in developing a large number of applications, including the protection of civil infrastructures, habitat monitoring, precision agriculture, toxic gas detection, supply chain management, and health care by the use of small devices called sensors. Due to their limited resources their used within large deployment need to allow the interconnection between them, thus forming a wireless sensor networks (WSNs) [4], [31]. In this chapter, the architecture and the applications of WSN are presented in Section 1.1; Thereafter the challenges faced by WSN, the type of routing and the different type of WSNs are presented in Section 1.2.

1.1 Architecture and applications

In this section, we present the components of a sensor node and a wireless sensor network. Several applications of WSNs are presented thereafter.

1.1.1 Sensor node

The recent evolution of wireless communication technologies, digital electronics, and MEMS technology which have seen the apparition of small and cheap devices called sensors. They are small in size and are able to collect information on its environment like temperature, pressure, humidity, water content, gas presence, or luminosity. Thus, a sensor node should have capabilities of sensing, processing and communicating the sensed data to the required destination [3], [32]. A typical architecture of a sensor node is presented in Figure 1.1 and it

consists of 05 modules: processing unit, storing unit, sensing unit, communications unit and a power source. The processing Unit is able to communicate with the other modules. In most architecture the processing and the storing units can be merged to an unique module. thus, the energy source powers the sensing, the processing and the communication units [33].

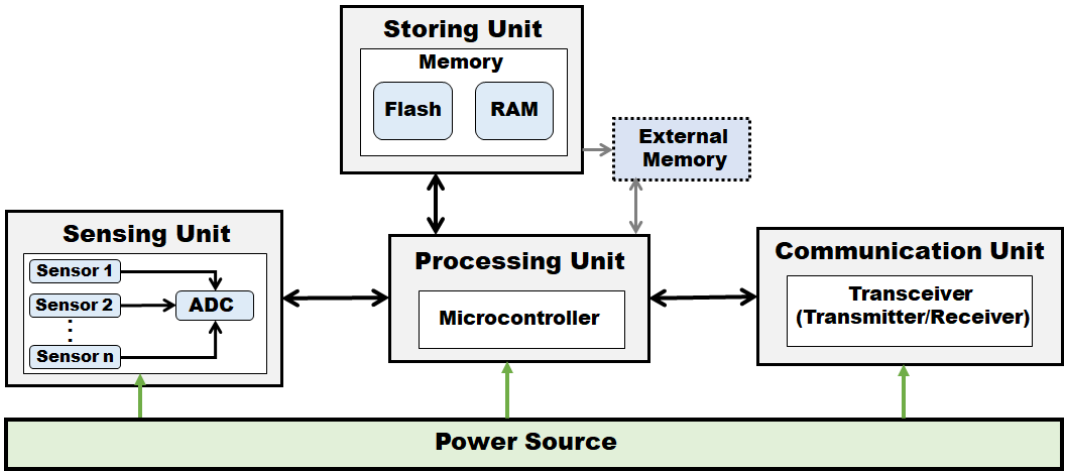

Figure 1.1: Architecture of a sensor node.

Processing Unit

The processing unit is the core of a sensor node. It is made up of a controller which performs tasks, processes data and controls the functionality of other components in the sensor node. While the most common controller is a microcontroller, other alternatives that can be used as a controller are: a general purpose desktop microprocessor, digital signal processors, a Field Programmable Gate Array (FPGA) or an Application Specific Integrated Circuit (ASIC). The microcontroller is often used in many embedded systems such as sensor nodes because of its low cost, flexibility to connect to other devices, ease of programming, and low power consumption. The energy consumption explains why a microcontroller is used is WSN instead of a microprocessor which has a a higher power consumption [34]. Moreover, a microcontroller can be chosen over other types of small-scale processors because of the programming flexibility it offers. Its compact construction, small size, low power consumption, and low cost make it suitable for building computationally less intensive, standalone applications. Most of the commercially available microcontrollers can be programmed with assembly language and the C programming language. The use of higher-level programming languages increases the programming speed and eases debugging. There are development environments that offer an abstraction of all the functionalities of a microcontroller. This enables application developers to program microcontrollers without the need to have a low-level knowledge of the hardware [3].

Storing Unit

This unit includes the RAM in which instructions are executed by the microcontroller. Mostly, the storing unit is integrated in the processing unit as parts of the microcontroller. This memory consumes most of the power allocated to the microcontroller, which is why it is often supplemented by a less energy-intensive memory (ROM) containing the operating system [35]. Several sensor node use an EPROM, an EEPROM, or a flash memory for storing relatively simple instruction program code [36]. Furthermore, due to the limited since of the flash memory on cheap node devices, an external memory can be added to store sensed data locally [33].

Sensing Unit

The most important task of a sensor node is to collect data. This is possible through the sensing unit which allows the node to capture or measure physical data from a target object. This unit consists of two sub-units: the receiver or sensor that recognizes the physical quantity to be captured and the transducer that converts the analog signal received into a digital signal (voltage). The physical data collected by sensor are the temperature, pressure, relative humidity, water level, soil moisture, gas presence, underground activities, etc. The transducer or the Analog-to-Digital Converter (ADC) converts the output of a sensor which is a continuous (or analog) signal into a digital signal. The first step is to quantify the analog signal by converting the continuous valued of the signal into a discrete valued signal. The most important decision at this stage is to determine the number of allowable discrete values. This decision in turn is influenced by the frequency of the signal and the available processing + storage resources [3]. During the last step, the frequency is Over-sampled due to noise. According to the application types, the sensing subsystem integrates one or more physical sensors and provides one or more ADCs.

Communication Unit

As the selection of a microcontroller instead of a microprocessor is vital to the performance as well as the energy consumption of a sensor node, the way the a node sends its collected data is also vital. This task is carried out by a communication unit which is directly connected to the processing unit and the power source. Wireless modules are commonly use instead of wired modules because they are more cheap and easy to install [30]. Thus, the communication unit of a node is made up of a transceiver (transmitter/receiver) to allow wireless communication. Because of the small size of nodes, parallel buses are never supported in node design. Therefore, serial interfaces such as the Serial Peripheral Interface (SPI) are used in most of the wireless modules of embedded systems like sensor node. The SPI bus consists of four pins: MOSI

(Master-Out/Slave-In), MISO (Master-In/Slave-Out), SCLK (Serial Clock), and CS (Chip Select) [37], [38]. Moreover, sensor nodes often make use of Industrial, Scientific and Medical (ISM) bands, which gives free radio, spectrum allocation and global availability. Portion of the RF spectrum globally for industrial, scientific and medical applications had originally reserved by the ITU[1]. ISM bands groups a part of the radio spectrum that can be used for any purpose without a license in most countries [39].

Power Source

This unit is used to supply power to the various components of the sensor node. Indeed, The sensor node consumes power for sensing, communicating and data processing. The Power is stored either in batteries or capacitors both can be rechargeable or not. Batteries and capacitors are the main source of power supply for sensor nodes. However, this resource is limited and generally non-replaceable due to the small size of the node [40]. The power can be classified according to the electrochemical material used for the electrodes such as NiCd (nickel-cadmium), NiZn (nickel-zinc), NiMH (nickel-metal hydrid), and lithium-ion. All this makes energy the most precious resource of a WSN because it has a direct influence on the lifetime of the sensors and therefore of the entire network [29].

In order to cover a more consequent space, several sensors are deployed and connected to each other, thereby forming a Sensor Network. When the communication is performed through wireless module, the sensor network becomes a Wireless Sensor Network (WSN) [3].

1.1.2 Wireless Sensor Network

A wireless sensor network consists of a group of sensor nodes able to monitor and record physical events at diverse locations within a deployment field. Commonly monitored physical parameters are temperature, humidity, pressure, wind direction and speed, light intensity, vibration intensity, sound power, chemical concentrations, air pollution levels and vital body functions. Sensor nodes are deployed randomly or through a predetermined manner according to the sensed fields. Contrary to ad-hoc networks, WSNs are made up of densely deployed sensor nodes in a large deployment field [33]. For this latter, nodes are not able to communicate directly with the user or the BS. To send data up to end-user or BS, nodes use their neighbor to forward the sensed data throughout the network. This mechanism known as multihop communication aims at reducing the energy consumption of each node by sending sensed data to nearest neighbors with high reliability [41], [42]. When the communication between source and destination is done

[1]ITU:International Telecommunication Union is a specialized agency of the United Nations that is responsible for issues that concern information and communication technologies.

without any forwarding a an intermediate node, the nodes communicate each other through a single-hop manner [43].

Hence, multihop communication in sensor networks is expected to consume less power than the single hop communication. Thus, the transmission power levels can be kept low. In a basic WSN (Figure 1.2), nodes within the sensor field collect data and send them throughout the network by using intermediate nodes in a multihop manner. A sink node located out of the sensor field get the sensed data. In order to avoid data reduncy, latency, energy wastage, sensor node send their collected data via a Time Division Multiple Access (TDMA) instead of a regular Carrier Sense Multiple Access with Collision Detection (CSMA/CD) [11], [44], [45], [46]. A pre-treatment of raw sensed data can be achieved by the sink node which has more resources (treatment, memory, communication, energy, etc.) than nodes of the field. The final user communicates with the the sink node through Internet or a LAN. The basic configuration of a WSN allows the user to send a collection request to the sink node which can deliver therefore the request. This configuration is possible because it is assumed that due to its higher resources, the sink node is able to communicate directly with each node of the sensor field, then deliver the collection request [3], [33]. In some WSN, the sink may be mobile and can get data directly from the nodes [47], [48]. Others researches consider several sink node instead of a unique sink in WSN [49].

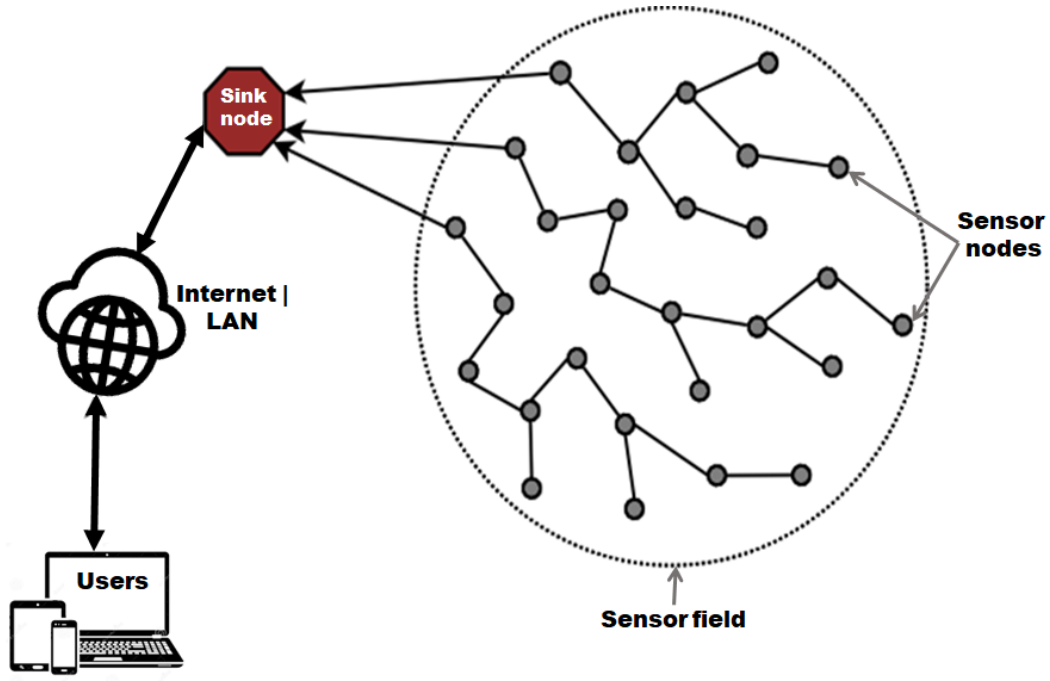

Figure 1.2: An example of a Wireless Sensor Network.

1.1.3 WSN applications

Nowadays, the WUSNs are widely used in varied domains. Their applications can be classified into Area monitoring, Health care monitoring, Environmental sensing, Industrial monitoring or threat detection according to Figure 1.3.

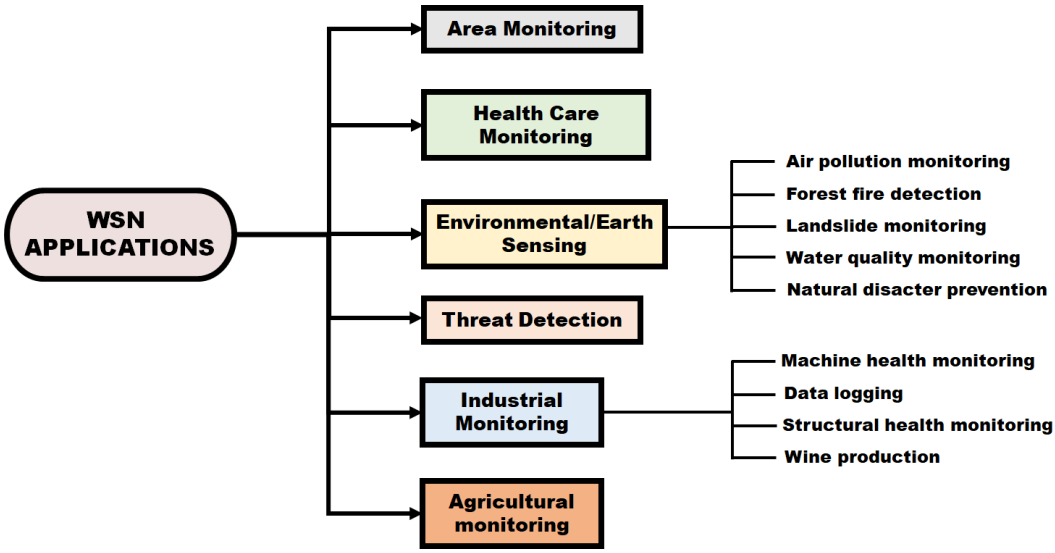

Figure 1.3: Applications of WSN.

Area monitoring

Area monitoring is a common application of WSNs. In area monitoring, the WSN is deployed over a region where some phenomenon is to be monitored. A military example is the use of sensors to detect enemy intrusion; a civilian example is the geo-fencing of gas or oil pipelines.

Health care monitoring

There are several types of sensor networks for medical applications: implanted, wearable, and environment-embedded. Implantable medical devices are those that are inserted inside the human body. Wearable devices are used on the body surface of a human or just at close proximity of the user. Environment-embedded systems employ sensors contained in the environment. Possible applications include body position measurement, location of persons, overall monitoring of ill patients in hospitals and at home. Devices embedded in the environment track the physical state of a person for continuous health diagnosis, using as input the data from a network of depth cameras, a sensing floor, or other similar devices. Body-area networks can collect information about an individual's health, fitness, and energy expenditure [50]. In health care applications the privacy and authenticity of user data has prime importance. Especially due to the integration

of sensor networks, with IoT, the user authentication becomes more challenging; however, a solution is presented in recent work [51].

Environmental/Earth sensing

There are many applications in monitoring environmental parameters [52], they can be subdivided into air pollution monitoring, fire forest detection, landslide monitoring, water quality monitoring and natural disaster prevention.

- *Air pollution monitoring*: WSN have been deployed in several cities (Stockholm, London, Brisbane, Toulouse, etc.) to monitor the concentration of dangerous gases for citizens. These can take advantage of the ad hoc wireless links rather than wired installations, which also make them more mobile for testing readings in different areas.
- *Forest fire detection*: A network of Sensor Nodes can be installed in a forest to detect when a fire has started. The nodes can be equipped with sensors to measure temperature, humidity and gases which are produced by fire in the trees or vegetation. The early detection is crucial for a successful action of the firefighters; thanks to WSN, the fire brigade will be able to know when a fire is started and how it is spreading.
- *Landslide monitoring*: A landslide detection system makes use of a wireless sensor network to detect the slight movements of soil and changes in various parameters that may occur before or during a landslide. Through the data gathered it may be possible to know the impending occurrence of landslides long before it actually happens.
- *Water quality monitoring*: It involves analyzing water properties in dams, rivers, lakes and oceans, as well as underground water reserves. The use of many wireless distributed sensors enables the creation of a more accurate map of the water status, and allows the permanent deployment of monitoring stations in locations of difficult access, without the need of manual data retrieval.
- *Natural disaster prevention*: WSNs can be effective in preventing adverse consequences of natural disasters, like floods. Wireless nodes have been deployed successfully in rivers, where changes in water levels must be monitored in real time.

Threat detection

A typical threat detection system is the Wide Area Tracking System (WATS) which is a prototype network for detecting a ground-based nuclear device such as a nuclear briefcase bomb. WATS is being developed at the Lawrence Livermore National Laboratory (LLNL). WATS

would be made up of wireless gamma and neutron sensors connected through a communications network. Data picked up by the sensors undergoes data fusion, which converts the information into easily interpreted forms; this data fusion is the most important aspect of the system. The data fusion process occurs within the sensor network rather than at a centralized computer and is performed by a specially developed algorithm based on Bayesian statistics. WATS would not use a centralized computer for analysis because researchers found that factors such as latency and available bandwidth tended to create significant bottlenecks. Data processed in the field by the network itself (by transferring small amounts of data between neighboring sensors) is faster and makes the network more scalable [53].

Industrial monitoring

The applications related to the industrial monitoring by the use of sensor nodes can be classified into: Machine health monitoring, data logging, structural health monitoring or wine production.

- *Machine health monitoring*: WSNs have been developed for machinery condition-based maintenance (CBM) as they offer significant cost savings and enable new functionality. Wireless sensors can be placed in locations difficult or impossible to reach with a wired system, such as rotating machinery and untethered vehicles
- *Data logging*: WSNs are also used for the collection of data for monitoring of environmental information [54]. This can be as simple as monitoring the temperature in a fridge or the level of water in overflow tanks in nuclear power plants. The statistical information can then be used to show how systems have been working. The advantage of WSNs over conventional loggers is the real time data feed that is possible.
- *structural health monitoring*: WSNs can be used to monitor the condition of civil infrastructure and related geophysical processes close to real time, and over long periods through data logging, using appropriately interfaced sensors.
- *Wine production*: WSNs are used in order to monitor the production of wine in such a way the harvest is triggered at the right time by farmers.

Agricultural monitoring

In agriculture, efforts to reduce operating costs while maintaining and improving crop yields have been consistently made. One of the efforts to more uniformly apply irrigation water is sprinkler irrigation with a center pivot system, which improves the efficiency of water use as well as of energy use [55]. This kind of intelligent watering system are widely used in smart agricultural field [56]. Moreover, WSN can be used to continuously and effectively monitor various critical

parameters in a fishpond, such as the water level, pH, temperature and dissolved oxygen. The data collected through the system can be used for long-term analysis and better decision-making, thereby improving resource utilization and maximizing profits. Several aquaculture are implemented in the literature [57].

1.2 Overview on WSN

In this section, we present an overview of WSN technology. We firstly describe the main challenges facing WSN; secondly the wireless technologies mostly used for WSN are presented; thirdly, we summarize and classify the routing approaches for WSN; finally, we briefly describe the types of WSN.

1.2.1 WSN challenges

WSNs allow a large number of applications and are widely used. However, due to sensors constraints (limited resources) the design of a WSN faces many constraints. Important constraints are presented below [3], [4], [33], [58], [59], [60].

Network cost

When designing a WSN, the cost of the whole network is the most important factor to take into consideration. Since the zone of study can be very large, the number of sensors within the field will significantly increase, in that case, sensor nodes should be less expensive as possible.

Node deployment

The deployment of sensor nodes within the sensor fields can be deterministic or self-organizing. In deterministic deployment, the different paths are pre-determined through the network, whereas in self-organizing deployment, the process of setting up routes is greatly influenced by energy consumption and is achieved by sensor nodes themselves. Even if an application like underground monitoring in ecology uses a deterministic deployment, nodes should self-organize themselves after failures of some nodes in order to enhance the fault tolerance of the network.

Nature of nodes

WSN facing the issue of node natures: they can be homogeneous or heterogeneous. Within a sensor field, nodes are homogeneous when all them have the same characteristics or resources

(microcontroller performance, available memory, communication range, energy level, etc.). However, the nodes are heterogeneous when there are within the field one or more special nodes with extended performance compared to normal nodes. In this last case, these special nodes are mostly set as sink node.

Energy consumption

The energy management is a big challenge for WSN. Due to their reduced size and their low cost, sensor nodes will have limited energy capacity because of the use of battery of which replacement or recharge is impossible and/or complex due to dangerous study fields. So when the energy of a sensor reaches a certain threshold, they become faulty and are not able to run properly thus affect the overall network performance and its lifetime.

Hardware restrictions

Due to their low price and small size, sensors have very limited resources like a restricted computation, reduced energy supply, limited memories (storage, programmable) and transmission coverage. The design of a WSN should consider the constraints of nodes.

Scalability

Since WSN are ad-hoc network, new sensors can be added to the initial network, then the number of sensor nodes deployed in the sensing field may be in the order of hundreds, thousands or more.

Fault tolerance

Some sensor nodes may fail or be blocked due to lack of power, physical damage, or environmental interference. The failure of sensor nodes should not affect the overall task of the sensor network. In order to avoid crashing, the network should perform mechanisms of resilience of data through the network.

Data delivery

On WSN, models of data delivery can be classified as continuous, event based, query based or multithreaded based. On a continuous model, data are delivered periodically up to the Base Station or the sink node. Meanwhile, on event and query based models, the nodes deliver the data after an event occurs. Moreover, in query based model, data are delivered after a request

of the sink node. Recent approach of delivering data on WSN is hybrid model such as the Multithreading Model for an Efficient Data Delivery (MMEDD) [43]. The presented approach allows to an intermediate node receiving and forwarding efficiently data without energy wastage cause initially by traditional multithreading on WSN.

Network topology

WSN deployment requires maintenance of the network topology due to the high density of nodes within the sensor field. Thus, sensor nodes should be able to adapt themselves their functionning in order to maintain the topology. The maintenance of the WSN topology consists of three phases:

- Deployment: Nodes are deployed either through a pre-defined or random manner. For random deployment, nodes self-organize.
- Post-deployment: During the exploitation phase, the network topology can change due to the modification of node positions or node failures.
- Re-deployment: Adding new sensor nodes within the field involves ipdating the network topology.

Wireless technology

When designing a WSN, another challenge to consider is the selection of the right or adapted wireless technology for an application. Moreover, the selection of a wireless technology must take into account the parameters like the bandwidth, the range, and the power requirements.

1.2.2 Wireless technologies for WSN

Wireless communication is vital for mobile handheld devices. In the development of mobile devices and electronics, the most used technologies can be resumed into: WiFi (IEEE 802.11), Bluetooth (IEEE 802.15.1), ZigBee (IEEE 802.15.4), 6LoWPAN, 6TiSCH, WirelessHART, Sigfox, LoRa (LoRaWAN) or specialized low-power RF.

WiFi (IEEE 802.11)

WiFi is the fastest of all popular wireless LAN technologies. Most deployed networks operate according to the IEEE 802.11n specification, which helps transfer data at a rate of up to 600 Mbps through MIMO technology (the use of multiple antennas that transmit and receive data

to generate several spatial radio channels that are weakly correlated). Wireless networks based on this technology can transmit large amounts of information and view videos of average quality. But for high-definition videos, WiFi (IEEE 802.11) is not enough, so new wireless LAN standards are introduced, such as IEEE 802.11ac and IEEE 802.11ad. IEEE 802.11ac (speed of up to 3.6 Gbps) is a development on WiFi for the 5 GHz band, which helps transfer high-resolution video streams, work with cloud services and hold video conferences over a wireless channel. IEEE 802.11ad (WiGig) is a new standard for wireless LANs operating in the 60 GHz band. It can transmit data at a speed of up to 7 Gbps. In addition to audio/video transmission, it also helps operate network storage [61].

Bluetooth

Bluetooth technology or standard IEEE 802.15.1 is widely used in mobile handheld devices for information exchange within a radius of 10 to 100 meters: cell phones, headsets, wireless manipulators and keyboards. Apart from its use in consumer electronics, Bluetooth is also utilized in embedded systems for industrial use. An example would be systems for local monitoring of remote objects (basic cell stations and electrical substations). Bluetooth technology is also developing in media and entertainment. For instance, it is applied in systems for transfer of advertising content in crowded places (supermarkets, shopping centers and expo shows). There are several Bluetooth specifications: v1.0 to v5.0. Bluetooth basic versions provide a data transfer rate of up to 723 kbps for unidirectional transfer and 433 kbps for bidirectional transfer. Bluetooth V5 is the latest version of the Bluetooth wireless communication standard. With Bluetooth 5.0, devices can use data transfer speeds of up to 2 Mbps, which is double what Bluetooth v4.2 supports. Devices can also communicate over distances of up to 800 feet (or 240 meters), which is four times the 200 feet (or 60 meters) allowed by Bluetooth 4.2. However, walls and other obstacles will weaken the signal, as they do with WiFi [61].

Zigbee (IEEE 802.15.4)

Zigbee is an IEEE 802.15.4 based specification for a suite of high-level communication protocols used to create personal area networks with small, low-power digital radios, such as for home automation, medical device data collection, and other low-power low-bandwidth needs, designed for small scale projects which need wireless connection. Hence, Zigbee is a low-power, low data rate, and close proximity (i.e., personal area) wireless ad hoc network. The technology defined by the Zigbee specification is intended to be simpler and less expensive than other wireless personal area networks (WPANs), such as Bluetooth or more general wireless networking such as WiFi. Applications include wireless light switches, home energy monitors, traffic management systems, and other consumer and industrial equipment that requires short-range low-rate

wireless data transfer [62], [63]. Zigbee is a low-cost, low-power, wireless mesh network standard targeted at battery-powered devices in wireless control and monitoring applications. Zigbee delivers low-latency communication. Zigbee chips are typically integrated with radios and with microcontrollers. Zigbee operates in the industrial, scientific and medical (ISM) radio bands: 2.4 GHz in most jurisdictions worldwide; though some devices also use 784 MHz in China, 868 MHz in Europe and 915 MHz in the US and Australia, however even those regions and countries still use 2.4 GHz for most commercial Zigbee devices for home use. Data rates vary from 20 kbps (868 MHz band) to 250 kbps (2.4 GHz band) [64].

6LoWPAN

The 6LoWPAN system is used for a variety of applications including WSNs. This form of wireless technology sends data as packets and using IPv6 proposed by the Internet Engineering Task Force (IETF) over Low power Wireless Personal Area Networks. 6LoWPAN provides a means of carrying packet data in the form of IPv6 over IEEE 802.15.4 and other networks. It provides end-to-end IPv6 and as such it is able to provide direct connectivity to a huge variety of networks including direct connectivity to the Internet. In order to send IPv6 packet data over 6LowPAN, a method of converting the packet data into a format that can be handled by the IEEE 802.15.4 lower layer system is performed. Moreover, IPv6 requires the maximum transmission unit (MTU) to be at least 1280 bytes in length. However, it is considerably longer than the IEEE 802.15.4's standard packet size of 127 octets used to keep short transmissions and thereby reduce power consumption. To overcome the address resolution issue, IPv6 nodes are given 128 bit addresses in a hierarchical manner. The IEEE 802.15.4 devices may use either of IEEE 64 bit extended addresses or 16 bit addresses that are unique within a PAN after devices have associated. There is also a PAN-ID for a group of physically co-located IEEE 802.15.4 devices [65], [66]. By using IPv6 packets, 6LoWPAN becomes a wireless IoT standard that has quietly gained significant ground. Although initially aimed at usage with IEEE 802.15.4, it is equally able to operate with other wireless standards making it an ideal choice for many applications [67].

6TiSCH

6TiSCH is the integration of IPv6 by the IETF over the Time Slotted Channel Hopping (TSCH) mode of IEEE 802.15.4e [68]. As the core technique in IEEE 802.15.4, TSCH splits time in multiple time slots that repeat over time. TSCH combines TDM with a form of frequency agility called Chanel Hopping in order to defeat all forms of interferences. Its structure is referred as a Slotframe [69]. The 6TiSCH aims to support best effort traffic on deterministic TSCH based networks. The 6TiSCH Architecture defines a remote monitoring and scheduling management

of a TSCH network by a path computation element protocol, which cooperates with an abstract Network Management Entity (NME) to manage time slots and device resources in such a way that the energy consumption on constrained devices such as sensor nodes is minimized. The PCE can lock some resources (namely hard cells) for deterministic flows along paths called tracks, so that traffic on a track cannot be influenced whatever by other flows [70].

WirelessHART

WirelessHART is a wireless sensor networking technology based on the Highway Addressable Remote Transducer Protocol (HART). HART is the global standard for sending and receiving digital information across the 4-20 mA analog current loops that connect the vast majority of field instruments with distributed control systems [71]. WirelessHART is a Time Division Multiple Access (TDMA) based network. All devices are time synchronized and communicates in prescheduled fixed length time slots. TDMA minimizes collisions and reduces the power consumption of the devices. WirelessHART uses several mechanisms in order to successfully coexist in the shared 2.4 GHz ISM band: Frequency Hopping Spread Spectrum (FHSS) allows WirelessHART to hop across the 16 channels defined in the IEEE 802.15.4 standard in order to avoid interference. All embedded systems like sensor node which work with WirelessHART technology must have routing capability, i.e., there are no reduced function devices like in ZigBee. Since all devices can be treated equally in terms of networking capability, installation, formation, and expansion of a WirelessHART network becomes simple as the network is self-organizing. WirelessHART forms mesh topology networks (star networks are also possible, but not recommended) [72].

Sigfox

Sigfox is a cellular system approach that allows end-devices connecting to base stations equipped with software-defined cognitive radios using the BPSK (Binary Phase Shift Keying) modulation [73]. It uses a frequency band of 868MHz, dividing the spectrum into 400 channels of 100Hz. Its coverage is about 30-50 km in rural areas and about 3-10 km in urban environments. An access point can manage around one million of end-devices and each end-device can send about 140 messages per day with a data rate of 100bps. Down link communication can only precede up link communication after each the end- device must wait to hear a response from the base station which makes it interesting for data acquisition. However, for command and control scenarios, it is not interesting [74].

LoRa/LoRaWANs

LoRa (Long Range) is a spread spectrum modulation technique derived from chirp spread spectrum (CSS) technology. LoRa is located at the physical layer. Semtech LoRa devices and wireless radio frequency technology is a long range, low power wireless platform that has become the st used technology for Internet of Things (IoT) networks. LoRa, essentially, is a clever way to get very good receiver sensitivity and low bit error rate (BER) from inexpensive chips. That means low-data rate applications can get much longer range using LoRa rather than using other comparably priced radio technologies. Furthermore, LoRa operates over ISM frequency bands under 1 GHz. For Europe it is designed to be used over 433/868 MHz band, while in USA it can be used over 915 MHz band. Nevertheless in Africa (south Africa), both frequency range can be used with LoRa modulation since there is not a regulation concerning Africa. Transmitting at higher power levels will increase a LoRa node,Äôs range. Nodes can adjust their output power to meet regulatory requirements [75]. For example, LoRaWANs (MAC layer) in Europe are limited to 10 channels, has duty cycle restrictions but no channel dwell time limitations. LoRaWANs in North America have 64 channels, also have duty cycle restrictions but no channel dwell time limitations. LoRaWAN has 3 common 125 kHz channels for the 868 MHz band namely 868.10, 868.30 and 868.50 MHz that devices use to join the network. Once a node has joined the network, the network server can provide additional channels to the device. In Europe, the same channels are used for up link and down link [73].

Specialized low-power RF modules

Low-power RF modules are a good solution for embedded systems where it is required to transmit small data chunks over a small distance using license-free radio frequency ranges of 433MHz, 868MHz and 2.4GHz. Electronic devices sometimes require some kind of remote control like a remote car alarm key or remote control for a multimedia device. Data amounts and transfer rates are rather low in such situations, while power consumption is crucial. It makes no sense to use complicated wireless stacks like Bluetooth, ZigBee or WiFi such remote control devices which do not require inter-operation with radio equipment by other manufacturers. A typical RF solution consists of a radio frequency transceiver or transmitter, a low-power microcontroller, an antenna and a crystal oscillator. RF chip manufacturers often combine a transceiver and a microcontroller into a single chip package [61].

1.2.3 Routing in WSNs

Routing in WSNs is very challenging due to the inherent characteristics that distinguish these networks from other wireless networks like MANET or cellular networks [58]. The main goal of

routing in WSN is to carry out data communication when trying at the same time to prolong the network lifetime and provide high quality of service during data delivery [76]. Based on the network structure, routing on WSN can be classified as data centric based routing, location based routing, group-based routing, or as hierarchical based routing [4].

Data centric based

In several sensor networks, it is not obvious to assign an identifier to each node because of the large number of nodes deployed. Besides the problem of identification of nodes, the random deployment of nodes makes it difficult to select a specific node during the routing of data through the network. Nevertheless, since data are usually transmitted from each node within the deployment region, the redundancy of these data can be significant then waste a lot of energy. The resolution of redundant data during routing has led to the data centric approach, which is different from the traditional address-based routing where routes are created between addressable nodes [31], [59], [77]. In data centric based routing, before data have to be sent by nodes in a selected region, the sink node should send queries to a selected region and wait for the incoming data [59]. The first and the most popular data centric protocol is the Sensor Protocols for Information via Negotiation (SPIN), in which negotiation between nodes is considered in order to eliminate redundant data and reduce the energy consumption. There are several kinds of data centric based routing like Directed Diffusion , Energy-aware routing, Rumor routing, or Gradient-Based Routing [77], [78].

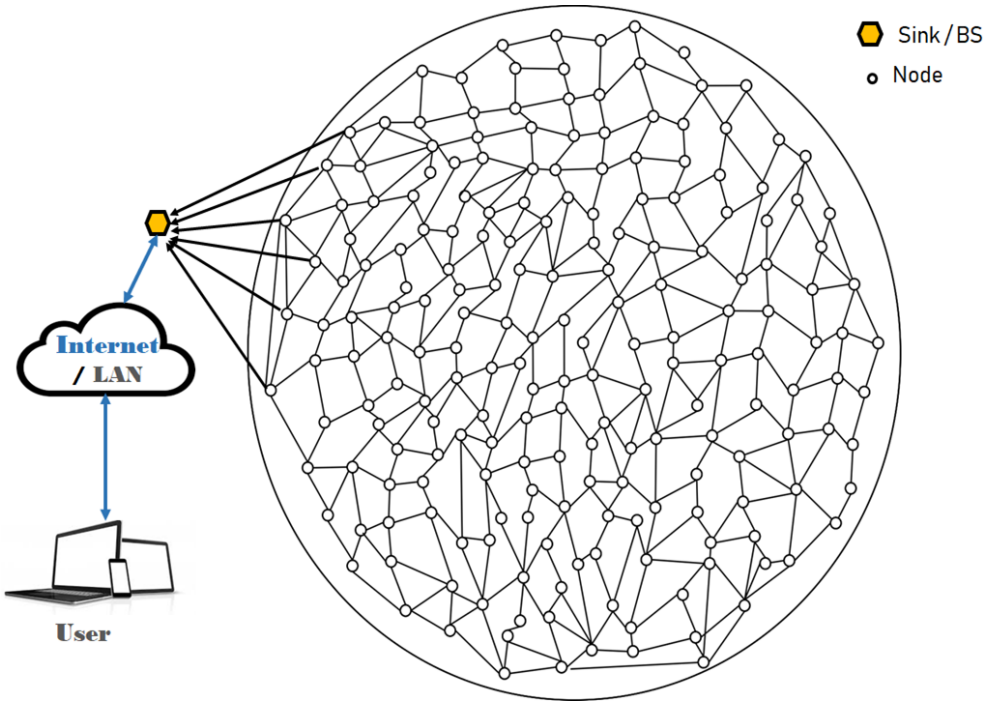

Figure 1.4: WSN based on data centric routing scheme.

Location based routing

The position of sensor node is required in applications like military tracking, ecology monitoring, or health care. Contrary to data centric based routing where the position of a node can be unknown, the location-based protocols are very interesting since they can significantly decrease the complexity of finding best routes through the network. The distance between two neighbor nodes can be therefore estimated by the Received Signal Strength Indicator (RSSI) [59]. When the study area is well known in advance, using the location of sensors will eliminate the number of transmissions significantly because the queries would be assigned only to a particular region at a particular time [59]. However, information about a position can be done through the use of a GPS (Global Positioning System) module on the sensor. Since the one goal when designing a sensor network is low cost and energy management, the use of GPS by sensors on a large scale network is quite expensive and energy consuming [79]. An example of location-based protocol is the Minimum Energy Communication Network (MECN), it reduces the energy consumption into the network by using a low power GPS module on each sensor node. Meanwhile, it is best applicable to sensor networks, which are not mobile [59]. Another well-known location-based algorithm is the Geographic Adaptive Fidelity (GAF) designed initially for mobile ad-hoc networks. Presentations of location-based protocols are conducted in [60], [80].

Group based routing

Having the location of each node within a field is not easy when the amount of sensors increases considerably. A more easy approach consists of deploying sensor nodes in groups. In this kind of routing, nodes in the same group are most of the time closed to each other [81], [82]. In group-based routing solutions, each group is able to perform its own application independently. Take, for example, the measurement of the environmental impact of an area made up of a small forest, a sandy place, and a marine reef. In this example, three groups can be deployed according to the measurements of each application (forest, sand, underwater). However, the deployment of group-based protocol within the study field needs to be meticulous. As explained by Liu et *al.* [82], in a group-based solution, each sensor node is assigned to its group before the deployment. There are several algorithms based on group routing. Lloret et *al.* [81] proposed the Group-Based Protocol for Large Wireless Ad Hoc and Sensor Networks called GBP-WAHSN. Another group-based algorithm is called Group based Mobile Agent Routing (GMAR) [83], which uses a mobile agent in order to aggregate data in each group.

Hierarchical based routing

Clustering is an efficient topology control approach for maximizing the lifetime and scalability of WSNs. The hierarchical based routing is a part of the group-based routing and consists of creating a virtual hierarchy among the nodes of the sensor network [84]. This class of routing techniques is generally designed for large scale networks and aims to efficiently maintain the energy consumption of sensor nodes and increase the network lifetime by cutting the whole network into clusters [31]. Each cluster is led by a node called Cluster Head (CH) which receives data from nodes within the cluster. CHs communicate each other in order to find a better route up to the sink node or the BS. This is done in order to reduce the energy consumption of sensor nodes by reducing the number of transmitted/received messages to the sink node. In addition to CH election, a second special node called Vice Cluster Head (VCH) can be elected in order to improve the lifetime of the CH as shown in [85]. Mechanisms like multihop communication, data aggregation, and data fusion are performed so that the energy is efficiently used within the cluster [59], [77]. The most popular clustering algorithm is the Low-Energy Adaptive Clustering Hierarchy (LEACH), it uses probability computing and the received signal strengths to locally select the CHs which have to serve as router of the data up to the BS. In LEACH, local data fusion and aggregation are performed by local CH [86]. For a large scale network, LEACH is able to increase the network lifetime [84]. However, due to its single hop configuration, the CH on LEACH is assumed to have a long communication range. Thus, the data sent by the CH has to reach the BS directly. Another approach subdivides the problem into two layers: an organization layer to manage communications and a distribution layer made up of cluster members [87]. Many hierarchical based routing algorithms are proposed in the literature, such as the PEGASIS, TEEN, EEHC, PEACH, or HEED. Authors of [79], [81], [82], [88] present several classical hierarchical algorithms and show how the scalability, the energy efficiency, network lifetime, data delivery, and the fault tolerance are greatly improved on large scale sensor network.

Regardless the network structure, routing protocols in WSN field can also be classified as follows [45], [58], [88], [89], [90]. Figure 1.6 below gives a global overview of this classification.

- Path establishment: The routing in WSN can be designed according to the way the path is set up in the network. For this kind of approach, the path can be established through a proactive, reactive or a hybrid manner. For proactive path establishment, the nodes build themselves the path from the field up to a BS or a sink node. This kind of routing are commonly known as distributed solution. When a supervisor outside the sensor field creates paths and sends them to each node, thus the routing is based on a reactive path establishment. Most of centralized routing solutions in WSN are based on reactive path establishment. Hybrid strategies combine the proactive and the reactive behaviours of

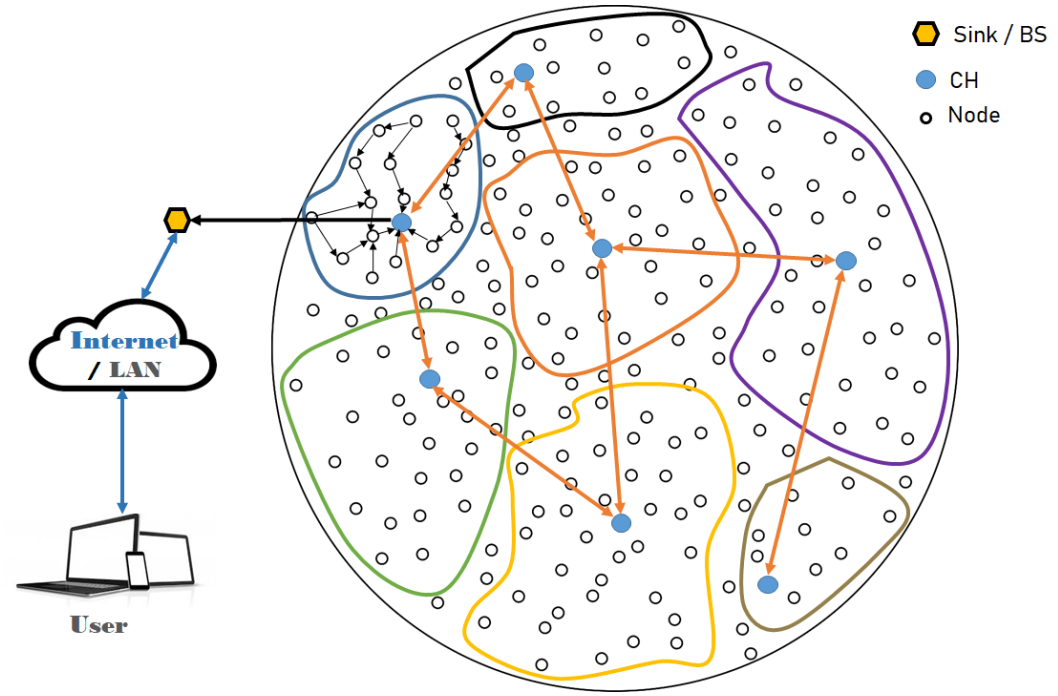

Figure 1.5: Architecture of hierarchical routing in WSN.

nodes for path establishment.

- Protocol operation: Another way to classify routing approaches in WSN is to consider the type of operations executed by the protocol. When nodes within the field start a particular task after the reception of a particular query, the routing protocol is query-based. For example, the sensing task sent by a source node through the network is forwarded by intermediate node to destination nodes. When a destination node receives a query that matches the query, it sends back the sensed data to the source node. However, when the node action is triggered by an event, the protocol is event-based. For approaches that use multiple paths rather than a single path, the routing is multipaths based. Due to the resiliency of paths in these type of routing protocols, the fault tolerant is higher than in single path based solutions. Another kind of protocol operation is based on negotiation between nodes. For this type, redundant data through the networks are eliminate contrary to simple query-based routing protocols. When the routing protocols aim at finding a tradeoff between the energy consumption and the data quality, they are named QoS-based. For routing solutions focus on the amount of data delivered at the BS or a sink node, the protocol operation is data delivery-based. Due to their limited resources, sensor nodes cooperate each other in processing the sensed data of the network. Thus, when the data are forwarded to an aggregator, the routing protocol is coherent-based. Contrary to coherent protocols, when the data are locally process by sensor nodes within the field, the routing algorithms are non coherent-based.

- Next hop selection: The limited communication range of sensor nodes is a key challenge in

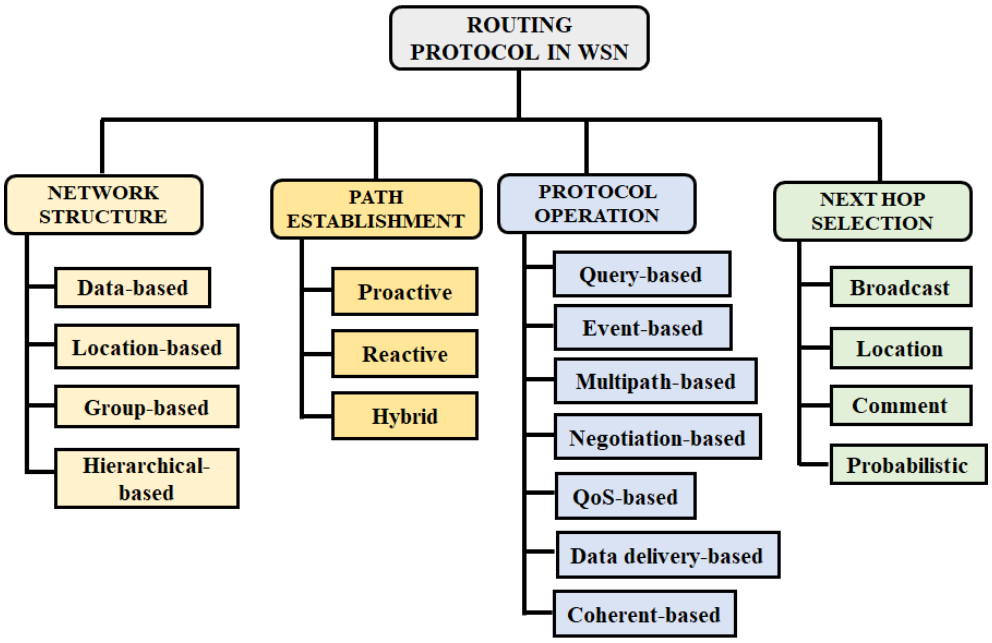

Figure 1.6: Classification of routing protocol in WSN.

WSN. To address this issue, nodes that are out of range can communicate through multi hop communication. Intermediate nodes are used to forward data sent by a source node to a far destination node. Routing protocols can be classified according to the selection process of the intermediate node (next hop). The next hop selection can be achieved by broadcasting a packet, thus nodes within the communication range of the source node could be the next hop. Another way in selecting the next hop is to use its location. In this type of routing protocols, the sensor nodes of the experimental field are equipped with a GPS module. The next hop selection can also be achieved through exchanges of comments between neighbor nodes or randomly by the computation of a probability.

Optimized routing solutions

Designing a routing protocol for WSN aims at optimizing the lifetime of the network. This optimization problem has conducted to recent and intelligent strategies based on Machine Learning (ML) and Computational Intelligence (CI). Routing approaches based on ML/CI improve the lifetime of the network by finding a trade off between the energy consumption and the performance of the WSN. Several ML/CI paradigms are used for routing in WSNs. They can be classified as follows: Fuzzy Logic, Genetic Algorithm, Neural Network, Reinforcement Learning, and Swarm Intelligence paradigms [76], [84], [91], [92], [93], [94].

- **Fuzzy Logic (FL)**: It is a mathematical discipline invented to express approximate human reasoning. Contrary to the classical set theory which enable elements to belong or not to a set, FL allows a measure of imprecision or uncertainly which is marked by the use

of linguistic variables like *most*, *many*, *frequently* through rules within a set called fuzzy set [91]. An example of a fuzzy set used for input variables of the distance between a node and the BS is presented in Figure 1.7. From the figure, the distance to BS is classified in *Close*, *Medium*, or *Far*. These later are the membership functions of the fuzzy set *Distance to Base Station*. Close and Far are

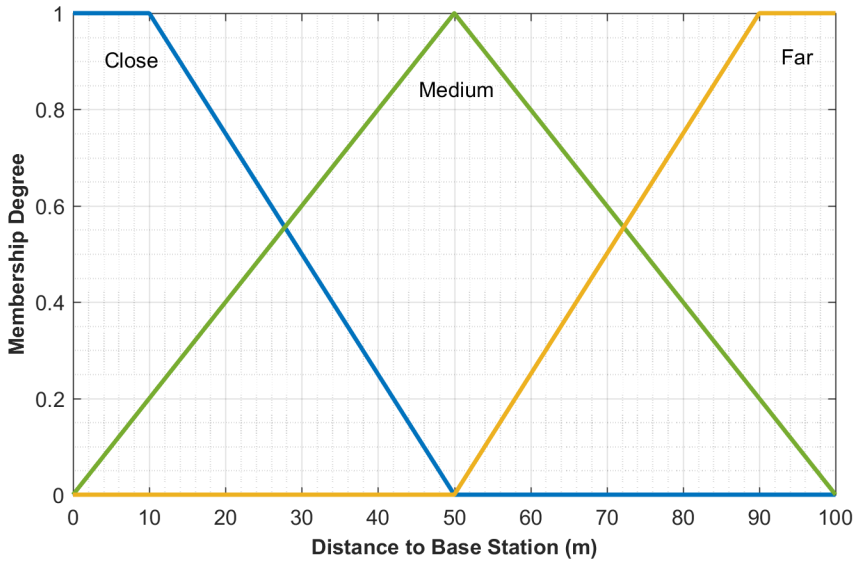

Figure 1.7: Fuzzy set for input variables of the distance between node and the BS.

- **Genetic Algorithm (GA)**: It is an adaptive heuristic approach based on biological genetic evolution for intelligent search and optimization. GA models the natural evolution by performing fitness tests on new structures to choose the best population [91]. With GA approaches, a population is made up of a group of chromosomes where a chromosome represents a complete solution to a relevant problem, and fitness shows the quality of a chromosome in function of concrete needs [95]. This kind of optimized algorithm is used for randomized search and optimization during routing of data. GA showed flexibility in solving dynamic problems and has been successfully applied within many NP-hard problems which include hierarchical routing on WSN [83], [93], [96], [97], [98].

- **Neural Networks (NNs)** : They are mathematical models inspired from biological networks of neurons. Similar to a large and dense network, each neuron is connected to many other neurons. A NN consists of a network of neurons organized in input, hidden, and output layers where the NN learns the different paths and determine their interrelationships [83], [99]. The NNs are used for solving the problems of search route, sensor fusion, data mining, and clustering [4], [100], [101], [102].

- **Reinforcement Learning (RL)**: It is a sub-domain of ML which teaches an agent on what to do and how to assign situations to particular actions so as to be intelligent [92].

The agent would try several actions, and learns from its experience the best action it has to choose in order to optimize the network performance [83], [91], [92], [98]. Most of the RL based protocols are used in some clustering algorithms in WSN finding optimal paths and prolonging network lifetime [76].

- **Swarm Intelligence (SI)**: It is defined in [103] as "*any attempt to design algorithms or distributed problem-solving devices inspired by the collective behavior of social insects and other animal societies*". Most of the proposed are based on the social behaviors of flocks of birds, schools of fishes, and insect cooperation like ants, bees, butterflies, etc. which have limited resources like sensor nodes used in WSN. SI approaches can be classify into Particle Swarm, Ant Colony, and Bee Colony Optimizations [76], [96], [98].

  - **Particle Swarm Optimization (PSO)** is an evolutionary computation technique and is related to the bird flocking, fishing schooling, and swarm theory. Like the other evolutionary computation techniques, PSO is a population-based search algorithm and is initialized with a population of random solutions, called particles. A particle will have a fitness value, which will be evaluated by a fitness function to be optimized in each generation [104], [105]. In order to increase the performances of WSNs, several routing strategies use PSO to improve the network lifetime [106], [107].
  - **Ant Colony Optimization (ACO)** is defined by [108] as a novel nature-inspired metaheuristic for the solution of hard combinatorial optimization problems. The ACO algorithm originates from the behavior of ants which communicate with each other by using chemical deposits called pheromones. When ants move, they lay pheromones on the ground, and they receive the current strength of pheromone [109]. The main idea of the ACO metaheuristic is to model the problem as a search for the best path by constructing a path-graph that represents the states of the problem [91]. Many works in the WSN field used clustering algorithms based on the ACO to improve the performance of sensor networks [110], [111].
  - **Bee Colony Optimization (BCO)** protocols are inspired from honeybees foraging behaviors. Insects are capable of individual proactive abilities and self-organizing capacity [77]. Honeybees can be grouped into a colony and living within a hive, and show impressive auto-solving problem capabilities. Scout bees explore the surrounding of the hive in order to detect possible sources of food, when a flower (food) is discovered, the scout bee returns back to the hive to recruit the forager bees through a special dance called waggle dance [112]. The BCO are widely used to solve efficiently routing NP hard problems like clustering [113], [114], [115].

1.2.4 Types of WSN

Mobile Wireless Sensor Networks (MWSNs)

Generally, most of used WSN have static sensor nodes, whereas, Mobile Wireless Sensor Networks (MWSNs) have mobile sensor node. Thus, these kind of networks consist of a collection of sensor nodes that can be moved on their own and can be interacted with the physical environment. In addition to the mobility possibility within the deployment field of sensor nodes, each of them can perform sensing and communication tasks.

MWSNs have more adaptability than the static WSNs because Mobile WSNs can be set up for any situation and they can operate with sudden topology changes [116]. The advantages of MWSN over the static WSNs include better coverage, better energy efficiency, superior channel capacity. However, due to the presence of a mobility entity and localisation system on each sensor node, the energy consumption can easily increase.

Wireless Multimedia Sensor Networks (WMSNs)

Another type of WSNs well-known are Wireless Multimedia Sensor Networks (WMSNs). They have been proposed initially to enable the tracking and the monitoring of events within a field in the form of multimedia. The media consist of imaging, video, and audio files. These networks are made up of low-cost sensor nodes equipped with microphones and/or cameras. The nodes within the sensor field are interconnected with each other over a wireless connection for data compression, data retrieval, and correlation [117], [118]. WMSNs are applicable in a wide range of areas including area monitoring and video surveillance. But due to unreliable error-prone communication medium and application specific QoS requirements, routing of real-time multimedia traffic in WMSNs poses a serious problem. The challenges with this kind of WSN are the high energy consumption, the requirement of high bandwidth, the data processing, and the compressing techniques. Moreover, multimedia contents require high bandwidth for the contents to be delivered properly and easily [119].

Terrestrial Wireless Sensor Networks (TWSNs)

Terrestrial WSNs (TWSNs) consist of numerous tiny sensor nodes. These nodes are randomly deployed in a specific area from where an ad-hoc network is used for communication between the nodes. These nodes can be organized by optimal placement, grid placement, or 2D and 3Dplacement models. recent reseaches investigated this for applications of the terrestrial wireless sensor network in Radio Frequence/Free Space Optics (RF/FSO) systems, including open research issues and challenges. The drawbacks of terrestrial applications are the effect of weather

such as rain and snow on an optical wireless communication link. The author has proposed a method to increase the lifetime performance of the network [120]. However, the difference between WSN and TWSN in the literature is often not noticeable, WSNs are assimilated to TWSNs.

UnderWater Wireless Sensor Networks (UWSNs)

Underwater wireless sensor networks (UWSN) is a kind of WSN in which sensor nodes are located under the water surface. It aims at studying different parameters such as natural disasters, marine life, climate change, and many more others. The deployment of sensor nodes are performed in shallow or deep water in order to observe the changes and these nodes transmit the report of changes to the sink node or directly to a BS. Similar to WMSNs, there is a need of an efficient communication among underwater devices to make these applications feasible. UWSNs are facing several challenges like limited bandwidth, the delay due to propagation of signal under the water, the limited battery power, a high bit error rate. These kind of network has more probability of failure because of battery life of sensor nodes and high attenuation of signal communication [121].

UWSN can consist of three types of sensor node: static nodes, semi-static nodes and mobile nodes [122]. Static sensor nodes are anchored to the dock, buoys, or the bottom of the ocean. Semi-static sensor nodes are used for monitoring for a short duration; it may be hours or some days. These nodes are hanged with the buoys and placed by the ship temporarily. Static and semi- static deployment of sensor nodes are mainly energy constrained. Mobile sensor nodes are attached with vehicles like as autonomous underwater vehicles (AUVs), Remotely Operated Vehicles (ROVs), and other underwater vehicles. Mobile nature of sensor nodes helps in covering maximum area in underwater but it raises the problem of network connectivity and localization of nodes. The designing of the UWSNs has some major challenges such as limited bandwidth, impaired channel due to fading and multipath, high propagation delay, high bit error rate, and limited battery power; and sensors are prone of fouling and corrosion [123]. Some disadvantages of underwater communication are as follows [121]:

- When it is needed to buffer the data (before dropping the data) for a long duration, it requires more storage.
- The sink node regularly transmits an enquiry message, if it does not receive any message from other nodes or base station. The regular transmission of enquiry messages raise the problem of power consumption

Wireless Underground Sensor Networks (WUSNs)

Wireless Underground Sensor Networks (WUSN) is a special type of WSN where some of the nodes are deployed below ground, either in soil or in a similar confined environment. For instance, sensors deployed inside walls or in the basement of a building may be considered WUSNs. Two communication technologies for underground channel have been proposed: radio ElectroMagnetic waves radiation (EM) [124], [125], [126] and Magnetic Induction (MI) [127]. Although specific WUSN applications can take advantage of one or the other technology, we believe that the future of most WUSNs lies in the strategic integration of both because the drawback of one technology can be compensated by the characteristics of the other technology. A variety of novel applications are enabled by the use of WUSNs, initially categorized [128] as follows: environmental monitoring, infrastructure monitoring, location determination, and security monitoring.

1.3 Conclusion

In this chapter, we introduction the concept of WSNs for a better understanding. We describe the architecture of the WSN and the different components of a sensor node. Furthermore, the constraints related to their design are discussed and the different related routing approaches. Each WSN can be classified into data centric based, localisation based, group based or hierarchical based.

The WSNs have a wide range of applications, from home application, military tracking, people rescue, innovative medical use, ecological monitoring and precision agriculture. For this latter, the sensor nodes are buried so that the sensed data are is directly use for the good plant growth. These data can be either the content of water in soil for an intelligent watering system or either the nutriment needed by the plant for an efficient use of fertilizers. The localisation of the sensor nodes under the ground aims at protecting the devices from damage due to surface activities like ploughing of the soil. However, for this kind of WSN, additional study must be done since the communication channel becomes the ground and the link quality of EM waves depends on the soil properties.

Chapter 2

State of Art on Wireless Underground Sensor Networks

The WSN are widely used nowadays because of its large and varied amount of applications [121]. Furthermore, the recent researches conducted on the IoT field has led to a promising sub-domain called IOUT in which a kind of WSN with buried sensor nodes is widely used in application such as precision agriculture for an efficient used of water and fertilizers resources [129], [130]. The resulting network is mostly known as WUSN. In this chapter, a state of art of WUSN is presented. The architecture of a typical WUSN and the main challenges in the design of WUSNs are presented in Section 2.1. Due to denser propagation medium of the electromagnetic waves, the wireless signal is widely attenuate in the soil. In order to give a good understanding of this phenomena, a comparison study of the existing path loss models is presented in Section 2.2. The presented path loss model are classified into underground and mixing models according to the type of wireless underground communication they consider. The chapter ends with a short conclusion in Section 2.3.

2.1 Generalities on WUSN

In this section, the architecture of WUSNs is briefly presented. Furthermore the communication types that can appear in a WUSN are presented.

2.1.1 Architecture of WUSN

Architecture

Typical WUSNs consist of buried sensor nodes, which are connected to subsurface underground sensors or gateways. The underground communications are performed by using EM waves or MI [126], [127]. WUSNs are capable of operating in environments where no other computer network has functioned before, and has the potential to provide real-time, robust, and energy efficient sensing, and communication in these environments.

Buried sensor nodes collect data of their environment and send them through multihop communication until a buried or an above-ground gateway which plays the same role as sink node. According to the requirements, the data can either be collected by a mobile user located at the ground surface, or either available by an user through a local network (LAN) or the Internet. Thus, for WUSN, the data collected by buried sensor nodes should reach an final user or BS located at the ground surface. The architecture of a WUSN is resumed in Figure 2.1.

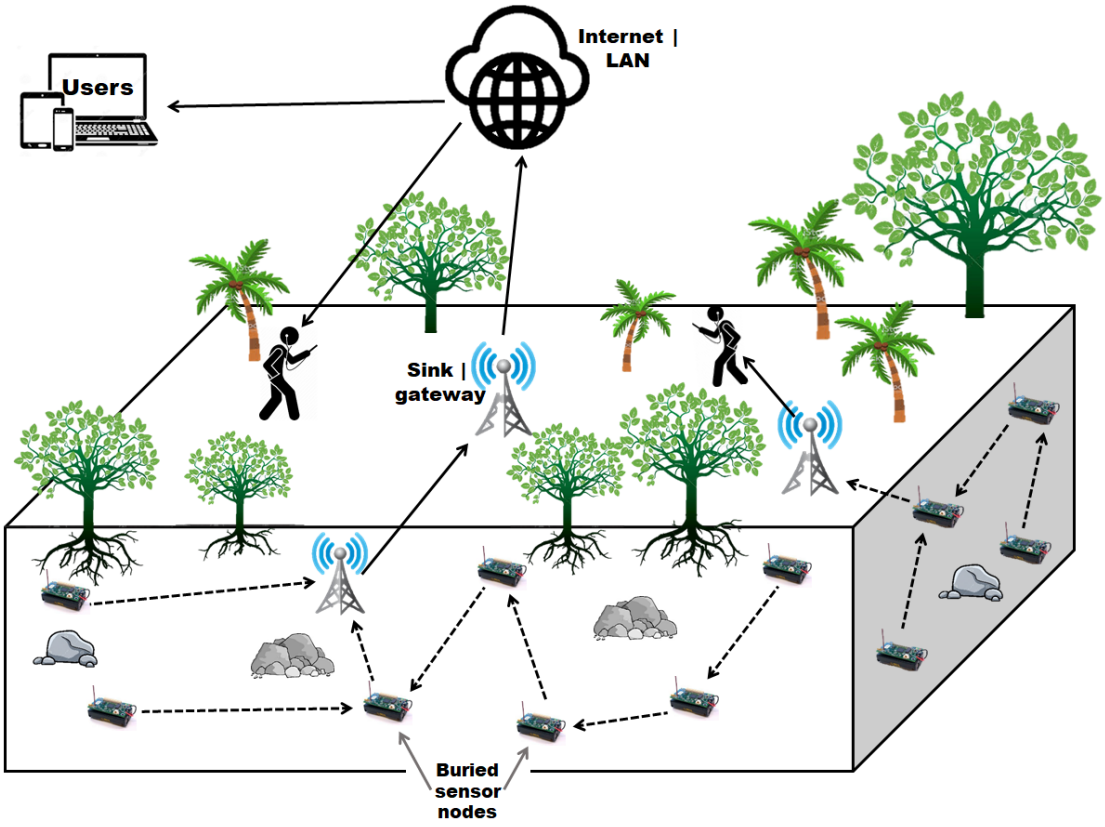

Figure 2.1: Architecture of a typical Wireless Underground Sensor Network.

Wireless Underground Communications

There are three main types of WUC [13]:

– Underground-to-Underground communication (UG2UG): here the two nodes are buried, the wave travels through the ground from a transmitter to a receiver. The soil is divided into two regions known as subsoil and topsoil. The topsoil considers the first 30cm depth; beyond 30cm, it is the subsoil region.

– Underground-to-Aboveground communication (UG2AG): in this case, a buried sensor node sends its collected data to another node or a BS located above the ground. The transmitter can either be located at the topsoil or the subsoil region according to the application. The wave crosses successively an underground and a free surface region.

– Aboveground-to-Underground communications (AG2UG): It is similar for UG2AG, but in this case, an above node (transmitter) or a BS sends data to another node buried in the soil. The buried node can be located either in the topsoil region or either in the subsoil region.

Figure 2.2 gives an overview of the different communications in WUSN.

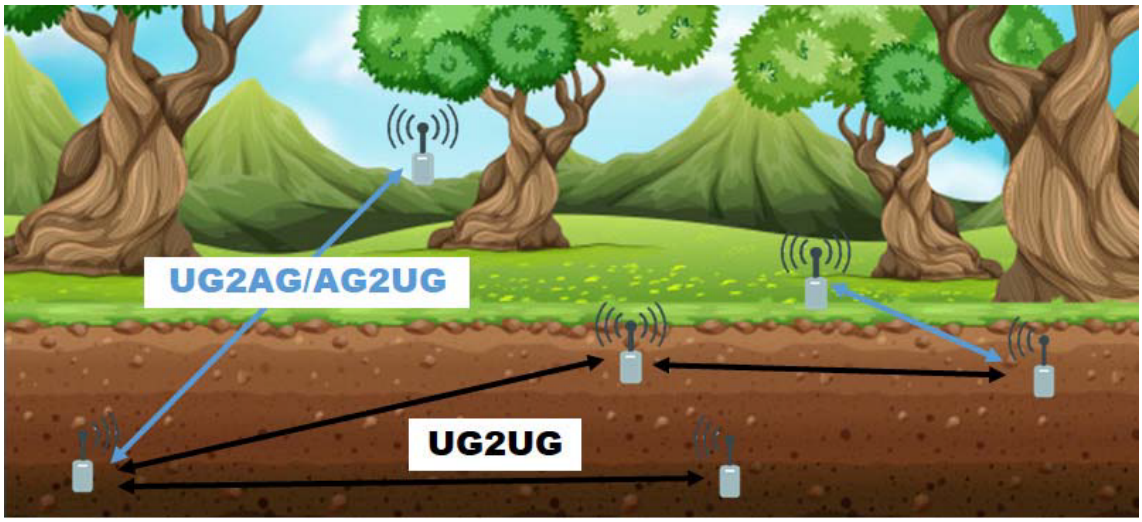

Figure 2.2: Types of wireless underground communications.

Electromagnetic waves in soil experience losses by absorption in soil and by diffusion attenuation due to soil permittivity, which is higher than that of air. Moreover, permittivity of soil changes with soil moisture, which causes changes in the wavelength. These changes in the wavelength impact the resonance of an underground antenna. Thus, designing a WUSN becomes more challenging than a basic WSN (TWSN) which uses the air as communication channel [131].

2.1.2 Design Challenges of WUSNs

WUSNs are an exciting and promising research area due to the nature of the underground environment in which sensors nodes are deployed. The use of underground channel led recent researches on the field to rethink terrestrial WSN paradigms. The design of a WUSN faces several challenges that can be resumed into: power conservation, topology design, antenna design, and environmental extremes [128].

Power conservation

Depending on the intended application, WUSN devices should have a lifetime of at least several years in order to make their deployment cost efficient. This challenge is complicated by the high wave attenuation in soil, which requires that WUSN devices have radios with greater transmission power than terrestrial WSN devices. As a result, power conservation is a primary concern in the design of WUSNs. Similar to terrestrial WSNs, the lifetime of WUSNs is limited by the self contained power source of each device. However, access to WUSN devices will be much more difficult than access to terrestrial WSN devices in most deployments, making retrieval of a device to recharge or replace its power supply less feasible. While recharging of devices deployed close to the surface may be possible with induction techniques, recharging deeper devices will be difficult, if not impossible. Deployment of new devices to replace failed ones is similarly difficult. Additionally, terrestrial WSN devices can be equipped with a solar cell [132], [133] to supplement or even replace a traditional power source, which is obviously not an option for WUSN devices. Scavenging opportunities for WUSN devices, such as converting seismic vibrations or thermal gradients to energy [134], [135] do exist, but it remains to be explored whether these methods can provide sufficient energy to operate a device in the absence of a traditional power supply.

Therefore, the Power conservation becomes a primary objective in the design of WUSNs. While it is possible to increase the lifetime of a device by providing it with a larger stored power source, this is not necessarily desirable since it will increase the cost and size of sensor devices, hence increase the cost deployment. Conservation can be achieved by utilizing power-efficient hardware and communication protocols

Topology design

The design of an appropriate topology for WUSNs is of critical importance to network reliability and power conservation. WUSN topologies will likely be significantly different from their terrestrial counterparts. For example, the location of a WUSN device will usually be carefully planned given the effort involved in the excavation necessary for deployment. Also three-

dimensional topologies will be common in WUSNs, with devices deployed at varying depths dictated by the sensing application. The integrated application of WUSNs will play an important role in dictating their topology, however, power usage minimization and deployment cost should also be considered in the design. A careful balance must be reached among these considerations to produce an optimal topology. Here, we provide concerns associated with each of these considerations as well as suggest new WUSN topologies.

- *Intended application*: Sensor devices must be located close to the phenomenon they are deployed to sense, which dictates the depth at which they are deployed. Some applications may require very dense deployments of sensors over a small physical area, while others may be interested in sensing phenomenon over a larger physical area but with less density. Security applications, for example, will require a dense deployment of underground pressure sensors, while soil monitoring applications may need fewer devices since differences in soil properties over very small distances may not be of interest.

- *Power usage minimization*: Intelligent topology design can help to conserve power in WUSNs. Since attenuation is proportional to the distance between a transmitter and receiver, power usage can be minimized by designing a topology with a large number of short distance hops rather than a smaller number of long-distance hops.

- *Cost*: Unlike terrestrial sensor devices, where deployment simply requires physically distributing devices, significant labor, and thus cost, is involved in the excavation necessary to deploy WUSNs. The deeper a sensor device is, the more excavation required to deploy it, and the greater the cost of deploying that device. Additional costs will be incurred when the power supply of each device has been exhausted and the device must be unearthed to replace or recharge it. Thus, when cost is a factor, deeper deployment of devices should be avoided if possible, and the number of devices should be minimized. Minimizing the deployment conflicts with the dense deployment strategy suggested by power considerations, and an appropriate trade-off must be established.

With the above considerations in mind, two possible topologies for WUSNs which should serve to address most underground sensing applications. These are the underground topology and the hybrid topology.

Underground topology : This consists of all sensor devices deployed underground (UG2UG), except for the sink, which may be deployed underground or aboveground as illustrated in Figure 2.2. Similar to terrestrial WSNs, the sink in a WUSN is the node at which all data from the sensor network is received. Underground topologies can be single depth, i.e., all sensor devices are at the same depth, or multi depth, i.e., the sensor devices are at varying depths. Both

communication protocols and sensor device hardware for multi depth networks require special consideration to ensure that data may be efficiently routed to a surface sink. The depth at which devices are deployed will depend upon the application of the network, e.g., pressure sensors must be placed close to the surface, while soil water sensors should be located deeper near the roots of the plants. This topology minimizes (or eliminates, in the case of an underground sink) the aboveground equipment, providing maximum concealment of the network. Devices deployed at a shallow depth may be able to make use of a ground air ground path for the channel, which should produce lower path losses than a ground to ground channel.

Hybrid Topology : This is composed of a mixture of underground and aboveground (UG2AG and AG2UG) sensor devices as shown in Figure 2.2. Since wireless signals are able to propagate through the air with lower loss than through soil, the aboveground sensor devices require a lower power output to transmit over a given distance than the underground sensor devices. A hybrid topology allows data to be routed out of the underground in fewer hops, thus trading power intensive underground hops for less expensive hops in a terrestrial network. Additionally, terrestrial devices are more accessible in the event that their power supply requires replacement or recharging. Thus, given a choice, power expenditures should be made by aboveground devices rather than underground devices. The disadvantage of a hybrid topology is that the network is not fully concealed as with a strictly underground topology.

A hybrid topology could also consist of underground sensors and a mobile terrestrial sink which moves around the surface of the underground network deployment area and collects data from the underground sensors or terrestrial relays. In the absence of terrestrial relays, deeper devices can route their data to the nearest shallow device (which is able to communicate with both underground and aboveground devices), which will store the data until a mobile sink is within range. This topology should promote energy savings in the network by reducing the number of hops to reach a sink, since effectively every shallow device can act as a sink. The drawback of this topology is the latency introduced by storing data until a mobile collector is within the range. Mobile sinks have already been used successfully for an aboveground WSN used for agricultural monitoring [136].

Antenna design

The selection of a suitable antenna for WUSN devices is another challenging problem. In particular, the challenges related to the antenna are:

- *Variable requirements*: Different devices may serve different communication purposes, and therefore may require antennas with differing characteristics. For example, devices deployed within several centimeters of the surface, may need special consideration due

to the reflection of EM radiation that will be experienced at the soil,Äìair interface. Additionally, near surface devices will likely act as relays between deeper devices and surface devices. Deeper devices acting as vertical relays to route data towards the surface may require antennas focused in both the horizontal and vertical directions.

- *Size*: Frequencies in the MHz or lower ranges will likely be necessary to achieve practical propagation distances of several meters. It is well known that the lower the frequency used, the larger antenna must be to efficiently transmit and receive at that frequency [3]. At a frequency of 100 MHz for example, a quarter-wavelength antenna would measure 0.75 m. Clearly this is a challenge for WUSNs since we desire to keep sensor devices small.

- *Directionality* ,Äì Future research must address whether an omnidirectional antenna or a group of independent directional antennas is most appropriate for a WUSN device. Communication with a single omnidirectional antenna will likely be challenging since WUSN topologies can consist of devices at varying depths, and common omnidirectional antennas experience nulls in their radiation patterns at each end. This implies that with a vertically oriented antenna, communication with devices above and below would be impaired [3]. This issue may be solved by equipping a device with antennas oriented for both horizontal and vertical communication.

Antenna design considerations will also vary depending on the physical layer technology that is utilized. The technologies mostly used are EM and MI [137], [127], [138], however it remains to final to select the appropriate technology according to the application requirements.

Environmental extremes

The underground environment is far from an ideal location for electronic devices. Water, temperature extremes, animals, insects, and excavation equipment all represent threats to a WUSN device, and it must be provided with adequate protection. Processors, radios, power supplies, and other components must be resilient to these factors. Addition- ally, the physical size of the WUSN device should be kept small, as the expense and time required for excavation increase for larger devices. Battery technology must be chosen carefully to be appropriate for the temperatures of the deployment environment while balancing environmental considerations with physical size and capacity concerns. Devices will also be subjected to pressure from people or objects moving overhead or, for deeply deployed devices, the inherent pressure of the soil above. The same environmental factors that make the underground a challenging environment for hardware also create extreme underground wireless channel conditions different from free space wireless channel.

2.2 Path Loss Models for WUSN

The characteristics of the wireless underground channel are much different as compared to the conventional free space wireless communication channel. These differences are caused by the wave propagation mechanism in the underground channel. EM waves interact with the soil medium exhibit distinct characteristics, and experience higher attenuation. Physical properties of the soil texture, soil moisture, soil temperature, and bulk density impact underground wave propagation. These interactions introduce channel impairments, which varies with space and time. In this section, we present path loss model designed for predicting the EM loss in the soil. We classified path loss models into two group: underground path loss models which are designed for fulled underground communication; Mixing path loss models which aim at predicting the wave attenuation for communications between the surface and the ground (UG2AG and AG2UG).

2.2.1 Underground Path Loss Models

Complex Refractive Index Model-Fresnel

The semi-empirical model proposed in [16] is a combination of the Complex Refractive Index Model (CRIM) [139] and Fresnel equations [140]. The proposed model assumes that the transmitter radiates equally in all directions. Furthermore, the authors highlight the path loss due to spherical divergence and the additional path losses caused by signal attenuation, reflection, refraction and diffraction. However, the signal attenuation in soils depends on the soil attenuation constant (2.1).

$$\alpha = 8.68 \frac{60\pi(2\pi f \epsilon_0 \epsilon^{''} + \sigma_b)}{\sqrt{\frac{\epsilon^{'}}{2}\left\{1 + \sqrt{1 + [\left(\epsilon^{''} + \frac{\sigma_b}{2\pi f \epsilon_0}\right))/\epsilon^{'}]^2}\right\}}} \tag{2.1}$$

f is the frequency in Hertz, $\epsilon_0 = 8.85 * 10^{-12} F.m^{-1}$ is the dielectric permittivity in free space, σ_b is the bulk density, $\epsilon^{'}$ and $\epsilon^{''}$ the real (Dielectric Constant DC) and imaginary (Loss Factor LF) parts of the mixing model respectively. The CRIM is used to find the complex dielectric permittivity of the soil based on the permittivity of solid, the complex permittivity of water and the permittivity of the air. However, authors assume that the water is the unique element responsible for the dielectric losses, thus the air and solid permittivity do not depend on the operating frequency.

In addition to the signal attenuation in the soil, the CRIM-Fresnel model considers the loss due to the wave reflection. It uses the Fresnel equation to calculate the reflection coefficient R.

The proposed model neglects the effect of the magnetic permeability, therefore, R is simplified by (2.2). The total signal attenuation Atot proposed by CRIM-Fresnel depends on the signal attenuation due to reflection R_c, the soil attenuation and the distance d between the transmitter and the receiver.

$$R = \left(\frac{1-\sqrt{\epsilon}}{1+\sqrt{\epsilon}}\right)^2 \tag{2.2}$$

$$A_{tot} = \alpha d + R_c \tag{2.3}$$

$$R_c = 10log\left(\frac{2R}{1+R}\right) \tag{2.4}$$

Meanwhile, the semi-empirical CRIM-Fresnel is not an accurate model because of the very limited type of soil used (sieved sand) that can be different from natural soil. The results of the comparisons presented in [16] are very different from the real experimentations.

Modified Friis Model

The Modified Friis or the Conventional Modified Friis is a path loss model based on Friis transmission equation initially designed for Free Space communication [15]. However, the Modified Friis model proposed in [14] takes into account the path loss due to wave attenuation in soil $L_s = L_{s1} + L_{s2}$. L_{s1} (2.5) denotes the attenuation loss due to the difference of the wavelength of the signal in soil and the wavelength of the signal in air. L_{s2} (2.6) represents the transmission loss caused by attenuation. Total attenuation L_{tot} considers the attenuation in free space [15] and the wave attenuation in soil L_s.

$$L_{s1}(dB) = 154 - 20log(f(Hz)) + 20log(\beta) \tag{2.5}$$

$$L_{s2}(dB) = 8.69\alpha d \tag{2.6}$$

The computed path loss L_{tot} (in dB) by the Modified Friis is simplified in Equation (2.7) below. The values α (1/m) and β (radian/m) depend on soil conditions. They are the attenuation due to material absorption and the phase shifting respectively.

$$L_{tot} = 6.4 + 20log(d) + 20log\,(\beta) + 8.69\alpha d \tag{2.7}$$

The constants α (2.8) and β (2.9) are the key elements of the Conventional Modified Friis path loss model and constitute the real and the imaginary parts of the complex propagation

constant γ.

$$\alpha = 2\pi f \sqrt{\frac{\mu_0 \mu_r \epsilon_0 \epsilon'}{2} \left(\sqrt{1 + \left(\frac{\epsilon''}{\epsilon'} \right)^2} - 1 \right)} \tag{2.8}$$

$$\beta = 2\pi f \sqrt{\frac{\mu_0 \mu_r \epsilon_0 \epsilon'}{2} \left(\sqrt{1 + \left(\frac{\epsilon''}{\epsilon'} \right)^2} + 1 \right)} \tag{2.9}$$

The permeability in vacuum μ_0 and the permittivity in free space ϵ_0 are related to the light velocity in vacuum by $\epsilon_0 \mu_0 c^2 = 1$. Moreover, most the soils are do not contain metal elements, the magnetic permeability is neglected ($\mu_r = 1$). The CDC is related on the semi-empirical mixing dielectric model proposed by Peplinski that uses the Debye relaxation spectrum of free water located out of the soil [17], [18].

NC Modified Friis

Chaamwe et *al.* [141] proposed a semi-empirical model merging the Conventional Modified Friis approach and that of CRIM-Fresnel. The model combined the reflection due to wave attenuation proposed in CRIM-Fresnel (2.4) and the Modified Friis model (2.7). Moreover, the authors consider the signal attenuation due to wave refraction by adding the attenuating factor K (2.10) of the angular defocussing.

$$K(dB) = 20log \left(\sqrt{\frac{\epsilon_1 \cos(\theta_1)}{\epsilon_2 \cos(\theta_2)}} \right) \tag{2.10}$$

θ_1 and θ_2 are the incoming and outgoing wave angle respectively, ϵ_1 and ϵ_1 denote the wave dielectric constant of the source and the destination environment respectively. The total path loss proposed in [141] is resumed in (2.11).

$$L_{tot}(dB) = 6.4 + 20log \left(d\beta K \sqrt{\frac{2R}{1+R}} \right) + 8.68\alpha d \tag{2.11}$$

The authors claim that their path loss model integrates better characteristics responsible for the signal attenuation than the Conventional Modified Friis and the CRIM-Fresnel models. Meanwhile, the path loss model presented in [141] also needs a laboratory analysis of a soil sample like the Conventional Modified Friis and the CRIM-Fresnel models. This analysis aims at finding the values of DC (ϵ') and the LF (ϵ'') of the soil also based on the Peplinski derivations like the Conventional Modified Friis. Moreover, in practice, the wave attenuation due to refraction occurs when the signal travels near the ground surface and most of the time is

neglected for topsoil region communications.

TDR Modified Friis

Sadeghioon et *al.* [142] proposed an *in situ* path loss prediction model by using measurements of the Time Domain Reflectometry (TDR). The TDR method is used to find the CDC values. This *in situ* method estimates the effective wave frequency of the TDR in soil that holds the most amount of the energy and thereafter gives accurate values of the dielectric permittivity. Moreover, in order to evaluate the path loss, this approach uses the output of the TDR measurements (real and imaginary parts of the CDC) as inputs in the Conventional Modified Friis model in (2.7). Experiments reveal that the proposed *in situ* path loss model of [13] is more accurate than the Conventional Modified Friis in 02 soil types (B and K of Table 2.1) and 03 configurations. In order to evaluate the TDR Modified Friis, the authors compared their approach to Conventional Modified Friis and to real measurements on the 03 configurations. The results have shown that the value of the root means squared error in the TDR Modified Friis is smaller than in the CRIM-Fresnel and the Conventional Modified Friis. The proposed model is assumed to more the more accurate than the existing path loss models. However, despite the slight increase in accuracy of the proposed model, the use of TDR equipment is very expensive and its deployment within a network is a costly problem.

Table 2.1: Characteristics of soil samples.

SOIL TYPES		**PROPORTIONS IN %**		
Ref.	**Name**	**Sand**	**Clay**	**Silt**
B	Sand(white)	98	0	2
D	Silty sand	88	4	8
F	Clay(gray)	1	51	48
K	Clayey silt	4	7	89

However, like the CRIM-Fresnel, this model needs to analyse a sample of soil in a laboratory so that to find the empirical values needed by the model. Thus, for a larger experimental field, soil conditions can be different, then, a sample of soil is not sufficient for an accurate path loss prediction. An example of some soil types widely used and their characteristics are presented in Table 2.1 [143].

2.2.2 Mixing Path Loss Models

ZS Free Space Modified Friis based model

Most of the mixing path losses in WUC adds to the free space path loss, the loss due to underground communication. Sun et *al.* [144] propose a path loss model for UG2AG and AG2UG communications. To achieve it, authors add to Free Space and to the Conventional Modified Friis models, the loss due to Soil-Air and Air-Soil refraction for UG2AG and AG2UG communications respectively. The resulting path losses are given in (2.12) and (2.13). Where θ is the incidence angle of the wave, $\epsilon^{'}$ is the dielectric constant, L_{ug} and L_{ag} are the Conventional Modified Friis (2.7) and the free space [15] path losses respectively.

$$L_{UG2AG} = L_{ug} + L_{ag} + 10log\left(\frac{\left(\sqrt{\epsilon^{'}}+1\right)^{2}}{4\sqrt{\epsilon^{'}}}\right) \tag{2.12}$$

$$L_{AUG2UG} = L_{ug} + L_{ag} + 10log\left(\frac{\left(cos\theta\sqrt{\epsilon^{'}-sin^{2}\theta}\right)^{2}}{4cos\theta\sqrt{\epsilon^{'}-sin^{2}\theta}}\right) \tag{2.13}$$

Similar to the Conventional Modified Friis and the NC Modified Friis, the model proposed by Sun et *al.* [144] does not consider the wave phenomena that can occur at different burial depth such as the loss due to wave reflection. However, the added refraction loss neglects the effect of the loss factor $\epsilon^{''}$ of the wave in soil and in practice, the incidence angle cannot be easily obtained in real *in-situ* application.

XD Free Space Modified Friis based model

Another mixing model for prediction of signal loss in UG2AG/AG2UG communications is proposed by Dong et *al.* [55]. Their approach is quite similar to the one proposed by Sun et *al.* [144], however, for UG2AG, the authors neglect the loss due to the wave refraction. This is because the signal travels perpendicularly from a higher density medium (soil) to a lower density one (air). Furthermore, for AG2UG communication, the loss due to refraction L_r depends on the refractive index of the soil n (2.14). In order to give an approximate value, Dong et al. assume that the signal incidence angle is zero degree, thus, the maximum power path taken by the signal. $\epsilon^{'}$ and $\epsilon^{''}$ are the dielectric constant and the loss factor respectively. The resulting path losses for UG2AG and AG2UG communications are resumed in (2.15) and (2.16).

$$L_r = 20log\left(\frac{n+1}{4}\right); n = \sqrt{\frac{\sqrt{(\epsilon^{'})^{2}+(\epsilon^{''})^{2}}+\epsilon^{'}}{2}} \tag{2.14}$$

$$L_{UG2AG} = L_{ug} + L_{ag} \tag{2.15}$$

$$L_{AUG2UG} = L_{ug} + L_{ag} + L_r \tag{2.16}$$

The overall path loss models are resumed in Table 2.2 in terms of the communication types, the CDC prediction approach and the input parameters. We observe that, the underground path loss models used either the Peplinski or either CRIM derivations in order to evaluate the CDC. However, the both approaches are similar in that sense they considered the same inputs (volumetric water content, the bulk density, particle size, wave frequency; clay and sand proportions) since they are based on the Debye relaxation spectrum of free water. Contrary to the Conventional Modified Friis, the CRIM-Fresnel and the NC Modified Friis consider additional losses due to wave reflection and the EM wave refraction in soil. Similar to existing underground path loss models, the mixing path loss models are based on Peplinski equations for the CDC prediction, thus the same inputs parameters are required for the path loss prediction. However, the mixing models only consider addition loss due to reflection phenomena of the EM wave and neglect the attenuation due to refraction in soil.

Table 2.2: Comparison of the path loss approaches.

Models	**Communication types**	**CDC**	**Inputs parameters**	**Additional losses**
Conventional Modified Friis	UG2UG	Peplinski	V, bulk density, particle size, wave frequency, clay and sand proportions.	-
CRIM-Fresnel	UG2UG	CRIM	V, bulk density, particle size, wave frequency, clay and sand proportions.	Reflection
NC Modified Friis	UG2UG	Peplinski	V, bulk density, particle size, wave frequency, clay and sand proportions.	Reflection + Refraction
TDR Modified Friis	UG2UG	TDR device	V, bulk density, particle size, wave frequency, clay and sand proportions.	-
ZS model	UG2AG/AG2UG	Peplinski	V, bulk density, particle size, wave frequency, clay and sand proportions.	Reflection
XD model	UG2AG/AG2UG	Peplinski	V, bulk density, particle size, wave frequency, clay and sand proportions.	Reflection

2.3 Conclusion

In this chapter, we described a typical architecture of a WUSN. Due to their deployment area, the WUSN faces additional challenges such as power consumption, antenna design and environmental extremes. These challenges are due to the communication channel that becomes the soil and widely affects the communications between nodes. In order to analyze the signal attenuation in soil, existing path loss models are presented and compared according to their input parameters or the additional losses they consider.

Wireless communications is the key challenge in WUSN since the soil properties must change along time, thus, they will directly affect the attenuation of EM waves in the ground. In order to analyze this loss,design a path loss model for wireless underground communications becomes a necessity before any deployment. This is because path loss model helps at predicting the RSSI received by a node according to the soil conditions. However, for an efficient use, the designed path loss model must be accurate as possible and should take into account the application requirements.

Chapter 3

A New Approach of Path Loss Prediction for Wireless Underground Sensor Networks

Despite the wide interest in WUSN applications, the location of sensor nodes becomes a relevant challenge because the soil widely affects the propagation of EM waves [145]. Thus, before the exploitation of a WUSN, a study on the signal attenuation of wireless underground communications is a necessity. To address this issue, an accurate path loss model for predicting the signal loss according to soil properties should be designed [14], [137], [146]. In this chapter, we propose a new accurate approach for path loss prediction in WUSN application. After stating the problem of the path loss models, we design the steps for the CDC prediction and for the path loss computation. the proposed approach focused on the accuracy of the CDC in order to increase the accuracy of a path loss model. For that, the more accurate model called MBSDM is used Instead of the widely used Peplinski derivations. Section 3.1 state the problem; the proposed approach is presented in Section 3.2; real experiment and sensor nodes are considered during the evaluation process of the proposed approach in Section 3.3; The chapter ends with a short conclusion and limitations of the presented approach in Section 3.4.

3.1 Problem Statement

Path loss models are widely used for predicting attenuation on WUSN, however their accuracy depends on the accuracy of the CDC which is directly related to the soil conditions [10], [142], [147], [148]. The key issue on path loss predictions is the difficulty of providing an accurate CDC without real *in situ* measurements.

3.2 New Approach for Path Loss Prediction

In this Section, we present the new approach for path loss prediction in wireless underground sensor networks.

3.2.1 Complex Dielectric Constant

The famous and useful CDC prediction model has been proposed by Peplinski et *al.* in [17], [18]. This model is based on the Debye′s relaxation spectrum of liquid water located out of the soil which is considered as a mixing of dry soil, air and water. The Peplinski model considers only the presence of free water inside the soil, however, as it is said by Topp et *al.* [19], bound water seems to dominate over free water. In order to predict with more accuracy the path loss, we consider a CDC prediction that takes into account free and bound water within moist soil. The models used is the Mineralogy-Based Soil Dielectric Model (MBSDM) [20]. It considers as input the wave frequency, the clay portion and the soil moisture (Volumetric Water Content V). This model can operate on frequency range between 45MHz and 26.5GHz. Furthermore, since the 433MHz operating frequency is widely used in WUSN field, we will consider this value in the rest of our tests. The real and the imaginary parts of the CDC (3.1) are derived from the Refractive Index n (3.2) and the Normalized Attenuation Coefficient k (3.3).

$$\epsilon^{'} = n^2 - k^2; \qquad \epsilon^{''} = 2nk \tag{3.1}$$

$$n = \begin{cases} n_d + (n_b - 1)V, \ if \ V < V_m \\ n_d + (n_b - 1)V_m + (n_f - 1)(V - V_m), \ else \end{cases} \tag{3.2}$$

$$k = \begin{cases} k_d + (k_b)V, \ if \ V < V_m \\ k_d + (k_b)V_m + (k_f)(V - V_m), \ else \end{cases} \tag{3.3}$$

$n_{d,b,f}$ (3.4) is the Refractive Index (RI) of dry soil, bound and free water respectively; $k_{d,b,f}$ (3.5) denote the Normalized Attenuation Coefficient (NAC) of dry soil, bound and free water respectively.

$$n_{b,f}\sqrt{2} = \sqrt{\sqrt{(\epsilon^{'}_{b,f})^2 + (\epsilon^{''}_{b,f})^2} + \epsilon^{'}_{b,f}} \tag{3.4}$$

$$k_{b,f}\sqrt{2} = \sqrt{\sqrt{(\epsilon^{'}_{b,f})^2 + (\epsilon^{''}_{b,f})^2} - \epsilon^{'}_{b,f}} \tag{3.5}$$

$$\begin{aligned} \epsilon'_{b,f} &= \epsilon_\infty + \frac{\epsilon_{0b,0f} - \epsilon_\infty}{1+(2\pi f \tau_{b,f})^2} \\ \epsilon''_{b,f} &= \frac{\epsilon_{0b,0f} - \epsilon_\infty}{1+(2\pi f \tau_{b,f})^2} 2\pi f \tau_{b,f} + \frac{\sigma_{b,f}}{2\pi f \epsilon_0} \end{aligned} \tag{3.6}$$

ϵ_d, ϵ_b and ϵ_f are complex dielectric values of dry soil, bound and free water respectively. The computation of their real and imaginary parts are given in (3.6). V_m is the maximum bound water fraction used to distinguish the two moisture regions (bound and free water). $\epsilon_\infty = 4.9$ is the dielectric constant in the high frequency limit; $\epsilon_{0b}, \epsilon_{0f}$ is the low frequency limit of the dielectric constant of bound and free water; τ_b and τ_f are the relaxation time of bound and free water; σ_b and σ_f denote the conductivity of bound and free water. The values of $n_d, k_d, V_m, \sigma_{b,f}, \tau_b$ and ϵ_{0b} are derived in function of the clay portion C (Eqs. 3.7 - 3.13). The low frequency limit of the dielectric constant and the relaxation time of free water are respectively $\epsilon_{0f} = 100$ and $\tau_f = 8.5 * 10^{-12}$.

$$n_d = 1.634 - 0.539 * 10^{-2}C + 0.2748 * 10^{-4}C^2 \tag{3.7}$$

$$k_d = 0.03952 - 0.04038 * 10^{-2}C \tag{3.8}$$

$$V_m = 0.02863 + 0.30673 * 10^{-2}C \tag{3.9}$$

$$\epsilon_{0b} = 79.8 - 85.4 * 10^{-2}C + 32.7 * 10^{-4}C^2 \tag{3.10}$$

$$\tau_b = 1.062 * 10^{-11} + 3.450 * 10^{-12} * 10^{-2}C \tag{3.11}$$

$$\sigma_b = 0.3112 + 0.467 * 10^{-2}C \tag{3.12}$$

$$\sigma_f = 0.3631 + 1.217 * 10^{-2}C \tag{3.13}$$

The computation of the CDC in the proposed approach for the path loss is resumed in Figure 3.1. Contrary the Peplinski and CRIM derivations, the MBSDM needs only 03 inputs parameters: the wave frequency (f), the clay portion in soil (C) and the volumetric water content V. The MBSDM has the lower amount of input parameters because it is based on a larger sample of soil types and a larger range on wave frequency. As output of MBSDM, the real (DC) and the imaginary part (LF) are computed.

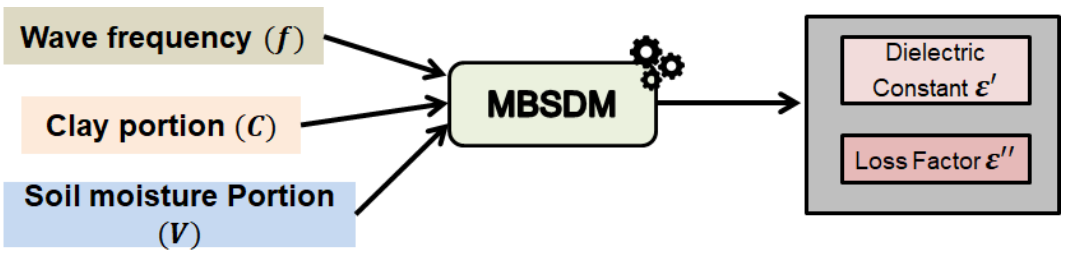

Figure 3.1: Computation of CDC based on MBSDM.

Another derivation of the MBSDM, is the Temperature and Mineralogy Dependable Soil

Dielectric Model (TMDM) proposed by Mironov et *al.* [149]. It considers the current temperature as input for predicting the mixing complex dielectric constant.

3.2.2 Path Loss Computation

Similar to TDR Modified Friis, we focus on the better way to predict the DC and the LF, thus, increase the accuracy of the Conventional Modified Friis (2.7). To calculate the values of α (2.8) and β (2.9), the real and imaginary parts of the CDC ($\epsilon^{'}$ and $\epsilon^{''}$ respectively) are computed according to the MBSDM equations (Eqs. 3.1 to 3.13). Thus, for evaluate the path loss, we need as inputs the soil moisture V, the clay portion C, the distance d between nodes and the operating frequency f. Figure 3.2 gives the overall architecture of the proposed approach for the path loss prediction in WUSN.

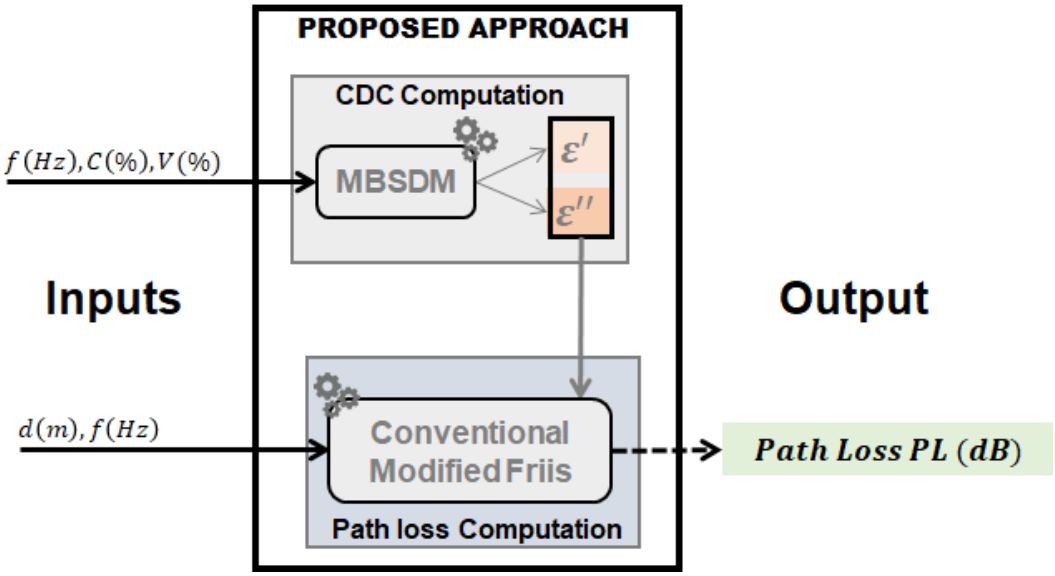

Figure 3.2: Architecture of the proposed scheme for path loss prediction.

3.3 Experimentations and Validation

In this section, we firstly compare the CDC predictions models to the TDR measurements done in [142]. Secondly, we evaluate our path loss model in real experimental field. We thereafter conduct additional tests and comparisons in order to validate our model.

3.3.1 Validation of the CDC Prediction

For our experimentations, we compare the MBSDM prediction with TDR data (Table 3.1) since the authors claim that it accurately predicts *in situ* the real and the imaginary part of the CDC.

For the prediction of the CDC, the wave frequency used is 433MHz and the temperature of experimentations is assumed to be 20°C like in [14] and [20]. The parameters used for the tests are presented in Table 3.1. Soils K and B are the same used for validation in [14]. Table 2.1 gives the corresponding sand and clay portions. The DC predictions of TMDM and MBSDM in Figure 3.3 are slightly identical because they have the both based on the Generalized Refractive Mixing Dielectric Model (GRMDM) [150]. Figure 3.3 gives the DC and LF predictions by using the Peplinski, TMDM and MBSDM of CDC predictions for soil K with 41.72% moisture. In this configuration, the TDR measurements of the DC and LF are 27.42 and 5.93 respectively. We observe that, the prediction of the DC in MBSDM and TMDM is closest to the measured values by the TDR. However, the LF prediction in MBSDM seems to be closer to real measurement. In Figure 3.3b, the soil B is used with 12.97% and 17.02% moistures. Similar to Figure 3.3a, the MBSDM and TMDM predictions are more accurate than Peplinski. However, the LF is more accurate in MBSDM than in TMDM and in Peplinski predictions.

The efficiency of the MBSDM over Peplinski can be explained by fact that it was derived from a larger set of soils than Peplinski derivations. Moreover, MBSDM considers both bound and free water within moist soil, contrary to Peplinski which only considers the presence of free water inside the soil. Moreover, the MBSDM seems to be more accurate than Peplinski due to the soil samples used for its derivation (more than 15 different soils).

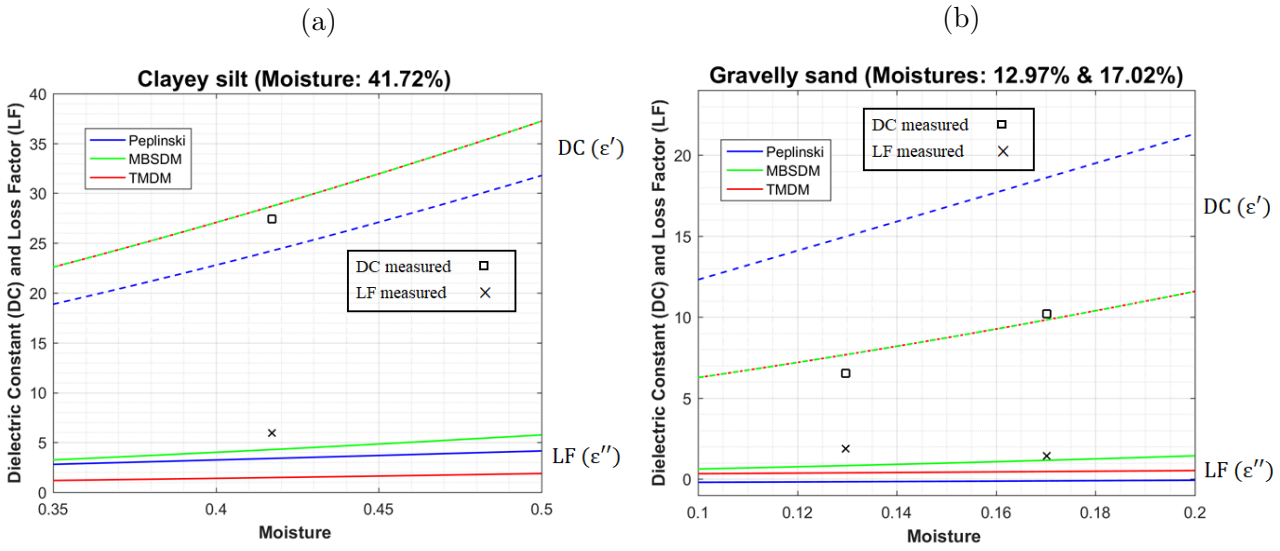

Figure 3.3: Evaluation of predicted and measured (TDR) values of DC and LF in K soil type (a) and in B soil type (b) at the 20°C temperature.

3.3.2 Experimental Field and Sensor Nodes

We have conducted our experimentations at the botanic garden of the University Cheikh Anta Diop in Senegal [151]. The soil is sandy clay type with a predominance of sand on the surface

Table 3.1: Soil Types and Parameters.

SOIL DETAILS			CDC MEASUREMENTS	
Ref.	**Name**	**Moisture**	**DC**	**LF**
#A	Gravelly sand	12.97%	6.53	1.88
#B	Gravelly sand	17.02%	10.21	1.42
#C	Clayey silt	41.72%	27.42	5.93

and the clay portion increases with the depth. For our tests, we fix the burial depth to 40cm, the field details are reported in Table 3.2.

Table 3.2: Features of the experimental Field [1], [2].

Name	**Sand(%)**	**Clay(%)**
Sandy clay#1	82.9	7.6
Sandy clay#2	95.3	3.3

Two nodes are used during our test: a transmitter and a receiver. Both nodes are based on Arduino UNO board and the wireless underground communications are performed by SX1278 LoRa transceiver at the 433MHz frequency (Figure 3.4). The transmitter senses physical values (soil, moisture, temperature) and sent them to the receiver through the SX1278 transceiver. The value of the soil moisture is given by YL-69 soil moisture at both the transmitter and receiver nodes. The received data are stored on receivers EEPROM. The transmitted power is fixed to $17dBm$ and the SX1278 antennas (transmitter and receiver) are $10cm$ height with a gain of $2.5dB$.

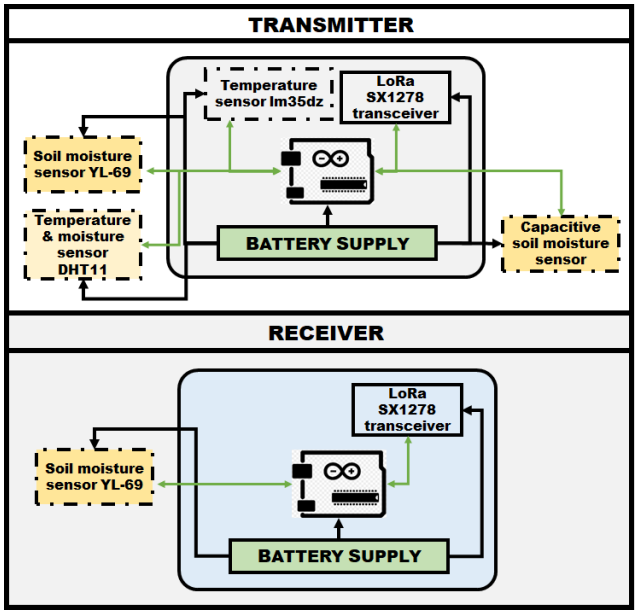

Figure 3.4: Transmitter and Receiver Nodes Based on Arduino UNO Boards.

3.3.3 Discussions and validation

We validate our model by analyzing the received power $P_r(dBm)$. In order to achieve it, we compare the RSSI received by the receiver and the receiver power given by the link budget (3.14). $PL(dB)$ is the total signal attenuation and is computed according to section 3; $P_t(dBm)$ is the output signal strength; G_r and G_t are the receiver and transmitter antenna gain respectively.

$$P_r = P_t + G_t + G_r - PL \tag{3.14}$$

The average soil moisture measured was around 20% over the 18 measurements done during our tests (Figure 3.5). The comparison of the received power in Sandy clay#1 with 20% moisture is resumed in Figure 3.5a. We observe that the received signal decreases with the distance. Moreover, the power received of the Conventional Modified Friis path loss and the NC Modified Friis looks more or less the same in function of the distance traveled by the EM wave. This is because NC Modified Friis improve the Conventional Modified Friis by adding a constant that defines the attenuation due to reflection (2.11). However, the Conventional Modified Friis is designed for topsoil region (more than 30cm depth) and assumes that in such region, the wave attenuation due to refraction on the NC Modified Friis are therefore neglected [141].

(a) (b)

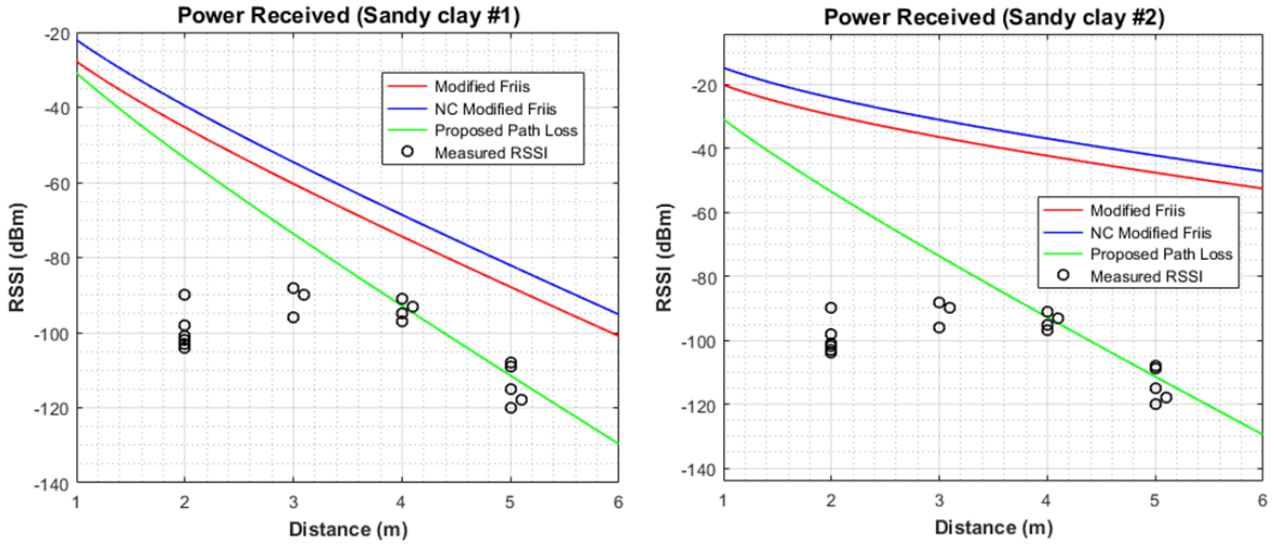

Figure 3.5: Received Power in Sandy Clay#1 (a) and Sandy Clay#2 (b) with 20% Mean Soil Moisture.

From Figure 3.5b, the conventional and the NC Modified Friis are far from real measurements. Moreover, our proposed approach seems to be more accurate than the other solutions. To validate our proposed model, we used the gap indicators: the Root Mean Square Error (RMSE), the Mean Absolute Error (MAE) and the Mean Absolute Percentage Error (MAPE) (3.15). For

a total of n measurements, p_i and o_i denote respectively the predicted and the observed values for the measurement i.

$$\begin{aligned} RMSE &= \sqrt{\frac{1}{n}\sum_{i=1}^{n}(p_i - o_i)^2} \\ MAE &= \frac{1}{n}\sum_{i=1}^{n}|p_i - o_i| \\ MAPE(\%) &= \frac{100}{n}\sum_{i=1}^{n}\left|\frac{p_i - o_i}{o_i}\right| \end{aligned} \tag{3.15}$$

In Table 3.3, we observe that our proposed approach has less RMSE (27.85, 27.87), MAE (20.02, 20.04) and MAPE (19.09, 19.14) in both sandy clay#1 and sandy clay#2. These values indicate that our approach is more accurate than the other existing path losses. Furthermore, The NC Modified Friis has the highest RMSE (43.09, 68.36), MAE (40.43, 67.79) and MAPE (40.25, 67.14) meaning that it is the less accurate model in each soil type.

Table 3.3: RMSE, MAE and MAPE Evaluation at 20% Soil Moisture.

PL Models	**Sandy clay #1**			**Sandy clay #2**		
	RMSE	MAE	MAPE	RMSE	MAE	MAPE
Conv. Modified Friis	37.73	34.66	34.49	63.01	62.40	61.75
NC. Modified Friis	43.09	40.43	40.25	68.36	67.79	67.14
Proposed approach	27.85	20.02	19.09	27.87	20.04	19.14

However, the soil moisture sensor YL-69 used during our experimentations is a cheaper sensor device. The study conducted by Zaman et *al.* [152] shows that this sensor is not very accurate compared to a professional sensor as the 5TM Decagon more expensive. Thus, we analyzed the accuracy of our model by considering the margin of $\pm 3\%$ for V compared to the 20% average measured moisture. In other words, we assumed that the real value of the soil moisture V is between 17% and 23%. Thus, the received power with 17% and 23% moistures are presented and compared in Figures 3.6 and 3.7 respectively.

Figure 3.6a gives the signal strength gets by the receiver node in sandy clay#1 with a moisture of 17% (-3% sensor inaccuracy). On sandy clay#2 (Figure 3.6b), Conventional and NC Modified Friis are too far for the real measurements. Meanwhile, The Conventional Modified Friis has a lower RMSE, MAE and MAPE than the NC Modified Friis. Nevertheless, the proposed approach is more close to real measurements than the other path loss approaches. Our proposed approach is then more accurate, thus, having the lowest RMSE (32.33, 32.35), MAE (26.74, 26.77) and MAPE (26.75, 26.78) regardless the type of sandy clay soil (Table 3.4). The received power comparison of path loss models at 23% moisture for sandy clay#1 and sandy clay#2 is shown in Figure 3.7aa and Figure 3.7b respectively. From these figures, our solution seems to be closer to the real measurements than the existing approaches despite

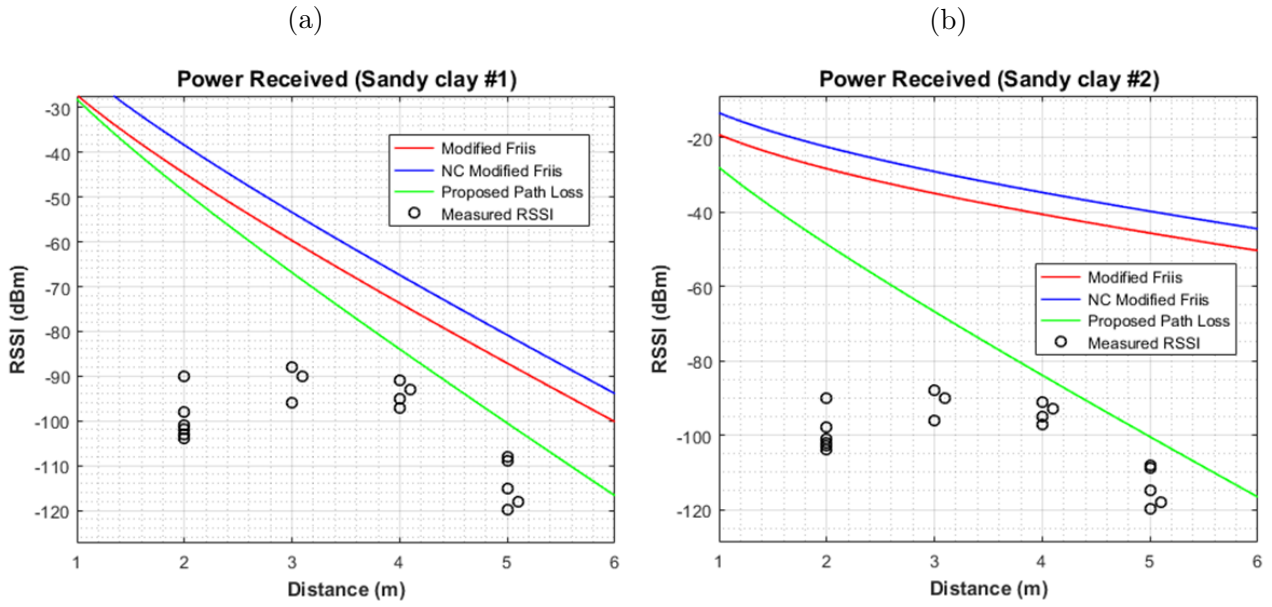

Figure 3.6: Received Power in Sandy Clay#1 (a) and Sandy Clay#2 (b) with 17% Mean Soil Moisture.

Table 3.4: RMSE, MAE and MAPE Evaluation at 17% Soil Moisture.

PL Models	**Sandy clay #1**			**Sandy clay #2**		
	RMSE	MAE	MAPE	RMSE	MAE	MAPE
Conv. Modified Friis	38.35	35.34	35.17	64.43	63.84	63.18
NC. Modified Friis	55.25	47.73	48.23	70.24	69.71	69.04
Proposed approach	32.33	26.74	26.75	32.35	26.77	26.78

the +3% inaccuracy of the soil moisture sensor (23% soil moisture). Thus, the accuracy of our model is shown by RMSE $\approx$ 25.3, MAE $\approx$ 19.7 and MAPE $\approx$ 11.5 either for sandy clay#1 or sandy clay#2 (Table 3.4).

Table 3.5: RMSE, MAE and MAPE Evaluation at 23% Soil Moisture.

PL Models	**Sandy clay #1**			**Sandy clay #2**		
	RMSE	MAE	MAPE	RMSE	MAE	MAPE
Conv. Modified Friis	37.14	34.00	33.84	61.69	61.06	60.43
NC. Modified Friis	32.74	31.38	31.01	66.66	66.07	65.44
Proposed approach	25.33	19.74	11.49	25.34	19.71	11.56

In definitive, despite the inaccuracy of low cost soil moisture sensor (YL-69), we propose here, a path loss approach that is more accurate than the existing path loss models with a maximum absolute percentage error less than 26.8% of the received power. The maximum RMSE and MAE observed by considering a $\pm$3% inaccuracy of the cheap soil moisture sensor

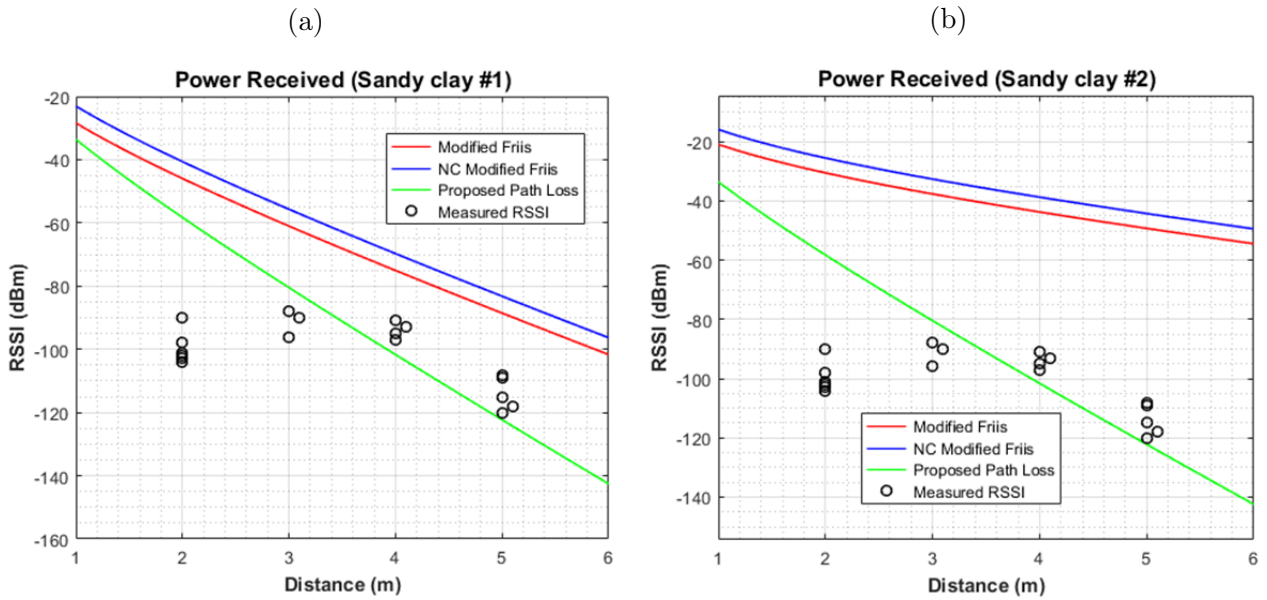

Figure 3.7: Received Power in Sandy Clay#1 (a) and Sandy clay#2 (b) with 23% Mean Soil Moisture.

are around 32.35 and 26.77 respectively. The proposed path loss model is then more accurate than the existing approach and can be efficiently used with low cost sensor devices.

3.4 Conclusion

In this chapter, we proposed a new approach of path loss prediction in WUSNs. In order to achieve this, we firstly conducted a review of existing path losses in WUSNs. Thereafter, we identified the key elements of the path loss prediction, among which we have the dielectric properties of the soil that are determined by the CDC. Then, we identified 03 main models for the prediction of CDC: Peplinski, MBSDM and TMDM. These models generally depend on several parameters like the temperature, bulk density, particle sizes, moisture, sand and clay portions. In order to compare and evaluate them, we used the TDR measurements done on three different configurations soil (moisture portion in percent): clayey silt (41.72%), gravelly sand (12.97%) and gravelly sand (17.02%). From our analysis, we observed that the most used Peplinski is the worst model according to the experimental parameters. The MBSDM seems to be more close to TDR measurements than TMDM and Peplinski. Finally, we proposed an accurate path loss model based on the MBDSM predictions for WUSNs. The experimentations revealed that our proposed model is more accurate to real measurements than the Conventional Modified Friis and NC Modified Friis. In order to validate our approach, we evaluated the RMSE, MAE and MAPE by taking into account the ±3% inaccuracy of the soil moisture sensor used. In each configuration, the RMSE and the MAPE were the less in our proposition.

Despite its better accuracy than the other path loss models, the proposed path loss model based on MBSDM is not suitable for real WUSN application like precision agriculture. This is because, the proposed approach is designed only for fully underground communications (UG2UG) between buried transmitter and receiver nodes. In application such as precision agriculture, the collected data from the ground must be analyze by an above ground user or BS, thus the communication between the underground sensor field and the aboveground final user should be possible. Thus, for a better growth of plants, the water content, the temperature or the nutriment presence directly get from soil near of the plant roots have to be received by the BS for an efficient watering or fertilizer addition. The design of a WUSN depends on a path loss model which can predict EM loss in UG2UG, UG2AG and AG2UG communications.

Chapter 4

A Wireless Underground Sensor Network Path Loss Model for Agriculture Precision

In the previous chapter, we proposed a new accurate path loss model based on MBSDM. Its validation in real experimental field and with real sensor devices have shown that it was more accurate than the existing path loss models regardless of the inaccuracy of low cost sensor devices [153]. However, the proposed approach is designed only for fully underground communications (UG2UG) and is not suitable for WUSN application like precision agriculture. In this application, the sensed data from soil must reach the user or the BS at the ground surface for a decision making such as deciding to watering a particular area of the field for an efficient use of the water resource. This chapter presents the Wireless Underground Sensor Network Path Loss Model for Precision Agriculture called WUSN-PLM. The proposed approach improve the path loss prediction in different communication types by allowing EM attenuation in UG2UG, UG2AG and AG2UG communications. the WUSN-PLM considers the limits and advantages of existing path loss models. The WUSN-PLM is designed for application of agriculture precision through buried cheap sensor node devices. The problem statement is discussed in Section 4.1, thereafter the proposed WUSN-PLM is described in Section 4.2; The results and intense discussion to validate the model is presented in Section 4.4; a short conclusion of the chapter and limitations of the WUSN-PLM are presented in Section 4.5.

4.1 Problem Statement

Despite a large number of path loss models for WUSN fields, there is any path loss models design for the 03 communication types to the best of our knowledge. Furthermore, the problem of accuracy and computation issues remain relevant in this research field. To find a trade off between accuracy and lowe *in situ* measurements, we designed the WUSN-PLM presented in

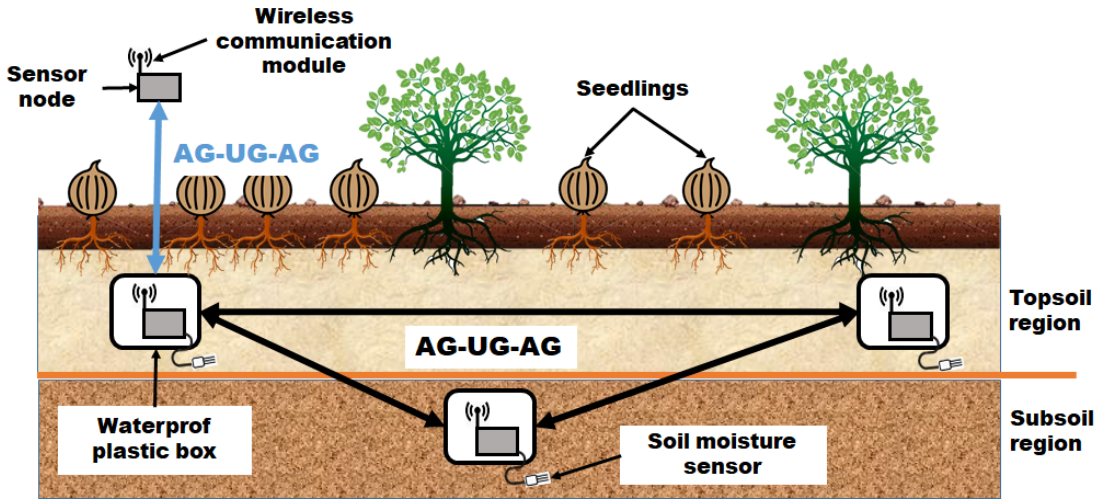

Figure 4.1: Design of wireless underground communications.

Section 4.2.

4.2 Proposed Approach

4.2.1 Wireless Underground Communications

The proposed WUSN-PLM considers the underground parts (topsoil and subsoil) because in agriculture the topsoil region or the subsoil can be ploughed before planting seeds or young plants. We classified the buried depth into two locations: *top_depth* and *sub_depth*. They denote the buried depth at topsoil (15cm to 30cm) and subsoil (more than 30cm) regions respectively.

In order to protect the electronic components from the water of other deteriorations, all the node components except sensors are put inside a plastic waterproof box that contains air. Thus, during the communication between two buried nodes (UG2UG), the wireless signal will successively cross the air inside the sender box, the ground and the air inside the receiver box (Figure 4.1). A buried node can communicate with another node located above the ground (UG2AG). Then, for that case, the wave crosses the air inside the box of the buried node, the ground that separates the buried node and the surface, and finally the air up to the receiver node. For the communication between an above ground node and a node placed under the ground (AG2UG), the scenario of wave propagation is slightly similar to UG2AG. In our model, the 03 communications types presented in Chapter 3 become AG2UG2AG (Figure 4.1).

4.2.2 Path Loss Computation

The proposed model $WUSN - PLM$ (4.1) is divided into two forms $WUSN - PLM_{\#1}$ (4.2) and $WUSN - PLM_{\#2}$ (4.3) for topsoil and subsoil regions respectively. For the topsoil region, the reflection effects due to ground surface proximity are added like [141] given by the equation (4.2). In subsoil regions, these effects are avoided, $WUSN - PLM$ is resumed to (4.3).

$$WUSN - PLM(dB) = L_{d1}(dB) + L_{ug}(dB) + L_{d2}(dB) \tag{4.1}$$

$$WUSN - PLM_{\#1}(dB) = -288.8 + 20\log\left(d_1.d_2.d_{ug}.\beta.f^2.\sqrt{\frac{2R}{1+R}}\right) + 8.69\alpha.d_{ug} \tag{4.2}$$

$$WUSN - PLM_{\#2}(dB) = -288.8 + 20\log\left(d_1.d_2.d_{ug}.\beta.f^2\right) + 8.69\alpha.d_{ug} \tag{4.3}$$

Where d_1 and d_2 are travelled distance in the aboveground region (air) by the wave; d_{ug} denotes the underground distance. For the communication between two buried nodes, d_1 and d_2 are the distance travelled by the signal inside the waterproof box. However, for a smaller distance (less than 1 m), the signal loss in free space can be neglected [16]. The α and β values are based on predicted $\epsilon^{'}$ and $\epsilon^{''}$ values like in the MBSDM Modified Friis model [153]. In the case of AG2UG communication, d_1 will represent the distance between the above ground node and the soil surface. For UG2AG communication, d_2 is the height of the buried node relative to the ground surface.

For fully underground communications, d_1 and d_2 are considered as the plastic waterproof width. Thus, they represent the distances travelled by the wave on the air inside each box. The underground distance between the two nodes is d_{ug}. Since at the topsoil region (top_depth), the wave reflection phenomenon is observed, we consider the loss due to reflection. The resulting path loss is resumed by $WUSN - PLM_{\#1}$ (4.2). However, for sub_depth, the reflection phenomenon is neglected, then the path loss becomes $WUSN - PLM_{\#2}$ (4.3).

For UG2AG communications, the sender is located below the ground and the receiver above the surface of the ground. d_1 is the distance travelled by the wave in the transmitter box, d'_{ug} denotes the buried depth and d_2 is the travelled distance in free space by the EM wave. The underground distance d_{ug} crossed by the wave is related to the burial depth d'_{ug} and the critical angle θ (Figure 4.2). The distance d'_{ug} is evaluated by assuming that all the sensor nodes are located within the same plan, thus the z-axis is avoided.

Furthermore, when the soil is dry, the critical angle $\theta \approx 15°$ and for moist soil it is slightly equal to 30° like it is shown in [16]. Thus, if the transmitter is located at the top_depth, the

overall path loss is expressed according to (4.2). Whereas, if the transmitter is located at the *sub_depth* the path loss is expressed through (4.3).

The path loss for AG2UG communications is slightly the same as the path loss in UG2AG. Meanwhile, for this kind of communication, additional attenuation caused by refraction (4.4) is considered as it is shown by Dong et *al.* [55]. Furthermore, if the receiver is located at *top_depth* and *sub_depth*, the corresponding path loss becomes $WUSN^{'} - PLM_{\#1}$ (4.5) and $WUSN^{'} - PLM_{\#2}$ (4.6) respectively.

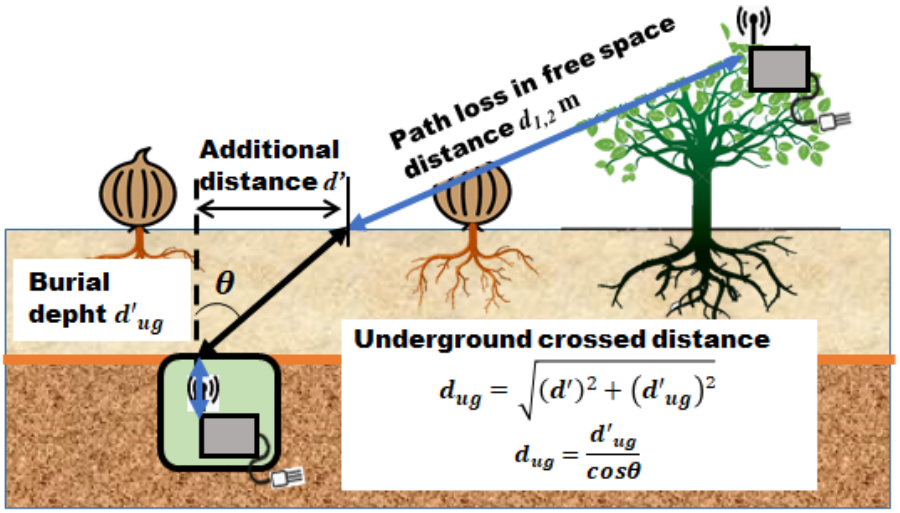

Figure 4.2: UG2AG and AG2UG path loss designing.

$$WUSN^{'} - PLM(dB) = WUSN - PLM + 20\log\left(\frac{n+1}{4}\right) \tag{4.4}$$

$$WUSN^{'} - PLM_{\#1}(dB) = -288.8 + 20\log\left(d_1.d_2.d_{ug}.\beta.f^2.\sqrt{\frac{2R}{1+R}}.\frac{(n+1)}{4}\right) + 8.69\alpha.d_{ug} \tag{4.5}$$

$$WUSN^{'} - PLM_{\#2}(dB) = -288.8 + 20\log\left(d_1.d_2.d_{ug}.\beta.f^2.\frac{(n+1)}{4}\right) + 8.69\alpha.d_{ug} \tag{4.6}$$

From equations (4.4 - 4.6) below, we note that when $n = 3$ the computed path loss is the same. In order words for soil with high proportion in silicium ($n = 3$), the path loss for AG2UG communications are the same regardless of the burial depth of the receiver node.

4.3 Experimentations

In this section, the experimentations processes are presented. The nodes used during the tests, the experimental field and the methodology are described in details.

4.3.1 Sensor Nodes

In order to evaluate the path loss, we designed a transmitter and a receiver, both based on Arduino UNO (Figure 3.4). The two nodes are powered by a $9V$ input. In order to sense the soil moisture and the temperature, the transmitter has four different sensors: a sensor LM35DZ to measure the temperature inside the box; a soil humidity sensor YL-69 and a capacitive soil moisture sensor resistant to corrosion; a DHT11 sensor is fixed outside the box in order to give the temperature and the humidity of the soil around the box. Contrary to the transmitter, the receiver node has only the soil moisture sensor YL-69. Except for the Arduino board, the transceivers, the batteries and the sensor LM35DZ from transmitter node, all other components are put outside a plastic box like the MoleNet [154]. The plastic box used in our model has a truncated square pyramid form with 13cm height. In addition to the schematic representation of sensor nodes presented in Figure 3.4, the wireless communication is also evaluated with a pair of LoRa SX1278 transceivers at 433MHz frequency.

The nRF905 and SX1278 transceivers parameters are found in Table 4.1. The Path loss is computed according to the link budget (3.14).

Table 4.1: Characteristics of transceivers.

Transceivers	**TX power (dBm)**	**Sensitivity (dBm)**	**Antenna gains**	**Maximum PL(dB)**
nRF905	+10	−100	$2dB$	114
SX1278	+17	−121	$2.5dB$	143

From Table 4.1 and the link budget equation of Chapter 3, the maximum acceptance path loss for nRF905 and SX1278 transceivers is $114dB$ and $143dB$ respectively. In other words, for the nRF905 transceiver, if the path loss is greater than $114dB$, the receiver will not get an incoming packet. However, if the signal attenuation is lower than this threshold, a node receives a new packet.

4.3.2 Experimental Field

We conducted our experimentation at the botanic garden of the University Cheikh Anta Diop of Dakar, Senegal (Figure 4.3). A $450m^2$ area for an onion plantation is considered; the present soil is a sandy clay type in which the clay proportion increase with the depth. Before putting the onion plants under the ground, the soil is ploughed beforehand on the first $20cm$ of the topsoil region (Figure 4.3a). Then, a drip irrigation system is installed and young onion seedlings are planted two days after the soil ploughing, thus, the soil is enough soft (Figure 4.3b and Figure 4.3c). The young onion seedlings are watered using a drip irrigation system connected to a pool dedicated to pisciculture. From Figure 4.3d and Figure 4.3e, the buried transmitter (green lid) and receiver (red lid) at different depth are presented. They are separated from each other by a certain distance in meter. The average distance between two onion plants of the same line (irrigation pipe) is $15cm$ and the distance between two lines is $50cm$ (Figure 4.3f).

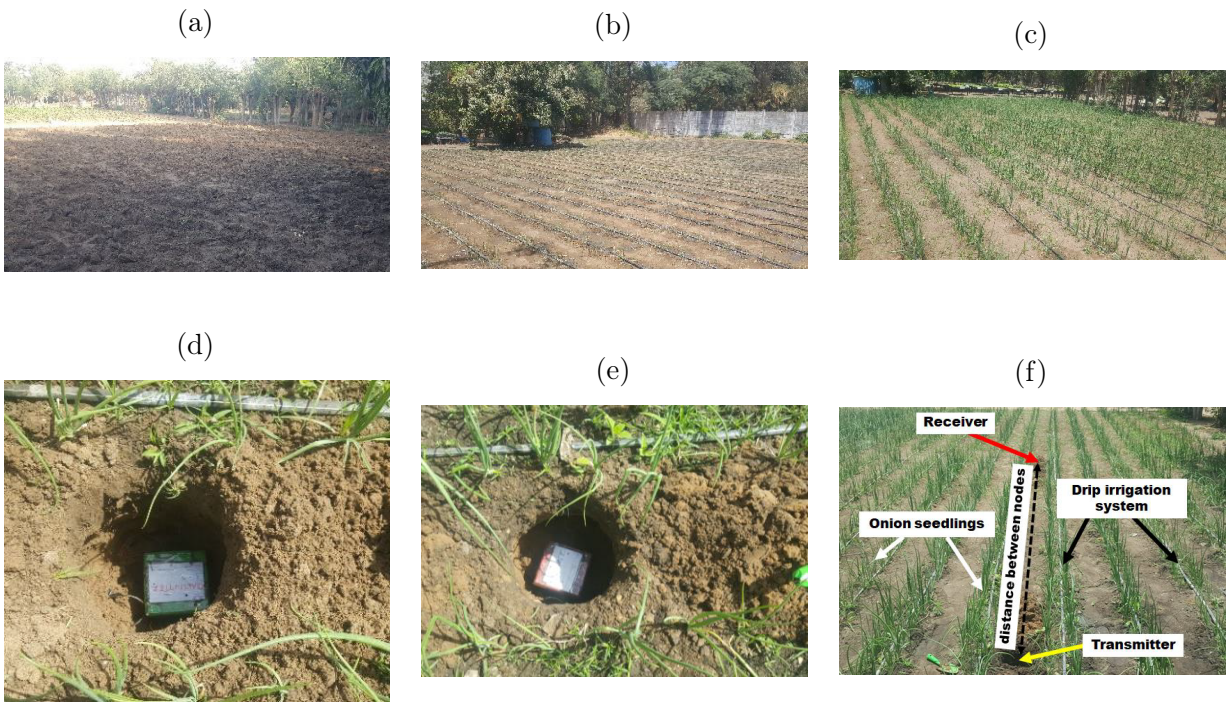

Figure 4.3: Experimentalfields at the botanic garden of the University Cheikh Anta Diop (UCAD), Senegal.

In order to have the clay and the sand portions of the area around the experimental field, we considered previous measurements conducted by [1], [2]. From these studies, sand and clay portions of sandy clay soil in Dakar could be grouped into two types, as shown in Table 3.2. Thus, because of the non-uniformity of these portions along the experimental field, both types of sandy clay are furthermore considered for the conducted experiments and tests.

4.3.3 Methodology

We have considered two scenarios for our measurements: Scenario #A when the soil is dry (Figure 4.3a) and Scenario #B for moist soil (Figure 4.3b and Figure 4.3c). On dry soil, there is no presence of moisture due to the heat released by the sunlight and the wind have dried the soil so that the soil moisture is around 0%. For each scenario, the distance between the transmitter and receiver nodes varies between $5m$, $10m$, $15m$ and $20m$. On each distance, the buried depth of nodes changes from the ground, $15cm$, $20cm$, $30cm$ and $40cm$ (Figure 4.4). The three types of communication presented in Figure 1 are considered in both topsoil and subsoil regions. Moreover, depths located at the first $30cm$ are considered as top_depth region and beyond $30cm$, they are considered as sub_depth.

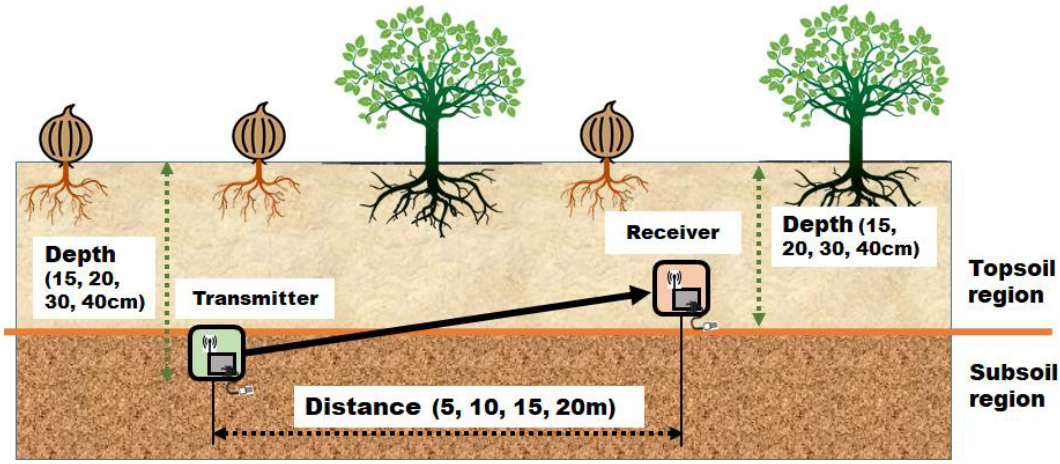

Figure 4.4: Methodology of measurement process.

The transmitter sends 170 packets to the receiver, each sent packet has 32-byte size and the interval between two transmissions is fixed to 02 seconds in order to avoid the latency due to sensor measurements. The structure of a radio packet in the nRF905 transceiver is presented in Figure 4.5, the Cyclic Redundancy Check (CRC) is used to detect errors in the received data. During each round, we get the different values of the DHT11 sensor (temperature and humidity), LM35DZ temperature, YL-69 soil moisture, capacitive soil moisture and the id of the current packet. The six sensed values are stored inside the transmitter EEPROM. Therefore, the packet thus constituted is sent to the receiver by the pure ALOHA communication scheme. At the receiver side, the node listens to any incoming packets from the transmitter. If it receives a packet, it gets the sensed value of its YL-69 sensor and stores it with the id of the received data on its EEPROM. Thus, we have an overview of the soil moisture between the transmitter and the receiver nodes at each round. The transmitter code and the receiver code are available on GitHub. The communication processes of nodes are resumed in Figure 4.6.

In order to evaluate the path loss prediction on each model with the nRF905 transceiver, we define the following classes:

Figure 4.5: Packet structure.

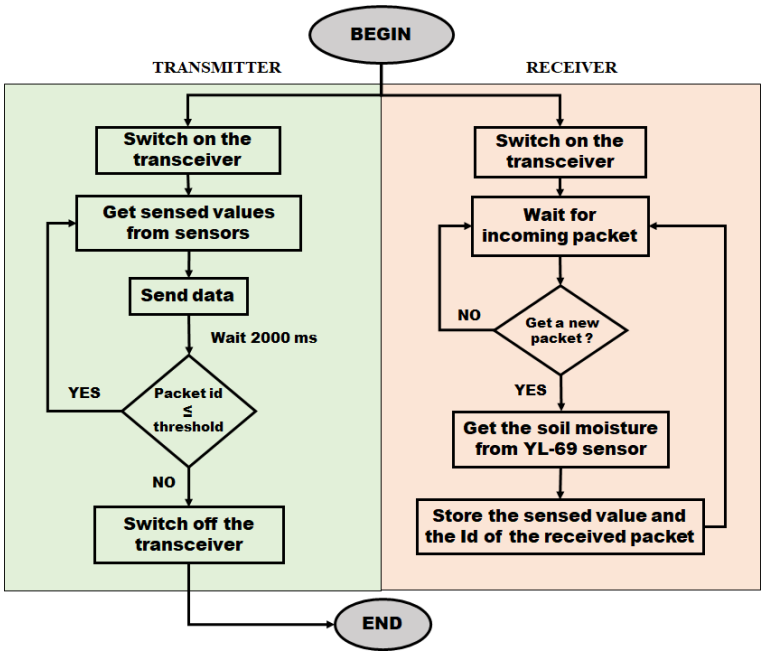

Figure 4.6: Overview of communication between transmitter and receiver nodes.

– Positive or Received class: the predicted path loss is less or equal to the maximum path loss of the transceiver (114 dB) from Table 4.1. In other words, the receiver node is able to get a packet sent by a transmitter node.

– Negative or Not received class: here, the computed path loss by the proposed approach is more than the maximum path loss of the transceiver. The receiver does not get incoming packets sent by the transmitter.

Moreover, according to the previous classes, we consider the 04 well-known metrics:

- **True Positive (TP)**: is a correct result when an approach successfully detects or predicts the positive class of an observation;
- **True Negative (TN)**: is a correct estimation when the approach successfully predicts a negative class;
- **False Positive (FP)**: is an error when predicting a positive class;
- **False Negative (FN)**: is an error when the approach does not successfully predict the negative class;

Furthermore, the number of good predictions is GP (TP+TN) and the amount of bad predictions is BP (FP+FN). GP gives the number of cases in which the prediction is equal to the observation. BP is simply the number of cases where the prediction is different from the observation.

4.4 Results and Discussions

We evaluate the proposed WUSN-PLM on two scenarios: #A for dry soil and #B for moist soil. For each scenario, the soil configurations presented in Table 3.2 are considered. Furthermore, in each scenario, we evaluated and compared the presented path loss models according to the type of communication.

4.4.1 Dry Soil (Scenario #A)

The path losses for UG2UG WUC for dry soils (0% moisture) are shown in Figure 9, where the distance crosses by the wave inside the plastic boxes is set to 13cm ($d_1 = d_2$) and can be neglected. Path losses in Sandy clay#1 (Figure 4.7a) and in Sandy clay #2 (Figure 4.7b) seem to be identical; this is because both soil samples are sandy clay with a high concentration of sand. Moreover, we conclude that, the clay portion in dry soil does not highly affect the signal attenuation in the same soil type (sandy clay).

(a) (b)

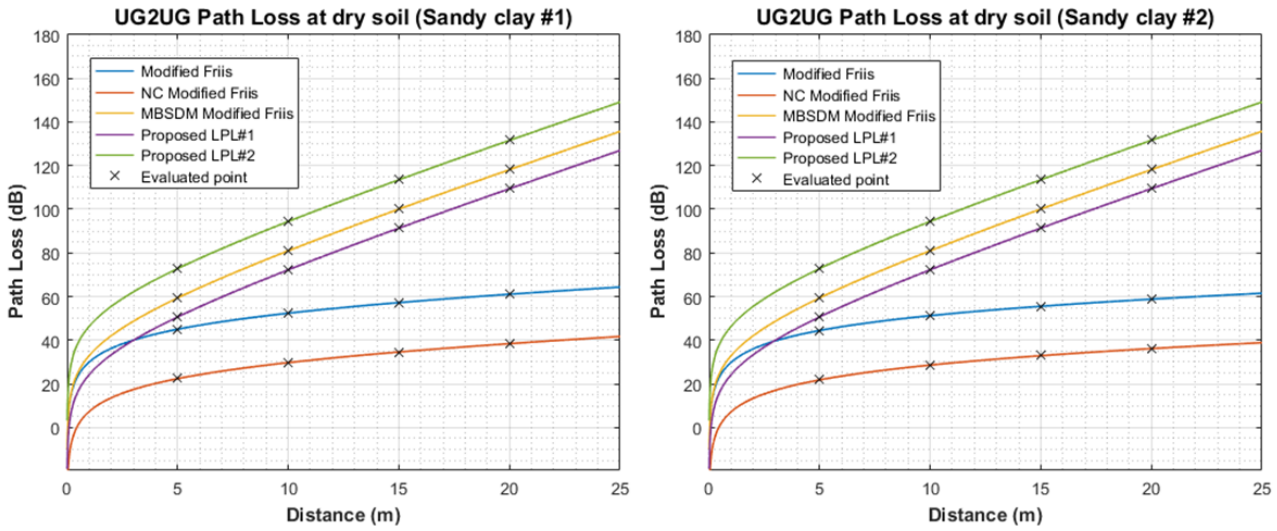

Figure 4.7: Path losses comparison on Dry soil. (a) is the path losses for sandy clay#1 soil whereas, (b) is the path losses for sandy clay#2 from Table 3.2.

From Figure 4.7, the Path losses on Conventional and NC Modified Friis have the same evolution; this is because both are based on the Peplinski derivations to predict the value of the CDC. Meanwhile, due to wave reflection phenomenon introduced by NC Modified Friis, the resulting path loss is slightly lower than the conventional Modified Friis. The path loss evolution on the proposed approach is different from the other path loss models since it is based on the accurate MBSDM for predicting the CDC. Nevertheless, the proposed approach additionally considers the presence or the absence of the wave reflection in soil according to the burial depths. Thus, we observed that the path loss at *sub_depth* ($WUSN - PLM_{\#2}$) is greater than the path loss on *top_depth* ($WUSN - PLM_{\#1}$).

To evaluate the UG2UG communications in each model for scenario #A, the number of TP, TN, FP and FN are compared based on the 48 measurements made. From Table 4.2, it is observed that the Conventional Modified Friis and the NC Modified Friis have the same results: 36GP (36 TP and 0 TN). However, our proposed model obtained the best prediction with 40GP (36TP and 4TN) and 8BP (8FP and 0FN). All the BP of our proposed approach are located in the *top_depth* and are caused by the wave interferences that appear in this region during reflection phenomenon but neglected by the authors of [16].

Table 4.2: Comparison of UG2UG path losses in Scenario #A.

	Conventional Modified Friis				**NC Modified Friis**				**Proposed WUSN-PLM**				**Observations**
Location	TP	TN	FP	FN	TP	TN	FP	FN	TP	TN	FP	FN	
top_depth	24	0	8	0	24	0	8	0	24	0	8	0	32
sub_depth	12	0	4	0	12	0	4	0	12	4	0	0	16
Total	36	0	12	0	36	0	12	0	36	4	8	0	48

In order to evaluate the performance of each approach, we calculate their precision (PRE) and their accuracy (ACC) according to (4.7). PRE simply stands for how consistent results are when measurements are repeated whereas ACC is used to describe the closeness of a measurement to the true value. Conventional and NC Modified Friis have the same performance, thus their corresponding precision and accuracy are the same (75%). PRE is equal to ACC in both approaches because all the GP are only TP; therefore, they are not able to predict the negative class (not a packet reception). However, the proposed WUSN-PLM obtained highest performance with 81.81% precision and 83.33% accuracy. The proportion of negative observations well predicted known as selectivity (SEL) and the ratio of correct prediction called sensitivity (SEN) are also evaluated according to (4.7). Likewise, the precision and the accuracy, our proposed path loss model has the best efficiency with a perfect Sensitivity ($SEN = 1$) and 0.33 selectivity. Furthermore, the same results are obtained for both sandy clay soils which configurations are presented in Table 3.2.

Knowing that the Conventional Modified Friis and NC Modified Friis are designed only for fully UG2UG communications, we compare and evaluate our proposed model WUSN-PLM to the mixing path losses models presented in subsection B of Section II. To evaluate ZS path loss for AG2UG communication, we assume the incidence angle to be null. Thus, the transmitted power is the maximum as in the XD path loss model.

$$\begin{aligned} SEN &= \frac{TP}{TP+FN} \\ SEL &= \frac{TN}{TN+FP} \\ PRE(\%) &= \frac{TP\times 100}{TP+FP} \\ ACC(\%) &= \frac{(TP+TN)\times 100}{TP+TN+FP+FN} \end{aligned} \tag{4.7}$$

For UG2AG communication, the predicted path loss models in scenario #A are presented in Figure 4.8. As for UG2UG communication, the path loss evolution in UG2AG type is the same despite the type of sandy clay soil used. We observe that the path loss models slightly increases with the burial depth and the distance between the nodes (Figure 4.8a, Figure 4.8b, Figure 4.8c and Figure 4.8d). Thus, there is a positive association between the path loss and the burial depth; and between the path loss and the distance between transmitter and receiver sensor nodes for UG2AG communications. Path loss predicted values of ZS and XD models can be confused for the low linear distance between transmitter and receiver (Figure 10a). However, the signal attenuation for 10, 15 and 20m linear distance between nodes, the ZS and XD path losses are closed each other. This is because both have slightly the same core and are based on Conventional Modified Friis and Free Space models.

Moreover, the expected path loss on each presented model seems to be lesser than the threshold path loss value of the transceiver nRF905 (114dB). Thus, in all the cases presented here, the communication between the transmitter (located under the ground) and the receiver (located on the ground surface) is reliable in the scenario #A independently of the burial depths of sensor nodes (up to 40cm) and for linear distance lesser or equal to 20m. To evaluate UG2AG these path loss models, 16 observations (12 in top_depth and 4 in sub_depth) have been made for each model. All the path loss models for UG2AG communications have the same perfect result in Scenario #A, the resulting confusion matrix is presented in Table 4.3. All the presented proposed approach obtained a perfect score with $16TP$. Thus, they obtained 100% of accuracy and precision with perfect sensitivity ($SEN = 1$) in Scenario #A.

The comparison of the path loss models in AG2UG for each linear distance (5, 10, 15 and 20m) is given in Figure 4.9. Contrary to UG2AG communications, ZS and XD path loss models are identical for all the linear distance. This is because both consider a zero angle of incidence; the maximum power is therefore considered to be transmitted. Furthermore, the calculated path

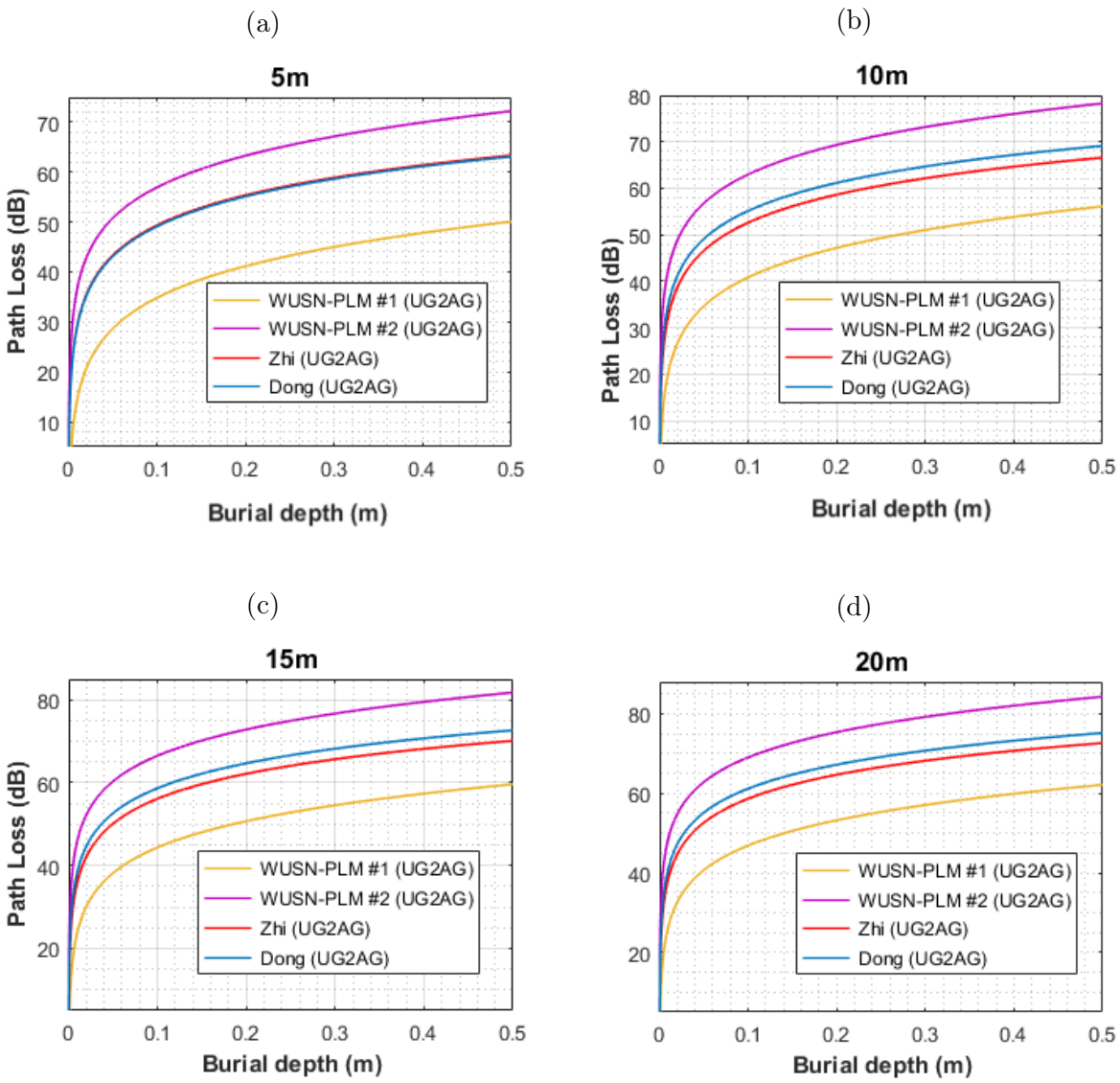

Figure 4.8: UG2AG path losses comparison in Scenario #A. The distance between nodes is 5m (a), 10m (b), 15 (c) and 20m (d) respectively. The burial depth of the transmitter node varies from 0 to 50cm.

losses in scenario #A for AG2UG communication are identical either for sandy clay #1 or for sandy clay #2 soil. As with UG2AG communication, the path loss for AG2UG is less than the maximum path loss acceptable by the nRF905 transceiver, which means that all sent packets are received despite the position of the nodes. The evaluation process of these models for AG2UG communication is similar to UG2AG evaluation process. However, for the WUSN-PLM, the computation of the predicted path loss is based on (4.5) and (4.6) for *top_depth* and *sub_depth* regions respectively. The resulting confusion matrix for each path loss model is identical to the confusion matric for UG2AG communication (Table 4.3) with $16TP$. Then, they have perfect accuracy ($ACC = 100\%$), precision ($PRE = 100\%$) and sensibility ($SEN = 1$).

80 measurements have been conducted in scenario #A in order to evaluate our proposed

Table 4.3: Resulting confusion matrix of ZS, XD and WUSN-PLM path loss for UG2AG and AG2UG in Scenario #A.

		Observation	
		Received	Not received
Prediction	Received	16 TP	0 FP
	Not received	0 FN	0 TN

path loss (Table 4.4) and only 48 measurements for the other existing path loss models since these are latter only designed for fully UG2UG communication.

Table 4.4: Overall confusion matrix of WUSN-PLM in Scenario #A.

		Observation	
		Received	Not received
Prediction	Received	68 TP	0 FP
	Not received	0 FN	12 TN

In order to evaluate the correlation between the prediction and the observation in WUSN-PLM, we used the Matthews Correlation Coefficient (MCC). Additionally, since the positive and the negative classes have different size (positive class is larger than the negative class), the balanced accuracy (bACC) is more suitable than the accuracy ACC (4.8). The positive value of MCC means that the proposed approach is better than a random prediction and therefore the correlation between the prediction of the path loss and the observation is good ($MCC = 0.55$). The overall performance evaluation of the proposed approach is resumed in Table 4.5.

$$\begin{aligned} bACC(\%) &= \frac{SEN+SEL}{2} \\ MCC &= \frac{TP.TN-FP.FN}{\sqrt{(TP+FP).(TP+FN).(TN+FP).(TN+FN)}} \end{aligned} \tag{4.8}$$

Table 4.5: Performance evaluation of WUSN-PLM in Scenario #A.

Precision (PRE)	**Accuracy (ACC)**	**Sensitivity (SEN)**	**Selectivity (SEL)**	**Balanced Accuracy (bACC)**	**MCC**
89.47%	90%	1	0.33	66.67%	0.55

4.4.2 Moist Soil (Scenario #B)

For moist soil configuration (scenario #B), the soil moisture portion varies according to each sensor measurement. In order to evaluate the path loss, we analyse each case and their

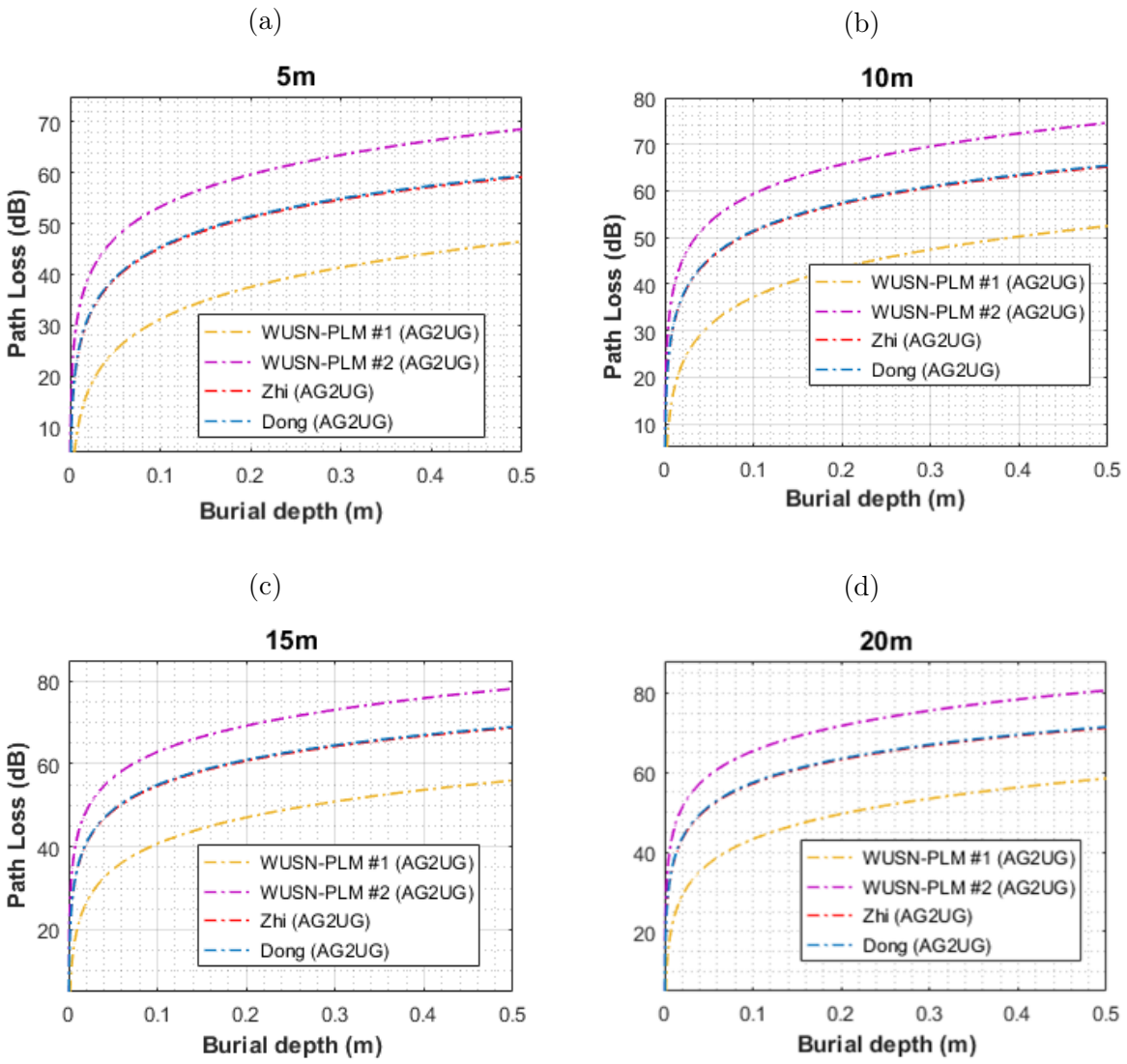

Figure 4.9: AG2UG path losses comparison in Scenario #A. The distance between nodes is 5m (a), 10m (b), 15 (c) and 20m (d) respectively. The burial depth of the receiver node varies from 0 to 50cm.

corresponding parameters. Due to the table size, the evaluation of path loss models on UG2UG in moist soil for 5m and 20m linear distances is taken from Appendix A.4. From the 18 observations of 5m and 20m linear distances from Appendix A.4, the proposed WUSN-PLM obtained the highest precision (100%) and selectivity ($SEL = 1$) for both sandy clay configurations.

Moreover, the same measurements in the previous example are conducted for 10m and 15m between the transmitter and the receiver. Thus, 36 comparisons have been observed in each soil (sand clay #1 and sandy clay #2). By observing the two types of soil, path loss predictions on the Conventional and the NC Modified Friis are different despite the same type of soil (sandy clay). This observation reveals that a minor change of the sand or clay portions would highly affect these path loss models. Thus, the use of Conventional and NC Modified Friis is

possible only for a uniform soil type in which sand and clay portions are the same. Contrary to Conventional and NC Modified Friis, WUSN-PLM gave the same prediction either for sandy clay #1 and sandy clay #2. Then, this path loss can be used for the same soil type despite a slight difference in sand or clay portions along the field. However, due to the inaccuracy of the low cost soil moisture sensor (YL-69) [153], [154], we consider an error margin of ±3% on the soil moisture value. In order words, for the underground communication at 20cm depth (20cm to 20cm), and by considering the distance between nodes to 5m, the measured moisture was 44%. Thus, by applying the ±3% margin, we assume that the exact value of the soil moisture is between 41% and 47%. Despite the ±3% margin error of the soil moisture sensor device, the predictions for 5m and 20 linear distance from Appendix A.4 no longer change. Thus, the prediction of the path loss can be done with the proposed model regardless of the use of a low cost sensor. Table 4.6 shows the corresponding confusion matrices of each path loss model for the 72 observations (36 in each sandy clay) made in full UG2UG communication (Appendix A.4. The NC Modified Friis obtained a higher number of TP whereas the proposed WUSN-PLM had the best amount of TN.

Table 4.6: Confusion matrices of path loss models for UG2UG communications in Scenario #B.

		Observation					
		Conventional Modified Friis		**NC Modified Friis**		**WUSN-PLM**	
		Rcv.	Not Rcv.	Rcv.	Not Rcv.	Rcv.	Not Rcv.
Prediction	Rcv.	9 TP	6 FP	13 TP	9 FP	2 TP	0 FP
	Not Rcv.	9 FN	48 TN	5 FN	45 TN	16 FN	54 TN

Furthermore, as in Scenario #A, we compared our proposed path loss model in UG2AG and AG2UG communications to ZS and XD path loss models. Appendices A.5 and A.6 resume the evaluation of mixing path loss models for UG2AG and AG2UG respectively. For each communication type, 12 observations are conducted based on the measured soil moisture. During UG2AG communications in Scenario #B (Appendix A.5), each path loss model obtains 75% precision and accuracy. As in Scenario #A, the recall or sensitivity is perfect ($SEN = 1$). In addition, the presented path loss models have an average balanced accuracy ($bACC = 50\%$). Thus, based on our data set, these path loss models have the same performance regardless of the scenarios in sandy clay #1 and sandy clay #2.

For AG2UG communication (Appendix A.6), ZS and XD path loss models have the same results (10TP and 2FP). Both obtained 83.33% precision and accuracy for AG2UG communication, however, their corresponding recall is perfect ($SEN = 1$) in Scenario #B. Nevertheless, the proposed WUSN-PLM outperforms ZS and XD models with a perfect prediction (10TP and 2TN). It obtained 100% Accuracy, precision and balanced accuracy, its correlation between

prediction and observation is perfect ($MCC = 1$).

The overall performance evaluation of our proposed WUSN-PLM in Scenario #B (UG2UG, UG2AG and AG2UG) is resumed in Table 4.7 and Table 4.8. Since the proposed approach gives the same results for sandy clay #1 and sandy clay #2, 60 tests were conducted in each soil type. The corresponding observations are presented in Table 4.7. From the 60 observations, our proposed obtained 47GP (20TP and 27TN). The corresponding precision and accuracy in Scenario #B are 80% and 78.33% respectively.

Table 4.7: Overall confusion matrix of WUSN-PLM in Scenario #B.

		Observation	
		Received	Not received
Prediction	Received	20 TP	5 FP
	Not received	8 FN	27 TN

Nevertheless, since the size of the negative class is higher than the size of the positive class (32 and 28 respectively), the F1 score is considered according to (4.9) instead of the balanced accuracy (bACC). Thus, the prediction reliability of the proposed approach despite the size of observed classes is 75.47% with a good correlation of 0.56 between the prediction and the observation (4.8).

$$F1Score(\%) = \frac{2\times TP}{2\times TP + FP + FN}\times 100 \tag{4.9}$$

Table 4.8: Performance evaluation of WUSN-PLM in Scenario #B.

Precision (PRE)	**Accuracy (ACC)**	**Sensitivity (SEN)**	**Selectivity (SEL)**	**F1 Score**	**MCC**
80%	78.33%	0.71	0.84	75.47%	0.56

To compare the path loss models in UG2UG communications (scenario #A and scenario #B), 168 observations have been conducted in sandy soil. The corresponding confusion matrices are given in Table 4.9 in which the size of the observed positive class is higher than the size of the observed negative class, i.e. 90 and 78 respectively. The proposed WUSN-PLM obtained the highest number of GP ($74TP$ and $62TN$). The Conventional Modified Friis performed the worst prediction with the highest number of BP ($9FN$ and $30FP$) directly follow by the NC Modified Friis ($38BP$).

Table 4.10 resumes the performance evaluation for UG2UG communications of the different path loss models presented in Section 3. The WUSN-PLM obtained the best precision and accuracy of 82.22%and 80.95% respectively. Meanwhile, the Conventional and NC Modified

Table 4.9: Confusion matrices of path loss models for UG2UG communications (Scenario #A and Scenario #B).

		Observation					
		Conventional Modified Friis		**NC Modified Friis**		**WUSN-PLM**	
		Rcv.	Not Rcv.	Rcv.	Not Rcv.	Rcv.	Not Rcv.
Prediction	Rcv.	81 TP	30 FP	85 TP	33 FP	74 TP	16 FP
	Not Rcv.	9 FN	48 TN	5 FN	45 TN	16 FN	62 TN

Friis performed the worst precision and accuracy. Moreover, despite the 77.38% accuracy in NC Modified Friis, we observe that, the correlation between its prediction and the observation is worst with the lowest MCC (0.35). In summary, the path loss in UG2UG communications regardless of the soil moisture is better predicted by WUSN-PLM. Due to the unbalanced size of classes (received and not received classes), the balanced accuracy is considered. Like the other metrics, the proposed path loss obtained the highest precision ($PRE = 82.22\%$), accuracy ($ACC = 80.95\%$), selectivity ($SEL = 0.79$), correlation between prediction and observation ($MCC = 0.62$) and balanced accuracy ($bACC = 80.85\%$). However, the WUSN-PLM performed the worst sensitivity ($SEN = 0.82$) because it badly predicts the positive classes. This can be caused by the wave interferences neglected at topsoil region by [16]. Despite the worst sensitivity, the proposed WUSN-PLM is more suitable than the Conventional and the NC Modified Friis.

Table 4.10: Performance evaluation of path loss models for UG2UG communications (Scenario #A and Scenario #B.

	PRE	**ACC**	**SEN**	**SEL**	**bACC**	**MCC**	**AUC**
Conventional Modified Friis	72.97%	76.79%	0.9	0.62	75.77%	0.542	0.831
NC Modified Friis	72.03%	77.38%	0.94	0.58	76.07%	0.350	0.871
WUSN-PLM	82.22%	80.95%	0.82	0.79	80.85%	0.62	0.9

Additionally, in order to evaluate the trade-off between the true and the false positive rate independently of the transceiver type, we use the *Receiver Operating Characteristic* (ROC) curve. It is used to evaluate a prediction model through graphical representation and regardless of the fixed threshold used to separate the positive and negative classes (reception and loss of an incoming packet). By varying the value of the maximum path loss bearable by transceiver from 0dB to 1150dB with a step of 10dB, the resulting ROC curves of each approach are presented in Figure 4.10. We observe that the ROC curves are all above the random guess. However, the proposed WUSN-PLM seems to be more above the random separation than the Conventional and NC Modified Friis. The value of the Area Under Curve (AUC) is calculated according to the trapezoidal rule describe in (4.10). The highest AUC value is obtained by the proposed

WUSN-PLM (0.9) follow by the NC Modified Friis (0.871). The Conventional Modified has the lowest AUC (0.831).

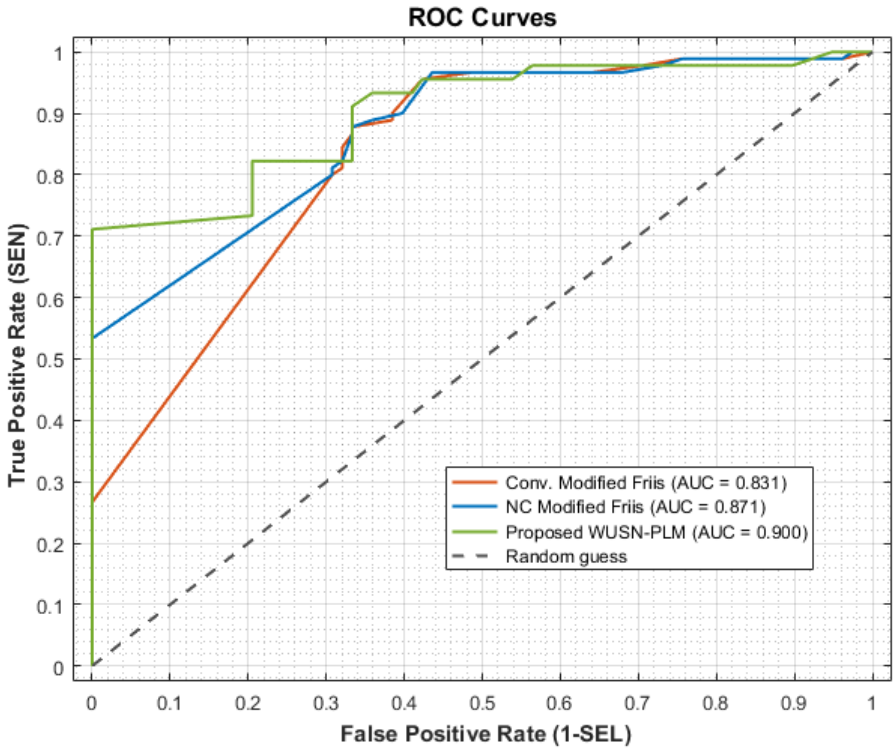

Figure 4.10: ROC curves comparison for UG2UG communications.

The performance evaluation of the mixing path loss models in UG2AG communication (Scenario #A and Scenario #B) is given in Table 4.11. Each of them gets 89.28% precision and accuracy, the balanced accuracy is average ($bACC = 50\%$).

Table 4.11: Performance evaluation of path loss models for UG2AG communications (Scenario #A and Scenario #B.

	PRE	**ACC**	**SEN**	**SEL**	**bACC**	**MCC**
Path loss models	89.28%	89.28%	1	0	50%	/

The overall performance evaluation of mixing path loss models in AG2UG communications (Scenarios #A and #B) is resumed Table 4.12.

Table 4.12: Performance evaluation of path loss models for AG2UG communications (Scenario #A and Scenario #B.

	PRE	**ACC**	**SEN**	**SEL**	**bACC**	**MCC**
ZS / XD models	92.85%	92.85%	1	0	50%	/
WUSN-PLM	100%	100%	1	1	100%	1

From Appendices A.5, A.6 and above evaluation, we observe that the prediction in both sandy clay soils is similar. Thus, the proposed WUSN-PLM is more efficient for UG2AG and

AG2UG communications than the presented mixing path loss models in the same soil type regardless of the slight variation of sand and clay portions. Additionally, despite the assumed ±3% error given by the sensor moisture device, the amount of GP no longer changes from Appendix A.5 and Appendix A.6.

The total number of observations conducted in each sandy clay soil was 140 (80 in scenario #A and 60 in scenario #B) for our proposed approach. From these observations, our proposed WUSN-PLM obtained a total of $119GP$ ($88TP$ and $31TN$) and $21BP$ ($13FP$ and $8FN$) like it is shown in Table 4.13. According to these observations, its corresponding performance evaluation is shown in Table 4.14. It has very good precision and accuracy (87.13% and 85% respectively), moreover, despite the different sizes of the observed classes, the proposed approach obtained a very good balanced accuracy (81.06%). Furthermore, the correlation between predictions and the real tests is high ($MCC = 0.64$), then our proposed model can be used for all the different types of communication (UG2UG, UG2AG and AG2UG) with very high sensitivity ($SEN = 0.92$) and selectivity ($SEL = 0.70$).

Table 4.13: Overall confusion matrix of WUSN-PLM in Scenarios #A and #B for each sandy clay configuration.

		Observation	
		Received	Not received
Prediction	Received	88 TP	13 FP
	Not received	8 FN	31 TN

Like for the evaluation of UG2UG communications, we evaluate the trade-off between the true and the false positive rate in our proposed path loss for all the communications types by the corresponding ROC curve presented in Figure 4.11. The computation of AUC is also based on the trapezoidal rule, thus, the area A_i of a trapezoid i delimitated by points x_i and x_{i+1} from Figure 4.11 and the AUC are given in (4.10). Where y_i denotes the sensibility according to the false positive rate x_i and n is the number of trapezoids used ($n = 41$). The calculated value of the AUC presented in Table 4.14 shows that the proposed model has 92.28% change to distinguish positive class (reception of a packet) from the negative class (not packet reception) independently of the communication types (UG2UG, UG2AG and AG2UG).

Table 4.14: Overall performance evaluation of WUSN-PLM in Scenarios #A and #B for each sandy clay configuration.

PRE	**ACC**	**SEN**	**SEL**	**bACC**	**MCC**	**AUC**
87.13%	85%	0.92	0.70	81.06%	0.64	0.92

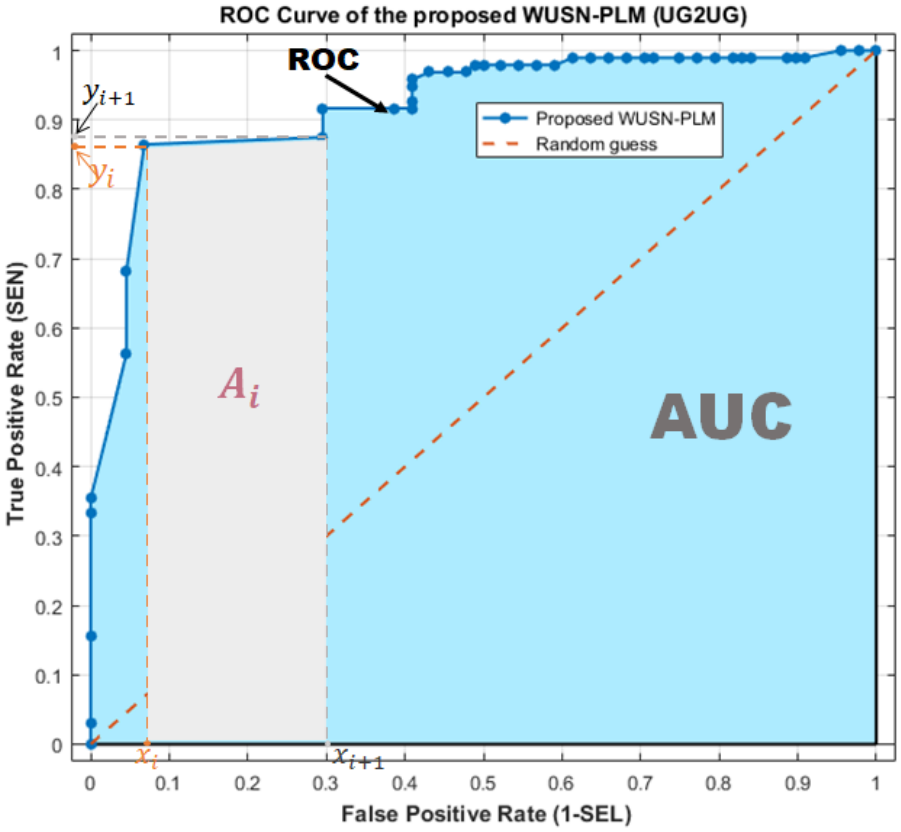

Figure 4.11: ROC curve and AUC of the proposed WUSN-PLM.

$$\begin{aligned} A_i &= \frac{(y_{i+1}+y_i)}{2} \times (x_{i+1} - x_i) \\ AUC &= \sum_{j=1}^{n} A_j \end{aligned} \tag{4.10}$$

4.5 Conclusion

In this chapter, we designed the Wireless Underground Sensor Network Path Loss Model for precision agriculture called WUSN-PLM. To achieve it, we first simplify the underground communication types to a generic model designed for precision agriculture. We integrated the accurate CDC prediction approach called MBSDM to our WUSN-PLM as in our previous work. The proposed model takes into account all the wireless communications (UG2UG, UG2AG and AG2UG) known in the WUSN field. Moreover, for each communication type and the node location, we consider phenomena like the wave attenuation or the wave refraction. To evaluate and validate the WUSN-PLM, intensive experimentations have been conducted in a real environment with two different pairs of wireless transceivers (nRF905 and LoRa SX1278). The resulting comparison has shown that the proposed WUSN-PLM outperforms the other approaches with the overall highest amount of Good Prediction GP (TP and TN) in dry soil (scenario #A) and in moist soil (scenario #B) for different communication type. Additional

experiments are conducted in fully UG2UG communication in order to compare the errors of the predicted power received and the real measured RSSI. The evaluation shown that our proposed approach has the lowest RSME, MAE and MAPE (32.7, 29.4 and 30.1 respectively).

Despite the higher performance of the WUSN-PLM, its implementation remains a key issue for real-time applications in WUSN. Indeed, in order to save the energy, the sensor node should be able to decide if a sent packet must be reach or not a destination node according to soil properties. However, the prediction of the CDC by the MBSDM need computational resources and more memory but sensor nodes have limited resources. Furthermore, in order to get soil properties such as clay portion, additional laboratory analyzes are required. Thus, the prediction *in situ* of the path loss remains highly challenging. An lightweight CI must allow a sensor node to evaluate the EM with lesser computation.

Chapter 5

A Powerful Approach for Reliable Wireless Underground Sensor Network Communications Based on Fuzzy Logic

In the previous chapter, we proposed an accurate Wireless Underground Sensork Network Path Loss Model called WUSN-PLM [155]. The proposed loss model is designed for precision application in WUSN, it addressed the prediction of EM wave in the different WUC types with a high correlation between the predicted values and the measured values. However, for real time application in which sensor nodes must be able to predict if a sent packet will be received or not by a destination node, the integration of WUSN-PLM becomes a key issue due to the required computation and memory resources. In this chapter, we extend our previous works of [153], and [155]. Due to relevant issues like inputs parameters, resources and laboratory tests needed to execute the path loss prediction, we propose a new approach for an *in situ* reliable communications for WUC. This chapter starts by introducing the concepts needed for the good functioning of a fuzzy inference system in Section 5.1; the problem is stated in Section 5.2 and the proposed approach for reliable link wireless underground communications is clearly presented in Section 5.3; The experimentation and the evaluation of the proposed model is given in Section 5.4.

5.1 Fuzzy Inference Systems

In this section, we present the overall functioning of fuzzy inference systems.

The functioning of a Fuzzy Inference System (FIS) is resumed on 3 steps (Figure 5.1): Fuzzification, application of rules within the Inference System and the Defuzzification process [156], [157], [158]. During the fuzzification process, the real inputs variables are converted into

$$\alpha_{TRI}^{A(x)}(x) = \begin{cases} 0 & \text{x} \leq a_1 \\ \frac{x-a_1}{b_1-a_1} & a_1 < \text{x} \leq b_1 \\ \frac{c_1-x}{c_1-b_1} & b_1 < \text{x} \leq c_1 \\ 0 & c_1 \leq \text{x} \end{cases}$$

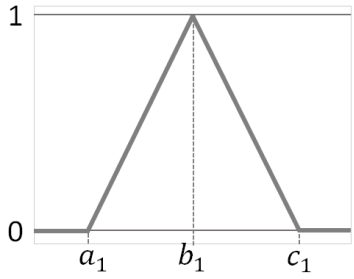

$$\alpha_{TRA}^{A(x)}(x) = \begin{cases} 0 & \text{x} \leq a_2 \\ \frac{x-a_2}{b_2-a_2} & a_2 < \text{x} \leq b_2 \\ 1 & b_2 < \text{x} \leq c_2 \\ \frac{d_2-x}{d_2-c_2} & c_2 < \text{x} \leq d_2 \\ 0 & d_2 \leq \text{x} \end{cases}$$

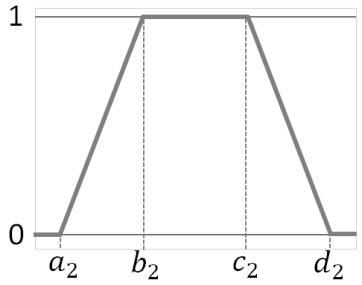

linguistic fuzzy variables. Then, the membership degree of the inputs is computed based on the membership functions before applying operations (AND, OR, NOT) according to the fuzzy rules defined in the inference system. The rules inside the inference system are mostly If-then rules where logical operators AND and OR are equivalent to minimum and maximum. An example of two fuzzy rules R_1 and R_2 are shown as follow:

$$R_1 \textbf{ :} \text{ if } A_1 \text{ is } X_1 \text{ AND } B_1 \text{ is } Y_1 \text{ then } C_1 \text{ is } Z_1$$
$$R_2 \textbf{ :} \text{ if } A_2 \text{ is } X_2 \text{ OR } B_2 \text{ is } Y_2 \text{ then } C_2 \text{ is } Z_2$$
$$\text{With } A_1 \text{ is } X_1 \text{ AND } B_1 \text{ is } Y_1 \Leftrightarrow min(A_1(X_1), B_1(Y_1))$$
$$\text{and '} A_2 \text{ is } X_2 \text{ OR } B_2 \text{ is } Y_2 \Leftrightarrow max(A_2(X_2), B_2(Y_2))$$

Where $A_{1,2}$, $B_{1,2}$ and $C_{1,2}$ are fuzzy sets where $A_{1,2}$ and $B_{1,2}$ are the input sets and $C_{1,2}$ the output sets. $X_{1,2}$, $Y_{1,2}$ and $Z_{1,2}$ are variables of the corresponding fuzzy sets. $A_{1,2}(X_{1,2})$ and $B_{1,2}(Y_{1,2})$ are the membership functions of fuzzy sets $A_{1,2}$ and $B_{1,2}$ respectively. The membership functions can be classified into four (04) types [159]: Piece-wise linear functions, Gaussian distribution function, sigmoid curve and quadratic-cubic polynomial curves. Among these function types, the most used are Piece-wise linear functions which can be either triangular (TRI) or trapezoidal (TRA). Thus, for a crisp input x, the corresponding membership degree $\alpha^{A(X)}(x) \in \{0, 1\}$ to a triangular or trapezoidal membership function $A(X)$ can be computed. Where A denotes a fuzzy set and X a fuzzy variable of A. According to its design, a FIS can either be MISO (Multiple Inputs and Single Output) or MIMO (Multiple Inputs and Multiple Outputs).

The output of the inference system is thereafter converted into a single crisp output through the defuzzification process. There are two famous and widely used FIS in the literature: Mamdani-type [27], [28] and Sugeno-type [160] fuzzy systems.

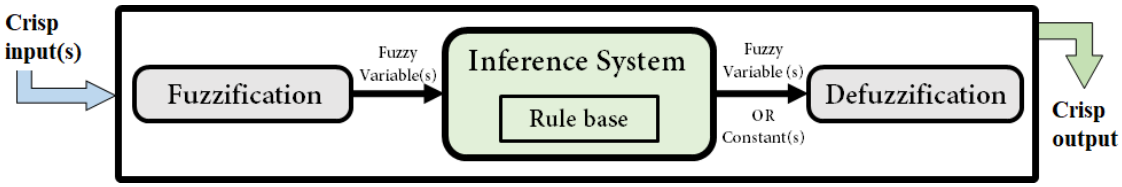

Figure 5.1: Functioning of a Fuzzy Inferrence System.

Another most used FIS is Sugeno-type [160] also known as Takagi-Sugeno-Kang (TSK) fuzzy system. This approach is similar to Mamdani except for the defuzzification process which is more computationally efficient. Moreover, all the Sugeno FIS are only MISO where the output can either be linear or a simple constant. From the previous example, the output $z_{1,2}$ is a linear function that depends on inputs. The resulting crisp output value z^* in Sugeno FIS is the weighted average of each rule inside the inference system according to (5.1).

$$Z^* = \frac{\sum_{i=1}^{n} \alpha_i \times z_i}{\sum_{i=1}^{n} \alpha_i} \tag{5.1}$$

n is the number of rules inside the inference system, α_i denotes the aggregated membership degree of each rule obtained by applying min or max operators. z_i represents the linear output of each rule i.

Despite a large number of FL applications and to the best of our knowledge, there is any previous study or research of reliable communication in WUNS based on FL, thus this presented study is a novel contribution in the fields of WUC and FL.

5.2 Problem Statement

The signal attenuation due to soil properties widely affects the overall reliability of a WUSN, thus the network topology. Despite a large amount of path loss models, the prediction *in situ* of the reception or the loss of a sent packet remains a key issue. To address this issue, we designed the following approach based on FL for a reliable WUC.

5.3 Proposed Approach

In this section, we present our approach for reliable communication in WUSN based on Sugeno FIS.

5.3.1 Design of the Proposed FIS

Our proposed approach is based on the famous Sugeno FIS because of the defuzzification process which is more suitable for a sensor node than in the Mamdani FIS. Our proposed approach is made up of the 04 following inputs (Figure 5.2):

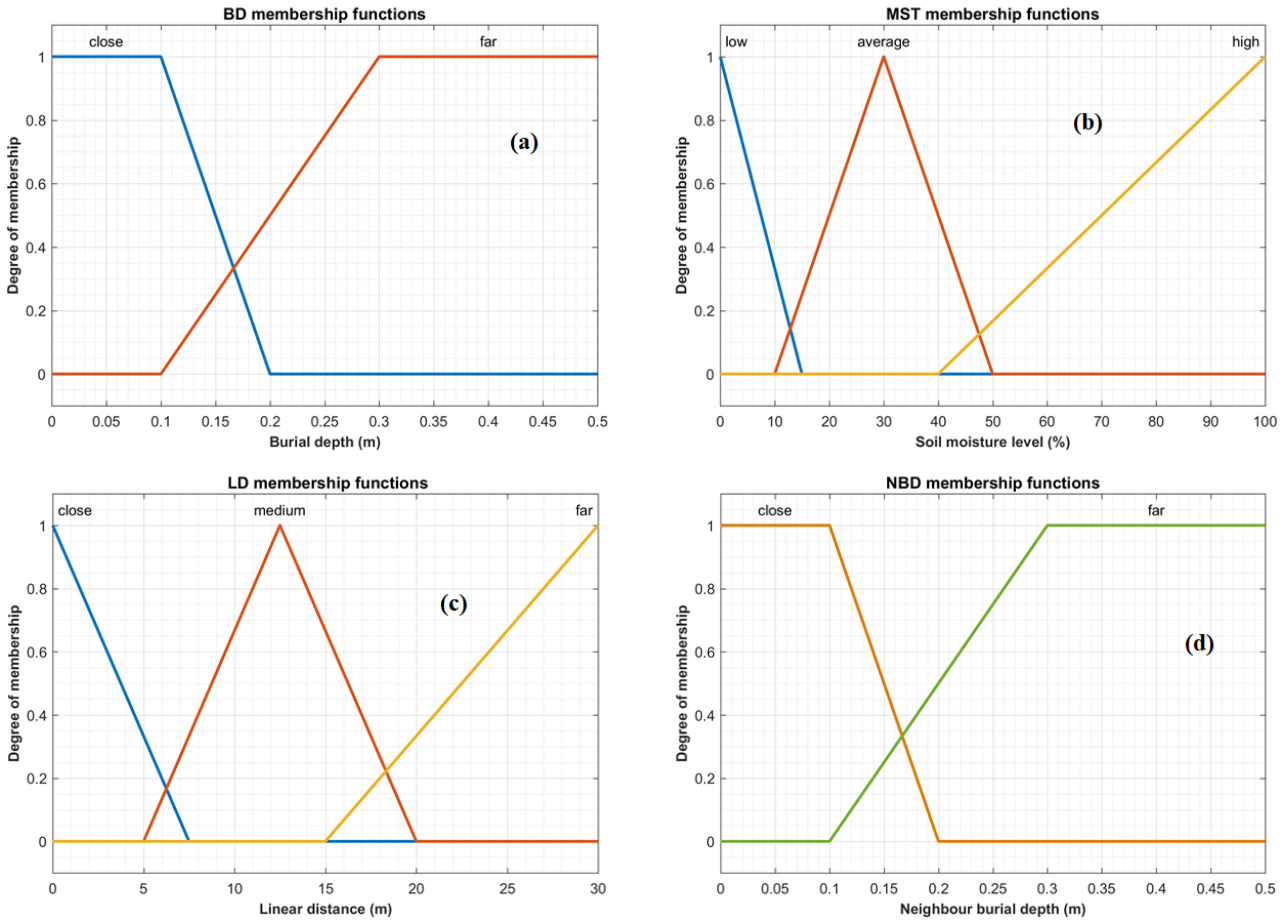

Figure 5.2: Different membership functions of the FIS. a) BD membership functions of FIS that represent the Burial Depth of Transmitter node. b) MST membership function for the soil moisture which varies from very dry (0%) to very moist (100%). c) is the graphical representation of the membership function LD that characterizes the linear distance between transmitter and receiver. d) NDB membership functions of the Burial Depth of Receiver node.

- The **Burial Depth (BD)**: this fuzzy variable describes the burial depth of the sender node which varies from the ground surface (zero meter) to the maximum depth set at $0.5meter$. Two (02) trapezoidal membership functions have been designed for BD fuzzy variable: *close* for depths near the ground surface in the topsoil region; *far* for subsoil depths up to the maximum depth (Figure 5.2a).

- The **Soil Moisture Level (MST)**: It represents the percentage of water within the soil given by one or more soil moisture sensors. Like it is shown in Figure 5.2b, three (03)

triangular membership functions are designed: *low, average* and *high*. They express the level of moisture inside the soil which can vary from 0% to 100%.

- The **Linear Distance (LD)**: It is the distance between a transmitter node and a receiver node regardless of their respective burial depths. We also designed 03 triangular membership functions like the fuzzy variable *MST*: *close, medium* and *far*. The graphical representation of its membership functions is illustrated in Figure 5.2c in which the real values of *LD* range from 0 to $30m$. The maximum range is set due to our experiments conducted at the botanic garden of the University Cheikh Anta Diop of Dakar in Senegal.
- The **Neighbour Burial Depth (NBD)**: this fuzzy variable is identical to BD, the membership functions are the same (Figure 5.2d).

According to the different fuzzy variables and their corresponding membership functions, the maximum number of rules is 36 according to Table 5.1. Furthermore, depending on the location of the transmitter node, the rule number can be reduced.

The output fuzzy variable of the proposed approach is the reliability degree that expresses the probability for a packet to be successfully got by a receiver node. This fuzzy variable has 05 constant values based on the Mamdani output. Thus, the reliability degree can be *Vhigh* (very high), *high*, *medium*, *low* or *Vlow* (very low). Furthermore, the fixed values of the reliability probability with the respective values $0.9, 0.7, 0.5, 0.3$ and 0.1 for each previous linear membership function.

The calculation of the membership degree α of a crisp input x for each of these membership functions is presented in Table 5.2.

The final crisp output of our proposed model is based on the default Sugeno FIS weighted average (5.1). The overview of the proposed fuzzy inference engine is shown by its high-level diagram in Figure 5.3.

5.3.2 Energy Model

In order to evaluate the energy consumption of our proposed, we assume that the membership degree of a rule is computed in one instruction *instr*. Thus, the membership degrees of n rules is performed in n instructions. By assuming that the energy waste by the microcontroller by one instruction is ϵ_{instr}. The time required for the execution of an instruction is t_{instr}. The total energy waste for the crisp output of the FIS is E_{tot} (5.2) and the required time is T_{tot} (5.3).

$$E_{tot} = (n+1) \times \epsilon_{instr} \tag{5.2}$$

Table 5.1: 36 rules in the proposed FIS.

$R1$. (BD=close) & (MST=low) & (LD=close) & (NBD=close) ⇒ (Reliability=Vhigh)
$R2$. (BD=close) & (MST=low) & (LD=close) & (NBD=far) ⇒ (Reliability=Vhigh)
$R3$. (BD=close) & (MST==low) & (LD=medium) & (NBD=close) ⇒ (Reliability=Vhigh)
$R4$. (BD=close) & (MST=low) & (LD=medium) & (NBD=far) ⇒ (Reliability=high)
$R5$. (BD==close) & (MST=low) & (LD=far) & (NBD=close) ⇒ (Reliability=medium)
$R6$. (BD=close) & (MST=low) & (LD=far) & (NBD=far) ⇒ (Reliability=medium)
$R7$. (BD=close) & (MST=average) & (LD=close) & (NBD=close) ⇒ (Reliability=Vhigh)
$R8$. (BD=close) & (MST=average) & (LD=close) & (NBD=far) ⇒ (Reliability=high)
$R9$. (BD=close) & (MST=average) & (LD=medium) & (NBD=close) ⇒ (Reliability=medium)
$R10$. (BD=close) & (MST==average) & (LD=medium) & (NBD=far) ⇒ (Reliability=medium)
$R11$. (BD=close) & (MST=average) & (LD=far) & (NBD=close) ⇒ (Reliability=high)
$R12$. (BD=close) & (MST=average) & (LD=far) & (NBD=far) ⇒ (Reliability=medium)
$R13$. (BD==close) & (MST==high) & (LD==close) & (NBD==close) ⇒ (Reliability=high)
$R14$. (BD=close) & (MST=high) & (LD=close) & (NBD=far) ⇒ (Reliability=high)
$R15$. (BD=close) & (MST=high) & (LD=medium) & (NBD=close) ⇒ (Reliability=high)
$R16$. (BD=close) & (MST=high) & (LD=medium) & (NBD=far) ⇒ (Reliability=medium)
$R17$. (BD=close) & (MST=high) & (LD=far) & (NBD=close) ⇒ (Reliability=medium)
$R18$. (BD=close) & (MST=high) & (LD=far) & (NBD=far) ⇒ (Reliability=low)
$R19$. (BD=far) & (MST=low) & (LD=close) & (NBD=close) ⇒ (Reliability=Vhigh)
$R20$. (BD=far) & (MST=low) & (LD=close) & (NBD=far) ⇒ (Reliability=Vhigh)
$R21$. (BD=far) & (MST=low) & (LD=medium) & (NBD=close) ⇒ (Reliability=Vhigh)
$R22$. (BD=far) & (MST=low) & (LD==medium) & (NBD==far) ⇒ (Reliability=medium)
$R23$. (BD=far) & (MST=low) & (LD=far) & (NBD=close) ⇒ (Reliability=medium)
$R24$. (BD=far) & (MST=low) & (LD=far) & (NBD=far) ⇒ (Reliability=low)
$R25$. (BD=far) & (MST=average) & (LD=close) & (NBD=close) ⇒ (Reliability=Vhigh)
$R26$. (BD=far) & (MST=average) & (LD=close) & (NBD=far) ⇒ (Reliability=medium)
$R27$. (BD=far) & (MST=average) & (LD=medium) & (NBD=close) ⇒ (Reliability=high)
$R28$. (BD=far) & (MST=average) & (LD=medium) & (NBD=far) ⇒ (Reliability=low)
$R29$. (BD=far) & (MST=average) & (LD=far) & (NBD=close) ⇒ (Reliability=medium)
$R30$. (BD=far) & (MST=average) & (LD=far) & (NBD=far) ⇒ (Reliability=low)
$R31$. (BD=far) & (MST=high) & (LD=close) & (NBD=close) ⇒ (Reliability=high)
$R32$. (BD=far) & (MST=high) & (LD=close) & (NBD=far) ⇒ (Reliability=medium)
$R33$. (BD==far) & (MST=high) & (LD=medium) & (NBD=close) ⇒ (Reliability=medium)
$R34$. (BD=far) & (MST=high) & (LD=medium) & (NBD=far) ⇒ (Reliability=low)
$R35$. (BD=far) & (MST=high) & (LD=far) & (NBD=close) ⇒ (Reliability=medium)
$R36$. (BD=far) & (MST=high) & (LD=far) & (NBD=far) ⇒ (Reliability=Vlow)

$$T_{tot} = (n+1) \times t_{instr} \tag{5.3}$$

Additional energy and time are considered to compute the value of z^* (5.1). Since, the proposed FIS used 36 rules, the total energy consumed and the required times to compute the

Table 5.2: Computation of the membership degrees.

Fuzzy sets	**Fuzzy variables**	**Membership degree**	
BD&NBD	close	1	$0 \leq x \leq 0.1$
		$2 - 10x$	$0.1 < x \leq 0.2$
		0	else
	far	0	$0 \leq x \leq 0.1$
		$5x - 1/2$	$0.1 < x \leq 0.3$
		1	else
MST	low	$1 - x/15$	$0 \leq x \leq 15$
		0	else
	average	$x/20 - 1/2$	$10 \leq x \leq 15$
		$5/2 - x/20$	$30 < x \leq 50$
		0	else
	high	$x/15 - 2/3$	$40 \leq x \leq 100$
		0	else
LD	close	$1 - 2x/15$	$0 \leq x \leq 7.5$
		0	else
	medium	$x/5 - 1$	$5 \leq x \leq 10$
		$3 - x/5$	$10 < x \leq 15$
		0	else
	far	$x/20 - 0.5$	$10 \leq x \leq 30$
		0	else

crisp output of the FIS is $37 \times \epsilon_{instr}$ and $37 \times t_{instr}$ respectively.

5.3.3 Reduction of Rules

Due to a large number of rules (36) within the proposed approach can be too much in terms of time processing. We reduced the number of rules according to several scenarios (Figure 5.4).

Sensor node location

On one hand, if the transmitter is placed at least $20cm$ after the ground surface, we assume that it is fully under the ground, thus, the first 18 rules in Appendix 5.1 could be dropped regardless the receiver location. From 5.2, when the burial depth of the transmitter is $\leq 0.2m$, the membership degree of *(BD = close)* is equal to 0. Thus, for rules with the relation *(BD =*

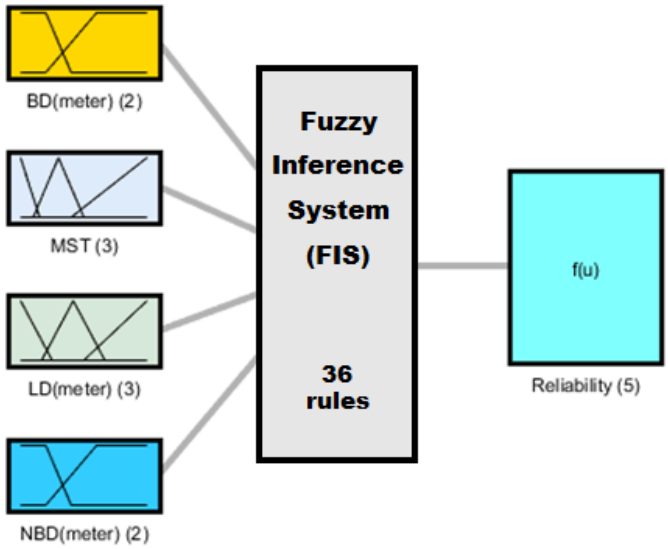

Figure 5.3: High-level diagram of the proposed FIS.

close), the resulting degree of these rules is 0 (Section 5.1). For example, the rule degree α_1 of rule $R1$ is given by:

$\alpha_1 = min$ *(BD (close), MST (low), LD (close), NBD (close))*

Since 0 is the lowest possible value for a membership degree and *BD (close)* $= 0$, we conclude that:

$\alpha_1 =$ *BD (close)* $= 0$

Where *BD (close)*, *MST (low)*, *LD (close)* and *NBD (close)* are the membership degrees of *(BD = close), (MST = low), (LD = close), (NBD = close)* respectively. The linear output z_1 of rule $R1$ is given by :

$z_1 =$ *Reliability (Vhigh)* (with *Reliability (Vhigh)* $= 0.9$)

The same approach is applied for Rules $R1$ to $R18$, and $\alpha_i = 0$ (for $i = 1$ to 18). Since the crisp output z^* (5.1) is based on the weighted average of each rule, the weighted of the 18 first rules will not affect its value, they can be avoided for the crisp output value.

On the other hand, if the receiver node is located after the $20cm$ depth, the rule number used for estimating the link reliability is reduced in half regardless of the location of the transmitter. 18 rules are canceled for the computation of z^*. Similar to buried transmitter scenario, all the rules with the relation *(NBD = close)* will have a null degree because *NBD (close)* $= 0$. When the receiver node is fully buried, only even-numbered rules are considered ($R2$, $R4$, $R8$, $R6$, ..., $R34$, $R36$).

By reducing the number of rules needed to compute the FIS crisp output from 36 to 18, we reduce the computation time in half. Furthermore, the energy consumed is reduced to $19 \times \epsilon_{instr}$ and the computational time is reduced to $19 \times t_{instr}$. When the transmitter or the receiver

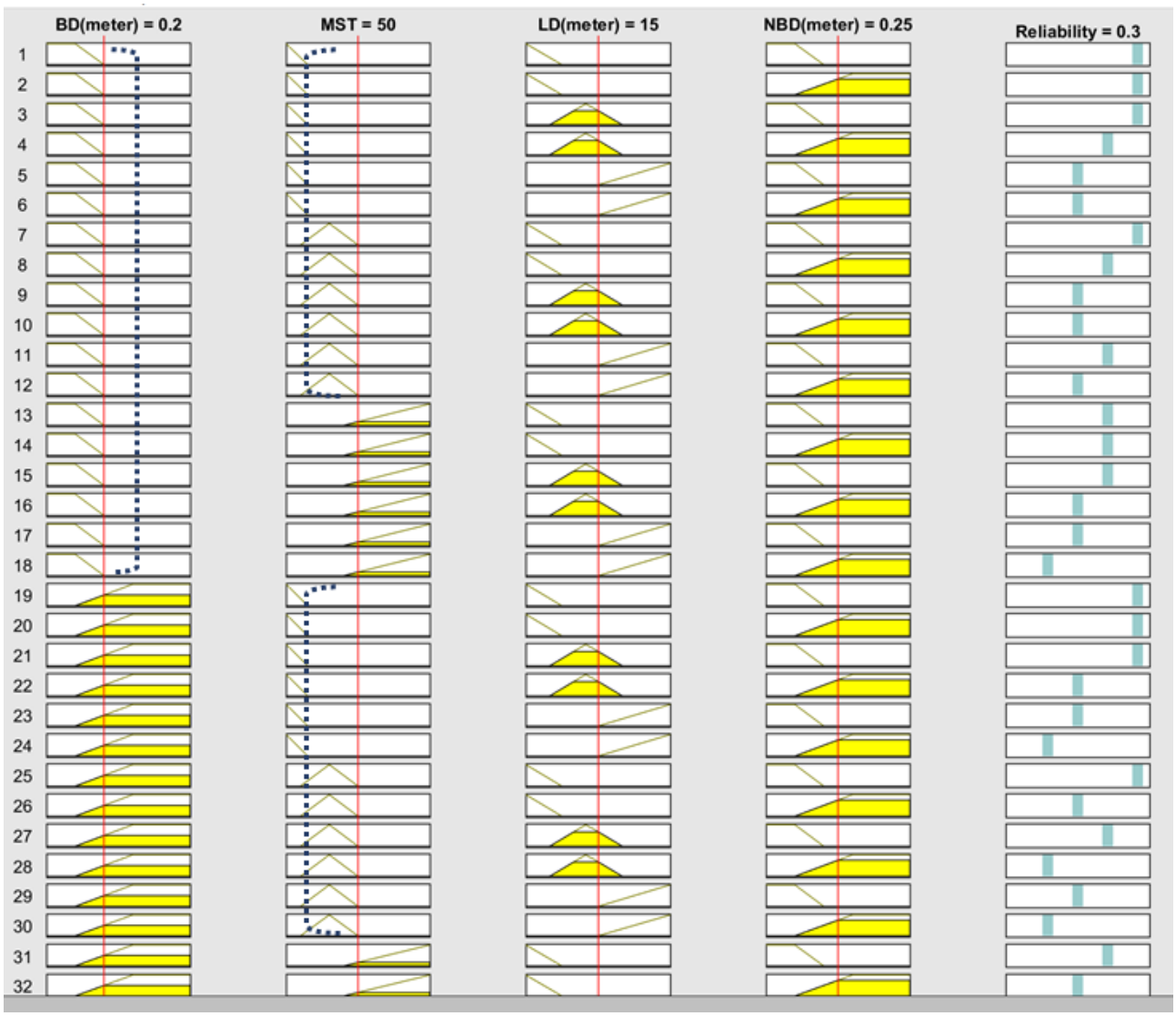

Figure 5.4: Reduction of rules according to the location of the transmitter (20cm Burial depth) and the soil moisture level (around 50%). The rules which no intersection with the inputs (BD=0.2 and MST=50) are neglected for link reliability computation.

sensor node is fully buried under the ground (depth at least 20cm).

However, for fully underground communication between the transmitter and the receiver, the previous 18 needed rule can be reduced. For this kind of communication, the transmitter and the receiver are located at least 20cm depth afer the ground surface. only 9 rules are taken into account for the calculation of z^*. This is because all the rules of Appendix 5.1 with relations *BD (close)* or *NBD (close)* are neglected. During underground communications, the proposed model uses rules $R20$, $R22$, $R24$, $R26$, $R28$, $R30$, $R32$, $R34$, and $R36$. The energy consumption is $10 \times \epsilon_{instr}$ and the computational time becomes $10 \times t_{instr}$.

Soil moisture level

When the soil is dry, the corresponding soil moisture is assumed to be around 0%. According to the computation of membership degrees of Table 5.2 and to the Appendix 5.1, a total of 24 rules can be canceled for the calculation of the crisp output. Only 12 rules are required for our proposed FIS. Furthermore, the rules $R7$ to $R18$ and rules $R25$ to $R36$ have the same null degree. This is because the membership degree for the membership functions *average* and *high* of the fuzzy set *MST* is equal to 0 for null soil moisture (dry soil). For example, the computation of the rule degree α_9 of the $R9$ is performed as follows:

$\alpha_9 = min$ (*BD (close), MST (average), LD (medium), NBD (close)*)

However, for dry soil, *MST (average)* = *MST (high)* = 0, thus,

α_9 = *MST (average)* = 0

Where *BD (close)*, *MST (average)*, *LD (medium)* and *NBD (close)* are the membership degrees of *(BD = close), (MST = average), (LD = medium), (NBD = close)* respectively. The corresponding linear output z_9 of the rule $R9$ is given by

z_9=*Reliability (medium)* (with *Reliability (medium)* = 0.5)

Similar to Section 5.3.3, all the rules with null degree are dropped. Thus, 24 rules are cancelled and 12 rules are used ($R1$ to $R6$ and $R19$ to $R24$).

Furthermore, according to the membership functions *low* and *average* of the fuzzy set MST in Figure 5.2b, the previous 12 rules needed to estimate the reliability of the channel are the same when the soil moisture is lesser than 10%. Thus, when the soil moisture $mst \in [0, 10\%]$ the 12 rules needed for the crisp output computation are the same as for dry soil, they are: $R1$, $R2$, $R3$, $R4$, $R5$, $R6$, $R19$, $R20$, $R21$, $R22$, $R23$, $R24$.

When the measured soil moisture $mst \in [15, 40\%]$, the membership functions low and high are null. Thus, all the rules with the relations *(MST = low)* or *(MST = high)* are removed for the crisp output computation. Therefore, *MST (low)* = *MST (high)* = 0, thus, all the rules with these relation are not taken into account. The rules dropped are : $R1$ to $R6$, $R13$ to $R24$ and $R31$ to $R36$. Similar to soil moisture from 0% to 10%, the needed rules are reduced to 12 when the sensed soil moisture $mst(\%) \in [15, 40\%]$. They are: $R7$, $R8$, $R9$, $R10$, $R11$, $R12$, $R25$, $R26$, $R27$, $R28$, $R29$, $R30$.

Similar to previous cases, if the moisture is between 50% and 100%, the membership functions *low* and *average* are null. In order terms, *MST (low)* = *MST (average)* = 0. The rules with the relations *(MST = low)* or *(MST = average)* are neglected. Thus, for the reliability computation when the collected soil moisture $mst \in [50, 100\%]$; the rules considered are $R13$ to $R18$ and $R31$

to $R36$.

When the sensed soil moisture $mst \in [0, 10\%] \cup [15, 40\%] \cup [50, 100\%]$ The time needed to compute the crisp output is $13 \times t_{instr}$. The overal energy consomed during the calculation the link reliability is $13 \times \epsilon_{instr}$.

Additionally, according to the sensor node location presented in Section 5.3.3, the 12 rules needed for the reliability computation can be further reduced.

When the transmitter is buried under the ground and the soil moisture $mst \in [0, 10\%]$, the rules with at least one of the relations *(BD = close)* or *(MST = average)* or *(MST = high)* are neglected. Thus only 6 rules are considered to compute the reliability of the channel. The needed rules are: $R19$, $R20$, $R21$, $R22$, $R23$ and $R24$. Similarly, when the soil moisture $mst \in [15, 40\%]$, the 6 rules used are $R25$, $R26$, $R27$, $R28$, $R29$ and $R30$. This is because the rules with at least one of the relations *(BD = close)* or *(MST = low)* or *(MST = high)*are dropped. Meanwhile, if the collected soil moisture $mst \in [50, 100\%]$, the rules with at least one relations *(BD = close)* or *(MST = low)* or *(MST = average)* are not considered. The 6 remaining rules are $R31$, $R32$, $R33$, $R34$, $R35$ and $R36$.

When the receiver is fully buried and the soil moisture $mst \in [0, 10\%]$, all the rules with at least on the relations *(MST = average)* or *(MST = high)* or *(NBD = close)* are not considered for the crisp output computation. The rules used for its calculation are $R2$, $R4$, $R6$, $R20$, $R22$ and $R24$. If the sensed soil moisture $mst \in [15, 40\%]$, the membership functions *close* (for the BD fuzzy set), *low* and *high* (MST fuzzy set) are null. the rules considered for the link estimation are $R8$, $R10$, $R12$, $R26$, $R28$ and $R30$. Nevertheless, when $mst \in [0, 10\%]$ and the receiver is buried under the ground surface, the rules with at least one of the relations *(MST = low)* or *(MST = average)* or *(NBD = close)* are neglected for the reliability computation. The rules $R14$, $R16$, $R18$, $R32$, $R34$ and $R36$ are used for the link reliability.

In short, when the transmitter or the receiver is buried under the ground surface and the soil moisture $mst \in [0, 10\%] \cup [15, 40\%] \cup [50, 100\%]$, the overall energy consumed is $7 \times \epsilon_{instr}$ and the needed computation time is $7 \times t_{instr}$.

For fully underground communication, the useful rules for the crisp output computation are reduced to 3. Indeed, when the soil moisture $mst \in [0, 10\%]$ all the rules with at least on of the relations *(BD = close)* or *(MST = average)* or *(MST = high)* or *(NBD = close)* are removed for the crisp output calculation. Therefore, the needed rules are $R20$, $R22$ and $R24$. However if $mst \in [15, 40\%]$, the same idea is executed, thus, the membership functions *close* (Burial Depth fuzzy set), *close* (Neighbour Burial Depth fuzzy set), *low* and *high* (Soil Moisture Level fuzzy set) are null. Only the rules $R26$, $R28$ and $R30$ are considered in order to calculate the crisp output z^*. Nevertheless, if $mst \in [50, 100\%]$, the soil moisture is assumed to be high. Thus,

for this range value, the membership functions *low* and *average* of the fuzzy set *MST* are null. for fully underground communication, the rules with at least of the relations *(BD = close)* or *(MST = low)* or *(MST = average)* or *(NBD = close)* are not required for the final evaluation of the link reliability. The rules used in this scenario are $R32$, $R34$ and $R36$.

For each of the previous scenarios, energy consumption is reduced to $4 \times \epsilon_{instr}$ and the corresponding processing time is $4 \times t_{instr}$.

Distance between sensor nodes

Similarly to section 5.3.3, the number of rules can be reduced according to the linear distance between nodes. Indeed, if the distance *ld* between the transmitter and the receiver $\in [0, 5] \cup [7.5, 15] \cup [20, 30]$, The 36 rules are reduced to 12 useful rules needed for the computation of the link reliability. Moreover, according to the location of the transmitter or the receiver node, the 12 rules are reduced to 6. Thus, for fully underground communication with sensor nodes buried under the ground surface, the rules needed for crisp output evaluation become 3.

By assuming that transmitter and receiver nodes are fully buried (depth more or equal to $20cm$); and the average soil moisture between them $\in [0, 10]$, the rules are reduced according to the linear distance *ld* between the sensor nodes. We subdivide the distance set into 5 ranges and the maximum number of rules needed for each range is at most 2 rules.

- *ld*$\in[0, 5]$: All the rules with at least one of the relations *(BD = close)* or *(MST = average)* or *(MST = high)* or *(LD = medium)* or *(LD = far)* or *(NBD = close)* are neglected. The initial 36 rules are reduced to just one (01) rule ($R20$: *(BD =far)* & *(MST = low)* & *(LD = close)* & *(NBD = far)* $\Rightarrow$ *(Reliability = Vhigh)*). Thus the computed crisp output related to the link reliability corresponds to the linear output. In orther words, $Z^* = z_{20} =$ *Reliability (Vhigh)* $= 0.9$. The energy used for its calculation is $2 \times \epsilon_{instr}$ and the execution time is $2 \times t_{instr}$.

- *ld*$\in]5, 7.5[$: For this case, the number of rule necessary for the computation of the crisp output used for decision-making is reduced to 2 rules (rules $R20$ and $R22$). This reduction is because the 34 dropped rules have at least one of the relations *(BD = close)* or *(MST = average)* or *(MST = high)* or *(LD = far)* or *(NBD = close)*. The calculation of the probability for the link reliability is based on (5.1) with $n = 2$, $z_1 =$ *Reliability (Vhigh)*$= 0.9$, $z_2 =$ *Reliability (medium)* $= 0.5$, α_1 and α_2 are the aggregated membership degrees of rules $R20$ and $R22$ respectively. A total energy consumed for the crisp output computation is reduced to $3 \times \epsilon_{instr}$. A time needed for its computation becomes $3 \times t_{instr}$.

- *ld*$\in[7.5, 15]$: The rule $R22$ (*(BD = far)* & *(MST = low)* & *(LD = medium)* & *(NBD = far)* $\Rightarrow$ *(Reliability = medium)*) is the unique rule important for decision-making in

our approach. All the rules with relations *(BD = close)* or *(MST = average)* or *(MST = high)* or *(LD = low)* or *(LD = far)* or *(NBD = close)* are not considered. Then, the crisp output $Z^* = z_{22} =$ *Reliability (medium)* $= 0.5$. Thus, the energy consumed and the execution time is $2 \times \epsilon_{instr}$ and $2 \times t_{instr}$ respectively.

- $ld \in]15, 20[$: Similar to the case when $ld \in]5, 7.5[$, the crisp output is computed based on 2 rules ($R22$ and $R24$). Where $z_1 =$ *Reliability (medium)* $= 0.5$ and $z_2 =$ *Reliability (low)* $= 0.3$. α_1 and α_2 are the degree of the rules $R22$ and $R24$ respectively. Similar to the case when $ld \in]5, 7.5[$, the energy consumed and the corresponding execution time for the crisp output computation is $3 \times \epsilon_{instr}$ and $3 \times t_{instr}$ respectively.

- $ld \in [20, 30]$: Similarly to $ld \in [7.5, 15] \cup [0, 5]$, a total of 35 rules can be neglected. The membership functions *close* (BD fuzzy set); *average* and *high* (MST fuzzy set); *close* and *medium* (LD fuzzy set); *close* (NBD fuzzy set) are null. Thus, only an unique rule ($R24$: *(BD = far)* & *(MST = low)* & *(LD = far)* & *(NBD = far)* $\Rightarrow$ *(Reliability = medium)*) is used for the computation of the crisp output (Z^* = *Reliability (low)* $= 0.3$). The energy consumed during the calculation of the link reliability is reduced to $2 \times \epsilon_{instr}$. The time elapsed for the computation of the reliability probability is $2 \times t_{instr}$.

5.4 Experimentation and Results

In this Section, experiments are conducted in order to evaluate our proposed model.

5.4.1 Data Collection

The data set uses to evaluate this approach is similar to the methodology processes of WUSN-PLM [155] presented in Section 4.3.3. The burial depths of nodes vary from the ground surface to $40cm$ and the linear distance between them ranges from $5m$ to $20m$ with steps of $5m$ (Figure 5.5). Moreover, when a sensor node is placed at the ground surface, its burial depth is set to zero (0). For our presented approach, we use two configurations: dry soil and moist soil. The dry soil will mean a soil with zero moisture, however, when the moisture will be different from 0, we will talk of moist soil. A total of 80 and 60 measurements are conducted for dry and moist soil configurations, thus a total of 140 real observations identical as our previous work on the WUSN-PLM [153],[155]. Since the proposed approach does not enable to give the value of the path loss, only the measurements conducted with the nRF905RF transceivers are considered (Figure 5.5).

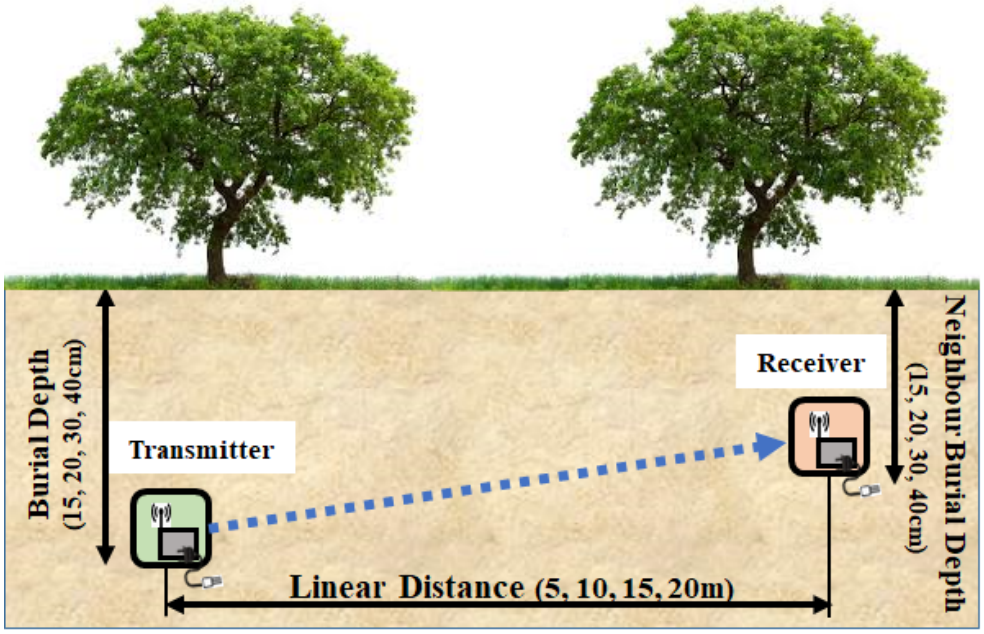

Figure 5.5: Measurement process of wireless underground communications between sensor nodes.

5.4.2 Results and Validation

For the evaluation of the proposed approach, we define the positive class as the reception of a packet (*received*) and the negative class for the not reception of a sent packet (*not received*).

According to each of the 140 observations performed, we associate $(bd, mst, ld, nbd) \in BD \times MST \times LD \times NBD$ related to the burial depth of the sensor nodes, the average sensed soil moisture and the distance between the nodes. The reliability is computed according to Section 5.3. Thus, for each scenario, we evaluate the crisp output of the proposed FIS according to the positive and the negative classes.

Knowing that the output of a Sugeno FIS is a crisp output (real value), the reliability of WUC is established by the following assumption.
Assumption: If the calculated probability for the link quality is less than 0.5***, a sent packet by a transmitter will not reach the receiver node: there is a packet loss. However, if the calculated reliability is equal or higher than*** 0.5 ***a packet is well received by the receiver: there is a packet reception.***

Appendices B.4, B.5 and B.8 present extract of the real experiments conducted in dry soil (Appendix B.4) and moist soil configurations (Appendices B.5 and B.8).

For each linear distance ($5m$, $10m$, $15m$ and $20m$) of dry soil configuration, 24 observations per linear distance are observed. Appendix B.4 below presents the computed reliability by our proposed FL approach and the observations in dry soil when the distance between the two nodes is $20m$. From Appendix B.4, the proposed approach has get 20 good predictions ($8TP$

Table 5.3: Confusion matrices comparison of WUSN-PLM and the proposed approach in dry soil configuration.

		Observation			
		WUSN-PLM		**Proposed FL**	
		Rcv.	Not rcv.	Rcv.	Not rcv.
Prediction	Rcv.	68TP	8FP	68TP	0FP
	Not rcv.	0FN	4TN	0FN	12TN

and $12TN$) over 20 observations. Thus, the proposed FL has a perfect sore with 0% error.

The same experiments of Appendix B.4 are repeated for $5m$ (Appendix B.1), $10m$ (Appendix B.2) and $15m$ (Appendix B.3) linear distances. Thus a total of 80 measurements for dry soil configuration. From the 80 tests conducted in dry soil configuration, the proposed approach obtains a perfect score with 80 good predictions ($68TP$ and $12TN$) i.e. 100% accuracy and 0% error. The comparison of the proposed approach and WUSN-PLM in dry soil configuration is resumed in the confusion matrix of Table 5.3. For dry soil configuration, WUSN-PLM performs 72 good predictions ($68TP$ and $4TN$) and 8 bad predictions ($0FN$ and $8FP$) over the 80 measurements. With 100% accuracy, the proposed FL approach outperforms the powerful path loss model WUSN-PLM which has 90% accuracy and a prediction error of 10%.

The slightly same experiments are conducted in moist soil, Meanwhile, the sensor burial depths vary from the ground surface to $30cm$ in depth for a practical reason. In each measurement carried out, the sensed soil moisture is taken into consideration as an input. Its value is given by the soil moisture sensors YL-69 equipped in each sensor node. Thus, the average sensed value of the soil moisture between the transmitter and the receiver nodes is considered for the observations. For example, Appendices B.5 and B.8 show the results of measurements conducted when the transmitter is either placed at the ground surface (burial depth is $0cm$) and at $30cm$ in depth respectively. Thus, a total of the 28 observations are presented for the Appendices B.5 and B.8, the proposed FL model for link reliability gives 5 wrong predictions ($1FP$ and $4FN$) and 23 good predictions ($14TP$ and $9TN$). The accuracy of the proposed approach is 82.14% for a prediction error of 17.86%.

The same measurements have been conducted for $15cm$ (Appendix B.6) and $20cm$ (Appendix B.7) burial depth of the transmitter node, therefore 32 additional measurements to Appendices B.5 and B.8. For the 4 depths ($0cm$, $15cm$, $20cm$ and $30cm$) from sensor nodes side, a total of 60 observations are conducted in moist soil configuration. The comparison of observations in moist soil of the WUSN-PLM is presented in the confusions matrices presented in Table 5.4. We observe that over the 60 measurements in moist soil both approaches get slightly the same predictions: The WUSN-PLM performs 49 good predictions ($20TP$ and $29TN$) and the proposed FL approach get a total of 48 good predictions ($25TP$ and $23TN$) over 60 measurements. The

Table 5.4: Confusion matrices comparison of WUSN-PLM and the proposed approach in moist soil configuration.

		Observation			
		WUSN-PLM		**Proposed FL**	
		Rcv.	Not rcv.	Rcv.	Not rcv.
Prediction	Rcv.	20TP	3FP	25TP	9FP
	Not rcv.	8FN	29TN	3FN	23TN

Table 5.5: Confusion matrices comparison of WUSN-PLM and the proposed approach in dry and moist soil configurations.

		Observation			
		WUSN-PLM		**Proposed FL**	
		Rcv.	Not rcv.	Rcv.	Not rcv.
Prediction	Rcv.	88TP	13FP	93TP	9FP
	Not rcv.	8FN	31TN	3FN	35TN

proposed approach is able to better predict the positive class (reception of a data) than the path loss model WUSN-PLM ($25TP$ against $20TP$).

The overall measurements conducted for dry and moist soils configuration is 140. The corresponding confusion matrices of the proposed approach and the WUSN-PLM are given in Table 5.5. Over the 140 cases, the proposed FIS outperforms the path loss model WUSN-PLM with 128 good predictions ($93TP$ and $35TN$) and 88 good predictions ($88TP$ and $31TN$) respectively. The proposed FIS gets a lower prediction error than the WUSN-PLM (Figure 5.6). To evaluate and compare the reliability of the proposed model to the WUSN-PLM, we use the metrics presented in (Eq. 4.7) in order to evaluate prediction models.

From Table 5.6, the proposed FL approach outpeforms the WUSN-PLM. Indeed, it peforms very good accuracy (91.429%) against 85% observed by the path loss model WUSN-PLM. Furthermore, it gets a higher *SEN* (0.969), *SEL* (0.795) and *PRE* (91.176%) than the path loss model WUSN-PLM which performs 0.917, 0.705 and 87.129% respectively.

Furthermore, due to the size inequality of the positive (*Received*) and the negative classes (*Not received*) (96 and 44 respectively), the previous accuracy ACC is not sufficient to evaluate the reliability of prediction models. For such case, the calculation of the balanced accuracy $bACC$ (4.8) instead of the accuracy is more suitable to evaluate the performance of a prediction model. From Table 5.6, we observe that despite the size inequality of the measurements considered, the proposed FIS obtains a higher balanced accuracy than the WUSN-PLM (88.21% and 81.061% respectively).

In order to evaluate the correlation between the prediction and the observation, the MCC is

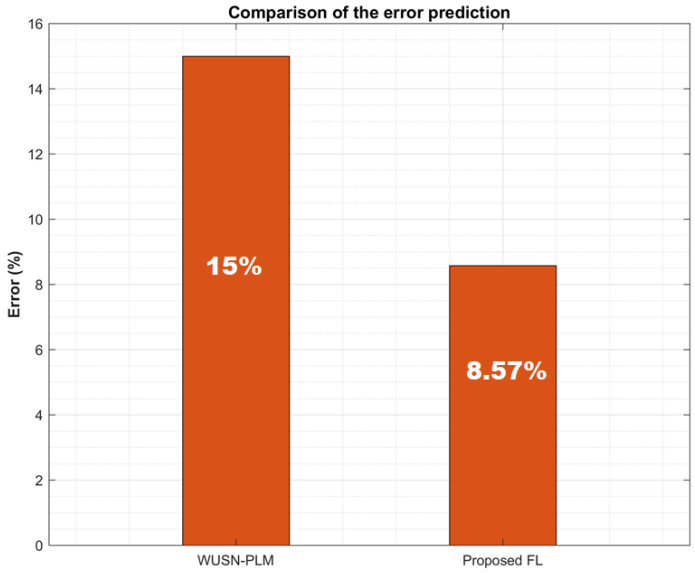

Figure 5.6: Comparison of the prediction errors of the proposed FL and the WUSN-PLM.

Table 5.6: Evaluation and comparison of the performance of the Proposed FIS.

	SEN	**SEL**	**PRE (%)**	**ACC (%)**	**bACC (%)**	**MCC**	**AUC**
WUSN-PLM	0.917	0.705	87.129	85	81.061	0.643	0.92
Proposed FL	0.969	0.795	91.176	91.429	88.21	0.798	0.92

calculated according to (4.8). From Table 5.6, the calculated *MCC* in the proposed FL approach is better than in the WUSN-PLM (0.643 and 0.785 respectively). In order words, it shows that the correlation between the prediction and the observation is higher in the proposed FL than in WUSN-PLM despite the unequal size of the observed classes.

Furthermore, in order to evaluate the proposed approach independently of the fixed threshold (0.5) and the insensibility to class distribution, we use the powerful *Receiver Operating Characteristic* (*ROC*) curve. The ROC curve evaluates the trade-off between the true and the false positive rate of our proposed approach through a graphical representation. By varying the threshold value from 0.00 to 1.00, the resulting ROC curve is presented in Figure 5.7. We observe that the *ROC Curve* is well above the random guess, thus confirms the good accuracy of the proposed approach.

Similar to the WUSN-PLM model, the value of the Area Under Curve (AUC) which quantifies the efficiency of the *ROC Curve* is calculated according to the trapezoidal rule describe in (4.10). From Figure 5.7, 21 trapezoids have been considered for the calculation of AUC.

By applying the relation (4.10) with $n = 21$ on the ROC curve (Figure 5.7), the proposed FL approach gets 0.92 in AUC. Thus, the proposed approach has 91.78% change to distinguish positive class (reception of a packet) from the negative class (not the reception of a packet)

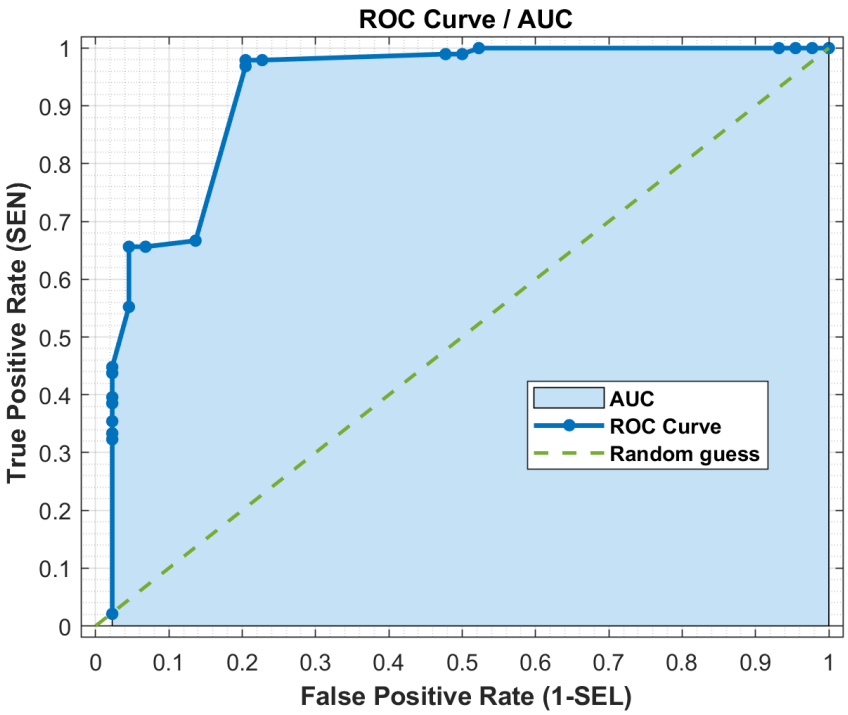

Figure 5.7: ROC curve and AUC of the proposed FIS.

regardless of the threshold used for the delimitation of classes. The AUC of the proposed FL based appraoch is slightly similar to the WUSN-PLM's AUC value.

5.5 Conclusion

In this chapter, we presented an intelligent and reliable WUSN communication based on FL. In order to achieve this, we use the Sugeno FIS due to its simplified defuzzification process. In order to find the probability of receiving a packet by a node, we considered in our model 4 fuzzy sets as inputs: the transmitter and receiver burial depths, the soil moisture, the linear distance between transmitter and receiver. 4 trapezoidal and 6 triangular membership functions have been designed for the input sets. The output fuzzy set represents the reliability degree of packet delivery classified into 5 constants. In order to evaluate the proposed FL approach, 140 observations from real experiments of our previous works have been considered. The results show that our proposal outperforms the path loss model WUSN-PLM with 88.21% balanced accuracy against 81.061%. Moreover, by comparing the MCC, we observe that obtains a higher correlation between the prediction and the actual case than the WUSN-PLM (0.798 and 0.643 respectively). Furthermore, despite the 36 rules defined within our proposed FIS, we showed that, according to some fixed parameters like the burial depth or the linear distance, the rules can be reduced to only one. Thus the energy and the computation time needed are widely reduced.

Conclusion and Future Directions

Conclusion

Advances in microelectronic mechanical systems and wireless communication technologies have led to the proliferation of wireless sensor networks (WSNs) and specially Wireless Underground Sensor Network (WUSN). WUSNs have attracted high attention for their great variety of novel applications, such as underground soil condition and power grid monitoring, mine disaster prevention and rescue, oil gas extraction, earthquake and landslide forecast, border patrol and security, ecological monitoring and precision agriculture. In such application, the sensors are buried under the ground in order to estimate the properties of soils and the water content necessary for the good growth of plants. Thus, the exact amount of water needed by the plant is supplied by an intelligent watering system for an efficient use of water resource. The final user can either decide to water a particular zone after receiving data from buried nodes of the same zone. He may either decide to not water a particular zone which has enough water, thus, saves water resource. However, due to underground environments, EM waves are widely attenuated in the soil. According to soil properties the topology of the WUSN would change. The design of a WUSN is related to the realization of reliable wireless underground communications between buried sensor nodes and aboveground user or BS.

In order to allow a reliable communications between buried sensor nodes, We firstly look at designing an accurate path loss model to predict the signal attenuation in the soil. The evaluation of the EM wave loss depends on several parameters such as the temperature, bulk density, particle sizes, moisture, sand and clay portions. Most of the existing path loss models consider the Peplinski derivations for the prediction of the CDC which characterize the soil properties according to the previous parameters. Contrary to famous Peplinski derivations used by the existing path loss models, we integrate a newer approach that considers in addition to free water presence in moist soil, the presence of bound water which seems to be higher. This approach is called the MBSDM. By using the MBSDM, we increase the accuracy of the existing path loss models. The validation of this approach is performer within a real experimental field

with real sensor node devices based on ARDUINO UNO boards. During the measurement process, the linear distance between the transmitter and receiver varies from 5 m, to 20 m with 5 meters steps. Similarly, we vary the burial depth of the transmistter and receiver nodes (from surface of the earth, 15 cm, 20 cm, 30 cm to 40 cm). The experimentations revealed that the proposed model is more accurate with lesser errors than the well-known conventional modified Friis and NC modified Friis. Furthermore, by taking into account an error of $\pm 3\%$ gives by the soil moisture device used, we observe that the propose approach is still better than the other models.

Secondly, we address the limits of the proposed approach by proposing a new path loss model called WUSN-PLM designed for an application of precision agriculture by taking into account the different types of wireless underground communications (UG2UG, UG2AG and AG2UG). In order to propose an unique model for the 3 communication types, the resumed the communication in precision agriculture in to AG2UG2AG by assuming that each buried node is placed into a waterproof plastic box which contains air and protect the node components. In type of communication, a signal sent by a transmitter will successively crosses the air, the ground and the air before reaching the destination node. In addition to wuc types, the proposed WUSN-PLM considers the different phenomena that occur in different depths of the soil. The soil is sub dived into topsoil (first 30cm of the surface) and into subsoil (after 30cm depth) regions. Thus, the WUSN-PLM is defined either for top depths or for sub depths. To evaluate the WUSN-PLM, intensive real experiments according to the measurement process describes previously within the botanic garden of the University Cheikh Anta Diop of Dakar in Senegal in a culture of onions. A total of 140 measurements have been conducted and the evaluation process considers furthermore two different pairs of transceivers for wireless communications (LoRa SX1278 and nRF905). From the 140 measurements, 80 measures have been conducted in dry soil and 60 measures in moist dry with varied soil moisture level. The proposed path model obtains the highest precision, balanced accuracy and MCC (87.13%, 81.01% and 0.64 respectively). Thus, there is a high correlation between the predicted values of the path loss and the real measurements. The comparison of the WUSN-PLM with existing path loss models shows that the proposed approach gets the lowest RSME, MAE and MAPE (32.7, 29.4 and 30.1 respectively).

Despite the high accuracy of the proposed WUSN-PLM, the real time prediction of wireless underground links remains a key challenge. In order to allow a reliable communication between buried sensor nodes, we propose a lightweight and easy to integrate in real device based on the well-known computational intelligence paradigm called fuzzy logic. The proposed scheme is based on the Sugeno FIS due to its simplified defuzzification process which gives as output a real value. This output is the probability of receiving a packet by another node. The proposed fuzzy inference system is made up of 04 fuzzy sets as inputs: the transmitter and receiver burial

depths, the soil moisture, the linear distance between transmitter and receiver. From the inputs sets, there are 4 trapezoidal and 06 triangular membership functions designed. The output set represents the reliability degree of packet delivery classified into 5 constants (0.9, 0.7, 0.5, 0.3 and 0.1). The FIS consists of 36 rules according the input parameters and the reliability output. The overall number of rules (36) can be reduced to only one according to several scenarios depending on the sensor node locations, the soil moisture level and the linear distance between buried nodes. Thus, the energy and the computation times needs for the FIS execution can be widely reduced. The evaluation process of the proposed solution considers the 140 observations from real experiments of the WUSN. The results have shown that our proposal outperforms the path loss model WUSN-PLM with 88.21% balanced accuracy against 81.061%. Moreover, by comparing the MCC a higher correlation between the prediction and the actual case than the WUSN-PLM (0.798 and 0.643 respectively) is noteworthy.

Future Works and Directions

Despite the promising results in the prediction of EM attenuation in soil according to soil properties, several improvements are possible:

- Additional evaluation in different sensor fields must be conducted in order to increase the portability and the reliability of the proposed WUSN-PLM:

  Indeed, during the validation of our model, only the soil type of the Botanic Garden (sandy clay type) of the University Cheikh Anta Diop has been considered. Knowing the MBSDM is related to clay portion in soil, another soil type with higher or lesser clay proportion than our experimental field should be considered for the evaluation and the portability of WUSN-PLM.

- The fuzzy based approach should be adapted for another type of application such as terrestrial or underwater WSNs:

  Since the proposed FIS is only designs for wireless underground communications, its investigation and behavior in TWSNs needs more investigation. Moreover, for WUSN application such as paddy culture in which the present of water in soil is around 100%, comparison between UWSN and WUSN path loss models should be performed so an unique path loss model for such culture could be investigated the deployment of sensor nodes.

- The integration of the fuzzy based solution for reliable wireless underground communication in recent routing protocol such as optimized clustering solution needs more investigation:

recent researches on WSN show that routing techniques widely increase the lifetime of a WSN. Most of these routing protocols aim at reducing the energy wastage in large scale WSN through the clustering techniques. These latter are based on recent researches conducted on Machine Learning or Computational Intelligence. Thus, merging a reliable communication model such as our proposal to an optimized clustering solution need more investigation for improving the Quality of Service and the lifetime in WSN especially in WUSN.

- The fault tolerance in such embedded system is a crucial issue to address:

  By using low-cost devices in application such as the precision agriculture in WUSN, sensor nodes can fail due to environmental parameters. In order to save the sensed data, the different failures must be investigated and thereafter appropriate approaches should have to be implemented by taking into account the limited resources of the sensor nodes.

Bibliography

[1] R. Maignien, "Carte Pédologique du Sénégal," tech. rep., Office de la Recherche Scientifique et Technique Outre-Mer (ORSTOM), Dakar, 1965.

[2] N. Aminata Badiane, "Etudes Cartographiques et Agro-Pedologiques des Sols de Plateau de Basse-Casamance," tech. rep., Institut Sénégalais de Recherches Agricoles (ISRA), Dakar, 1984.

[3] W. Dargie and C. Poellabauer, *Fundamentals of Wireless Sensor Networks*. Chichester, UK: John Wiley & Sons, Ltd, 2010.

[4] D. Wohwe Sambo, B. O. Yenke, A. Förster, and P. Dayang, "Optimized Clustering Algorithms for Large Wireless Sensor Networks: A Review," *Sensors*, vol. 19, no. 2, pp. 1–27, 2019.

[5] M. R. Senouci and A. Mellouk, "Wireless Sensor Networks," in *Deploying Wireless Sensor Networks*, pp. 1–19, Elsevier, 2016.

[6] A. Salam, M. C. Vuran, and S. Irmak, "Di-Sense: In situ real-time permittivity estimation and soil moisture sensing using wireless underground communications," *Computer Networks*, vol. 151, no. January, pp. 31–41, 2019.

[7] X. Dong and M. C. Vuran, "Impacts of soil moisture on cognitive radio underground networks," *2013 1st International Black Sea Conference on Communications and Networking, BlackSeaCom 2013*, pp. 222–227, 2013.

[8] G. Shan, Y. Sun, Q. Cheng, Z. Wang, H. Zhou, L. Wang, X. Xue, B. Chen, S. B. Jones, P. S. Lammers, A. Berg, and L. Damerow, "Monitoring tomato root zone water content variation and partitioning evapotranspiration with a novel horizontally-oriented mobile dielectric sensor," *Agricultural and Forest Meteorology*, vol. 228-229, pp. 85–95, 2016.

[9] Z. Sun, I. F. Akyildiz, and G. P. Hancke, "Dynamic Connectivity in Wireless Underground Sensor Networks," *IEEE Transactions on Wireless Communications*, vol. 10, no. 12, pp. 4334–4344, 2011.

[10] X. Yu, W. Han, and Z. Zhang, "Path Loss Estimation for Wireless Underground Sensor Network in Agricultural Application," *Agricultural Research*, vol. 6, no. 1, pp. 97–102, 2017.

[11] Y. Zhang, J. Wang, D. Han, H. Wu, and R. Zhou, "Fuzzy-Logic Based Distributed Energy-Efficient Clustering Algorithm for Wireless Sensor Networks," *Sensors*, vol. 17, no. 7, p. 1554, 2017.

[12] E. Stuntebeck, D. Pompili, and T. Melodia, "Underground Wireless Sensor Networks Using Commodity Terrestrial Motes," *Poster Presentation at IEEE SECON 2006*, pp. 1088–1090, 2006.

[13] M. C. Vuran and A. R. Silva, "Communication Through Soil in Wireless Underground Sensor Networks - Theory and Practice," in *Signals and Communication Technology*, pp. 309–347, Berlin: Springer, Berlin, Heidelberg, 2010.

[14] L. Li, M. C. Vuran, and I. F. Akyildiz, "Characteristics of Underground Channel for Wireless Underground Sensor Networks," in *The 6th Annual Mediterranean Ad Hoc Networking WorkShop*, pp. 92–99, 2007.

[15] H. Friis, "A Note on a Simple Transmission Formula," *Proceedings of the IRE*, vol. 34, pp. 254–256, may 1946.

[16] H. R. Bogena, J. A. Huisman, H. Meier, U. Rosenbaum, and A. Weuthen, "Hybrid Wireless Underground Sensor Networks: Quantification of Signal Attenuation in Soil," *Vadose Zone Journal*, vol. 8, no. 3, pp. 755–761, 2009.

[17] N. R. Peplinski, F. T. Ulaby, and M. C. Dobson, "Dielectric Properties of Soils in the 0.3 - 1.3GHz Range," *IEEE Transactions on Geoscience and Remote Sensing*, vol. 33, no. 3, pp. 803–807, 1995.

[18] N. R. Peplinski, F. T. Ulaby, and M. C. Dobson, "Corrections to Dielectric Properties of Soils in the 0.3 - 1.3GHz Range," *IEEE Transactions on Geoscience and Remote Sensing*, vol. 33, no. 6, 1995.

[19] G. C. Topp, J. L. Davis, and A. P. Annan, "Electromagnetic determination of soil water content: Measurements in coaxial transmission lines," *Water Resources Research*, vol. 16, no. 3, pp. 574–582, 1980.

[20] V. L. Mironov, L. G. Kosolapova, and S. V. Fomin, "Physically and mineralogically based spectroscopic dielectric model for moist soils," *IEEE Transactions on Geoscience and Remote Sensing*, vol. 47, no. 7, pp. 2059–2070, 2009.

[21] T. Gui, C. Ma, F. Wang, and D. E. Wilkins, "Survey On Swarm Intelligence based Routing Protocols for Wireless Sensor Networks: An Extensive Study," in *2016 IEEE International Conference on Industrial Technology (ICIT)*, pp. 1944–1949, IEEE, 2016.

[22] J. J. Jassbi, P. J. A. Serra, R. A. Ribeiro, and A. Donati, "A Comparison of Mandani and Sugeno Inference Systems for a Space Fault Detection Application," in *2006 World Automation Congress*, pp. 1–8, IEEE, 2006.

[23] A. Hamam and N. D. Georganas, "A comparison of mamdani and sugeno fuzzy inference systems for evaluating the quality of experience of hapto-audio-visual applications," in *2008 IEEE International Workshop on Haptic Audio Visual Environments and Games (HAVE 2008)*, pp. 87–92, 2008.

[24] J. Singla, "Comparative Study of Mamdani-Type and Sugeno- Type Fuzzy Inference Systems for Diagnosis of Diabetes," in *2015 International Conference on Advances in Computer Engineering and Applications (ICACEA)*, (Ghaziabad, India), pp. 1–7, 2015.

[25] M. Dhimish, V. Holmes, B. Mehrdadi, and M. Dales, "Comparing Mamdani Sugeno fuzzy logic and RBF ANN network for PV fault detection," *Renewable Energy*, 2017.

[26] S. Maurya and V. K. Jain, "Fuzzy based energy efficient sensor network protocol for precision agriculture," *Computers and Electronics in Agriculture*, vol. 130, no. November, pp. 20–37, 2016.

[27] E. Mamdani, "Application of fuzzy algorithms for control of simple dynamic plant," *Proceedings of the Institution of Electrical Engineers*, vol. 121, no. 12, p. 1585, 1974.

[28] E. Mamdani and S. Assilian, "An Experiment in Linguistic Synthesis with a Fuzzy Logic Controller," *International Journal of Human-Computer Studies*, vol. 51, no. 2, pp. 135–147, 1999.

[29] J. L. Hill, *System Architecture for Wireless Sensor Networks*. Ph.d., University of California, Berkeley, 2003.

[30] A. B. Noel, A. Abdaoui, T. Elfouly, M. H. Ahmed, A. Badawy, and M. S. Shehata, "Structural Health Monitoring Using Wireless Sensor Networks: A Comprehensive Survey," *IEEE Communications Surveys and Tutorials*, vol. 19, no. 3, pp. 1403–1423, 2017.

[31] A. A. Adamou Ado, G. Abdelhak, N. Labraoui, and B. Omer, "Concepts and Evolution of Research in the Field of Wireless Sensor Networks," *International Journal of Computer Networks and Communications*, vol. 7, no. 1, pp. 81–98, 2015.

[32] M. Elhoseny and A. E. Hassanien, "Hierarchical and Clustering WSN Models: Their Requirements for Complex Applications," in *Dynamic Wireless Sensor Networks. Studies in Systems, Decision and Control*, vol. 165, pp. 53–71, Cham: Springer, 2019.

[33] I. F. Akyildiz, W. Su, Y. Sankarasubramaniam, and E. Cayirci, "Wireless sensor networks: A survey," *Computer Networks*, vol. 38, no. 4, pp. 393–422, 2002.

[34] A. Sinha and A. Chandrakasan, "Dynamic power management in wireless sensor networks," *IEEE Design and Test of Computers*, vol. 18, no. 2, pp. 62–74, 2001.

[35] R. Kacimi, *Techniques de conservation d'énergie pour les réseaux de capteurs sans fil*. Phd thesis, Université de Toulouse, 2009.

[36] G. Anastasi, a. Falchi, a. Passarella, M. Conti, and E. Gregori, "Performance measurements of motes sensor networks," *Proceedings of the 7th ACM international symposium on Modeling, analysis and simulation of wireless and mobile systems - MSWiM '04*, p. 174, 2004.

[37] N. Xu, S. Rangwala, K. K. Chintalapudi, D. Ganesan, A. Broad, R. Govindan, and D. Estrin, "A wireless sensor network for structural monitoring," *SenSys'04 - Proceedings of the Second International Conference on Embedded Networked Sensor Systems*, pp. 13–24, 2004.

[38] G. Werner-Allen, K. Lorincz, M. Welsh, O. Marcillo, J. Johnson, M. Ruiz, and J. Lees, "Deploying a wireless sensor network on an active volcano," *IEEE Internet Computing*, vol. 10, no. 2, pp. 18–25, 2006.

[39] V. C. Gungor and G. P. Hancke, "Industrial wireless sensor networks: Challenges, design principles, and technical approaches," *IEEE Transactions on Industrial Electronics*, vol. 56, no. 10, pp. 4258–4265, 2009.

[40] D. Ovalle, D. Restrepo, and Alcides, "Artificial Intelligence for Wireless Sensor Networks Enhancement," in *Smart Wireless Sensor Networks*, ch. 4, pp. 73–81, InTech, 2010.

[41] F. K. Shaikh and S. Zeadally, "Energy harvesting in wireless sensor networks: A comprehensive review," *Renewable and Sustainable Energy Reviews*, vol. 55, pp. 1041–1054, 2016.

[42] H. Yetgin, K. T. K. Cheung, M. El-Hajjar, and L. Hanzo, "A Survey of Network Lifetime Maximization Techniques in Wireless Sensor Networks," *IEEE Communications Surveys and Tutorials*, vol. 19, no. 2, pp. 828–854, 2017.

[43] B. O. Yenke, D. Wohwe Sambo, A. A. Adamo Ado, and A. Gueroui, "MMEDD : Multi-threading Model for an Efficient Data Delivery in wireless sensor networks," *International Journal of Communication Networks and Information Security (IJCNIS)*, vol. 8, no. 3, pp. 179–186, 2016.

[44] W. Heinzelman, A. Chandrakasan, and H. Balakrishnan, "Energy-efficient communication protocol for wireless microsensor networks," *Proceedings of the 33rd Annual Hawaii International Conference on System Sciences*, vol. vol.1, p. 10, 2000.

[45] A. Adamou Abba Ari, B. Omer Yenke, N. Labraoui, I. Damakoa, and A. Gueroui, "A power efficient cluster-based routing algorithm for wireless sensor networks: Honeybees swarm intelligence based approach," *Journal of Network and Computer Applications*, vol. 69, pp. 77–97, 2016.

[46] Z. Molay, R. Akbari, M. Shokouhifar, and F. Safaei, "Swarm intelligence based fuzzy routing protocol for clustered wireless sensor networks," *Expert Systems With Applications*, vol. 55, pp. 313–328, 2016.

[47] D. Shang, X. Liu, Y. Yan, C. Li, and B. Zhang, "A ring-based bidirectional routing protocol for wireless sensor network with mobile sinks," *2016 IEEE International Conference on Communications, ICC 2016*, pp. 5–10, 2016.

[48] J. Wang, Y. Cao, B. Li, H.-j. Kim, S. Lee, J. Wang, Y. Cao, B. Li, H.-j. Kim, and S. Lee, "Particle Swarm Optimization based Clustering Algorithm with Mobile Sink for WSNs," *Future Generation Computer Systems*, 2016.

[49] A. Förster, "Machine Learning Techniques Applied to Wireless Ad-Hoc Networks: Guide and Survey," *2007 3rd International Conference on Intelligent Sensors, Sensor Networks and Information*, pp. 365–370, 2007.

[50] T. O'Donovan, J. O'Donoghue, C. Sreenan, D. Sammon, P. O'Reilly, and K. A. O'Connor, "A context aware wireless Body Area Network (BAN)," in *2009 3rd International Conference on Pervasive Computing Technologies for Healthcare - Pervasive Health 2009, PCTHealth 2009*, pp. 1–8, 2009.

[51] M. Bilal and S. G. Kang, "An Authentication Protocol for Future Sensor Networks," *Sensors*, vol. 17, no. 5, pp. 1–29, 2017.

[52] J. K. Hart and K. Martinez, "Environmental Sensor Networks : A revolution in the earth system science ?," *Earth-Science Reviews*, vol. 78, no. 3-4, pp. 177–191, 2006.

[53] N. Rajendran, P. Kamal, D. Nayak, and S. A. Rabara, "Wats-sn: a wireless asset tracking system using sensor networks," in *2005 IEEE International Conference on Personal Wireless Communications, 2005. ICPWC 2005.*, pp. 237–243, 2005.

[54] K. Saleem, N. Fisal, and J. Al-muhtadi, "Empirical Studies of Bio-Inspired Self-Organized Secure Autonomous Routing Protocol," *IEEE Sensors Journal*, vol. 14, no. 7, pp. 2232–2239, 2014.

[55] X. Dong, M. C. Vuran, and S. Irmak, "Autonomous precision agriculture through integration of wireless underground sensor networks with center pivot irrigation systems," *Ad Hoc Networks*, vol. 11, no. 7, pp. 1975–1987, 2013.

[56] Y. Hamouda and M. Msallam, "Variable sampling interval for energy-efficient heterogeneous precision agriculture using Wireless Sensor Networks," *Journal of King Saud University - Computer and Information Sciences*, vol. 32, no. 1, pp. 88–98, 2020.

[57] G. Gao, K. Xiao, and M. Chen, "An intelligent IoT-based control and traceability system to forecast and maintain water quality in freshwater fish farms," *Computers and Electronics in Agriculture*, vol. 166, no. March, p. 105013, 2019.

[58] J. Al-Karaki and A. Kamal, "Routing Techniques in Wireless Sensor Networks : A Survey," *IEEE Wireless Communications*, vol. 11, no. 6, pp. 6–28, 2004.

[59] K. Akkaya and M. Younis, "A survey on routing protocols for wireless sensor networks," *Ad hoc networks*, vol. 3, no. 3, pp. 325–349, 2005.

[60] A. Boukerche, M. Z. Ahmad, B. Turgut, and D. Turgut, "A Taxonomy of Routing Protocols in Sensor Networks," in *Algorithms and Protocols for Wireless Sensor Networks*, pp. 129–160, Hoboken, NJ, USA: John Wiley & Sons, Inc., 2008.

[61] "Wireless technologies in embedded systems," [Online]. Available: https://promwad.com/technologies/wireless-technologies. [Accessed:04-Jul-2020].

[62] K. Gill, S. H. Yang, F. Yao, and X. Lu, "A ZigBee-based home automation system," *IEEE Transactions on Consumer Electronics*, vol. 55, no. 2, pp. 422–430, 2009.

[63] H. R. Chi, K. F. Tsang, C. K. Wu, and F. H. Hung, "ZigBee based wireless sensor network in smart metering," in *IECON 2016 - 42nd Annual Conference of the IEEE Industrial Electronics Society*, pp. 5663–5666, 2016.

[64] "Home - Zigbee Alliance."

[65] G. Mulligan, "The 6LoWPAN architecture," *Proceedings of the 4th workshop on Embedded networked sensors - EmNets '07*, p. 78, 2007.

[66] D. Culler, "6lowPAN Tutorial: IP on IEEE 802.15. 4 Low Power Wireless Networks," *Arch Rock Corporation*, 2007.

[67] V. H. La, R. Fuentes, and A. R. Cavalli, "A novel monitoring solution for 6LoWPAN-based Wireless Sensor Networks," *Proceedings - Asia-Pacific Conference on Communications, APCC 2016*, pp. 230–237, 2016.

[68] X. Vilajosana, T. Watteyne, T. Chang, M. Vucinic, S. Duquennoy, and P. Thubert, "IETF 6TiSCH: A Tutorial," *IEEE Communications Surveys and Tutorials*, vol. 22, no. 1, pp. 595–615, 2020.

[69] A. Mavromatis, G. Z. Papadopoulos, X. Fafoutis, A. Goulianos, G. Oikonomou, P. Chatzimisios, and T. Tryfonas, "Link quality and path based clustering in IEEE 802.15.4-2015 TSCH networks," *Proceedings - IEEE Symposium on Computers and Communications*, pp. 798–803, 2017.

[70] P. Thubert, M. R. Palattella, and T. Engel, "6TiSCH centralized scheduling: When SDN meet IoT," *2015 IEEE Conference on Standards for Communications and Networking, CSCN 2015*, pp. 42–47, 2016.

[71] "HART | FieldComm Group," [Online]. Available: https://www.fieldcommgroup.org/technologies/hart. [Accessed:04-Jul-2020].

[72] T. Lennvall, S. Svensson, and F. Hekland, "A comparison of WirelessHART and ZigBee for industrial applications," *IEEE International Workshop on Factory Communication Systems - Proceedings, WFCS*, pp. 85–88, 2008.

[73] U. Raza, P. Kulkarni, and M. Sooriyabandara, "Low Power Wide Area Networks: An Overview," *IEEE Communications Surveys and Tutorials*, vol. 19, no. 2, pp. 855–873, 2017.

[74] J. de Carvalho Silva, J. J. P. C. Rodrigues, A. M. Alberti, P. Solic, and A. L. L. Aquino, "LoRaWAN - A low power WAN protocol for Internet of Things: A review and opportunities," *2017 2nd International Multidisciplinary Conference on Computer and Energy Science (SpliTech)*, pp. 1–6, 2017.

[75] J. M. Marais, R. Malekian, and A. M. Abu-Mahfouz, "LoRa and LoRaWAN Testbeds : a Review," *2017 Ieee Africon*, pp. 1544–1549, 2017.

[76] A. Arya, A. Malik, and R. Garg, "Reinforcement Learning based Routing Protocols in WSNs: A Survey," *International Journal of Computer Science & Engineering Technology (IJCSET) Anju Arya et al. International Journal of Computer Science & Engineering Technology*, vol. 4, no. 11, pp. 1401–1404, 2013.

[77] K. Jeevan and T. Sachin, "A survey on routing protocols for wireless sensor networks using swarm intelligence," *International Journal of Internet Technology and Secured Transactions*, vol. 6, no. 2, 2016.

[78] I. Chalermek, G. Ramesh, and E. Deborah, "Directed diffusion: a scalable and robust communication paradigm for sensor networks," *Algorithmica*, vol. 43, no. 1-2, pp. 5–15, 2005.

[79] Z. Jin, Y. Jian-Ping, Z. Si-Wang, L. Ya-Ping, and L. Guang, "A Survey on Position-Based Routing Algorithms in Wireless Sensor Networks," *Algorithms*, vol. 2, no. 1, pp. 158–182, 2009.

[80] A. G. G. Kumar, R. Thiyagarajan, and N. Sripriya, "Data Centric Based Routing Protocols for Wireless Sensor Networks : A Survey," *International Journal of Scientific and Research Publications*, vol. 4, no. 12, pp. 1–5, 2014.

[81] J. Lloret, M. Garcia, J. Tomás, and F. Boronat, "GBP-WAHSN: A group-based protocol for large wireless ad hoc and sensor networks," *Journal of Computer Science and Technology*, vol. 23, no. 3, pp. 461–480, 2008.

[82] D. Liu, P. Ning, and W. Du, "Group-Based Key Pre-Distribution in Wireless Sensor Networks," in *ACM Transactions on Sensor Networks (TOSN)*, pp. 1–20, 2008.

[83] G. Wu, H. Li, and L. Yao, "A group-based mobile agent routing protocol for multitype wireless sensor networks," *Proceedings - 2010 IEEE/ACM International Conference on Green Computing and Communications, GreenCom 2010, 2010 IEEE/ACM International Conference on Cyber, Physical and Social Computing, CPSCom 2010*, pp. 42–49, 2010.

[84] X. Liu, "A survey on clustering routing protocols in wireless sensor networks," *Sensors (Switzerland)*, vol. 12, no. 8, pp. 11113–11153, 2012.

[85] A. Mehmood, J. Lloret, M. Noman, and H. Song, "Improvement of the wireless sensor network lifetime using LEACH with vice-cluster head," *Ad-Hoc and Sensor Wireless Networks*, vol. 28, no. 1-2, pp. 1–17, 2015.

[86] A. Boukerche, M. Z. Ahmad, D. Turgut, and B. Turgut, "A Taxonomy of Routing Protocols in Sensor Networks," in *Algorithms and Protocols for Wireless Sensor Networks*, pp. 129–160, Hoboken, NJ, USA: John Wiley & Sons, Inc., mar 2008.

[87] J. Lloret, M. Garcia, D. Bri, and J. R. Diaz, "A cluster-based architecture to structure the topology of parallel wireless sensor networks," *Sensors*, vol. 9, no. 12, pp. 10513–10544, 2009.

[88] N. Sabor, S. Sasaki, M. Abo-Zahhad, and S. M. Ahmed, "A Comprehensive Survey on Hierarchical-Based Routing Protocols for Mobile Wireless Sensor Networks : Review , Taxonomy , and Future Directions," *Wireless Communications and Mobile Computing*, vol. 2017, pp. 1–23, 2017.

[89] P. Vyas and M. Chouhan, "Survey on Clustering Techniques in Wireless Sensor Network," *International Journal of Computer Science and Information Technologies*, vol. 5, no. 5, pp. 6614–6619, 2014.

[90] S. P. Singh and S. C. Sharma, "A Survey on Cluster Based Routing Protocols in Wireless Sensor Networks," in *International Conference on Advanced Computing Technologies ans Applications (ICACTA-2015)*, vol. 45, pp. 687–695, 2015.

[91] R. V. Kulkarni, A. Förster, and G. K. Venayagamoorthy, "Computational intelligence in wireless sensor networks: A survey," *IEEE Communications Surveys and Tutorials*, vol. 13, no. 1, pp. 68–96, 2011.

[92] M. Bhanderi and H. Shah, "Machine Learning for Wireless Sensor Network: A Review, Challenges and Applications," *Advance in Electronic and Electric Engineering*, vol. 4, no. 5, pp. 475–486, 2014.

[93] S. Sirsikar and K. Wankhede, "Comparison of clustering algorithms to design new clustering approach," *Procedia Computer Science*, vol. 49, no. 1, pp. 147–154, 2015.

[94] D. Praveen Kumar, T. Amgoth, and C. S. R. Annavarapu, "Machine learning algorithms for wireless sensor networks: A survey," *Information Fusion*, vol. 49, pp. 1–25, 2019.

[95] M. Abdullah and A. Ehsan, "Routing Protocols for Wireless Sensor Networks: Classifications and Challenges," *Journal of Electronics and Communication Engineering Research*, vol. 2, no. 2, pp. 5–15, 2015.

[96] S. Wazed, A. Bari, A. Jaekel, and S. Bandyopadhyay, "Genetic algorithm based approach for extending the lifetime of two-tiered sensor networks," *2007 2nd International Symposium on Wireless Pervasive Computing*, pp. 83–87, 2007.

[97] S. Hussain, A. W. Matin, and O. Islam, "Genetic algorithm for hierarchical wireless sensor networks," *Journal of Networks*, vol. 2, no. 5, pp. 87–97, 2007.

[98] B. Solaiman and A. Sheta, "Computational Intelligence for Wireless Sensor Networks : Applications and Clustering Algorithms," *International Journal of Computer Applications*, vol. 73, no. 15, pp. 1–8, 2013.

[99] A. Hosseingholizadeh and A. Abhari, "A Neural Network approach for Wireless sensor network power management," in *28th IEEE International Symposium on*, 2009.

[100] M. Cordina and C. J. Debono, "Increasing wireless sensor network lifetime through the application of SOM neural networks," *2008 3rd International Symposium on Communications, Control, and Signal Processing, ISCCSP 2008*, no. March, pp. 467–471, 2008.

[101] N. Kumar, M. Kumar, and R. B. Patel, "Neural network based energy efficient clustering and routing in wireless sensor networks," *1st International Conference on Networks and Communications, NetCoM 2009*, pp. 34–39, 2009.

[102] W. Liu, Z. Wang, X. Liu, N. Zeng, Y. Liu, and F. E. Alsaadi, "A survey of deep neural network architectures and their applications," *Neurocomputing*, vol. 234, no. 4, pp. 11–26, 2017.

[103] M. Saleem, G. A. Di Caro, and M. Farooq, "Swarm intelligence based routing protocol for wireless sensor networks: Survey and future directions," *Information Sciences*, vol. 181, no. 20, pp. 4597–4624, 2011.

[104] T. Gui, C. Ma, F. Wang, and D. E. Wilkins, "Survey On Swarm Intelligence based Routing Protocols for Wireless Sensor Networks: An Extensive Study," in *2016 IEEE International Conference on Industrial Technology (ICIT)*, pp. 1944–1949, IEEE, 2016.

[105] R. Poli, J. Kennedy, and T. Blackwell, "Particle swarm optimization," *Swarm Intelligence*, vol. 1, no. 1, pp. 33–57, 2007.

[106] R. S. Y. Elhabyan and M. C. E. Yagoub, "Two-tier particle swarm optimization protocol for clustering and routing in wireless sensor network," *Journal of Network and Computer Applications*, vol. 52, pp. 116–128, 2015.

[107] P. C. S. Rao, P. K. Jana, and H. Banka, "A particle swarm optimization based energy efficient cluster head selection algorithm for wireless sensor networks," *Wireless Networks*, vol. 23, no. 7, pp. 2005–2020, 2017.

[108] M. Dorigo and C. Blum, "Ant colony optimization theory: A survey," *Theoretical Computer Science*, vol. 344, no. 2-3, pp. 243–278, 2005.

[109] H. Munot and P. H. Kulkarni, "Survey on Computational Intelligence Based Routing Protocols in WSN," *International Research Journal of Engineering and Technology (IRJET)*, vol. 3, no. 9, pp. 122–127, 2016.

[110] L. Wang, R. Zhang, and a. N. Model, "An Energy-Balanced Ant-Based Routing Protocol for Wireless Sensor Networks," in *2009 5th International Conference on Wireless Communications, Networking and Mobile Computing*, pp. 1–4, IEEE, sep 2009.

[111] J. Yang, M. Xu, W. Zhao, and B. Xu, "A multipath routing protocol based on clustering and ant colony optimization for wireless sensor networks," *Sensors*, vol. 10, no. 5, pp. 4521–4540, 2010.

[112] X. Cai, Y. Duan, Y. He, J. Yang, and C. Li, "Bee-sensor-C: An energy-efficient and scalable multipath routing protocol for wireless sensor networks," *International Journal of Distributed Sensor Networks*, vol. 2015, pp. 1–14, 2015.

[113] M. Saleem and M. Farooq, "BeeSensor : A Bee-Inspired Power Aware Routing Protocol for Wireless Sensor Networks," *Lecture Notes in Computer Science*, pp. 81–90, 2007.

[114] D. Karaboga, S. Okdem, and C. Ozturk, "Cluster based wireless sensor network routing using artificial bee colony algorithm," *Wireless Networks*, vol. 18, no. 7, pp. 847–860, 2012.

[115] P. S. Mann and S. Singh, "Energy-Efficient Hierarchical Routing for Wireless Sensor Networks: A Swarm Intelligence Approach," *Wireless Personal Communications*, pp. 1–21, 2016.

[116] M. K. Singh, S. I. Amin, S. A. Imam, V. K. Sachan, and A. Choudhary, "A Survey of Wireless Sensor Network and its types," *Proceedings - IEEE 2018 International Conference on Advances in Computing, Communication Control and Networking, ICACCCN 2018*, pp. 326–330, 2018.

[117] I. F. Akyildiz, T. Melodia, and K. R. Chowdhury, "A survey on wireless multimedia sensor networks," *Computer Networks*, vol. 51, no. 4, pp. 921–960, 2007.

[118] I. F. Akyildiz, T. Melodia, and K. R. Chowdhury, "Wireless multimedia sensor networks: applications and testbeds," *Proceedings of the IEEE*, vol. 96, no. 10, pp. 1588–1605, 2008.

[119] V. Bhandary, A. Malik, and S. Kumar, "Routing in wireless multimedia sensor networks: A survey of existing protocols and open research issues," *Journal of Engineering (United Kingdom)*, vol. 2016, 2016.

[120] A. Ali, Y. Ming, S. Chakraborty, and S. Iram, "A comprehensive survey on real-time applications of WSN," *Future Internet*, vol. 9, no. 4, pp. 1–22, 2017.

[121] B. Gupta, G. Martinez Pérez, D. P. Agrawal, and D. Gupta, *Handbook of computer networks and cyber security principles and paradigms*. Springer, 2020.

[122] J. Heidemann, M. Stojanovic, and M. Zorzi, "Underwater sensor networks: Applications, advances and challenges," *Philosophical Transactions of the Royal Society A: Mathematical, Physical and Engineering Sciences*, vol. 370, no. 1958, pp. 158–175, 2012.

[123] J. G. Proakis, E. M. Sozer, J. A. Rice, and M. Stojanovic, "Shallow water acoustic networks," *IEEE Communications Magazine*, vol. 39, no. 11, pp. 114–119, 2001.

[124] B. Silva, R. M. Fisher, A. Kumar, and G. P. Hancke, "Experimental Link Quality Characterization of Wireless Sensor Networks for Underground Monitoring," *IEEE Transactions on Industrial Informatics*, vol. 11, no. 5, pp. 1099–1110, 2015.

[125] M. C. Vuran and I. F. Akyildiz, "Channel model and analysis for wireless underground sensor networks in soil medium," *Physical Communication*, vol. 3, no. 4, pp. 245–254, 2010.

[126] A. Salam, M. C. Vuran, and S. Irmak, "Towards Internet of Underground Things in smart lighting: A statistical model of wireless underground channel," *Proceedings of the 2017 IEEE 14th International Conference on Networking, Sensing and Control, ICNSC 2017*, pp. 574–579, 2017.

[127] S. Kisseleff, B. Sackenreuter, I. F. Akyildiz, and W. Gerstacker, "On capacity of active relaying in magnetic induction based wireless underground sensor networks," in *2015 IEEE International Conference on Communications (ICC)*, pp. 6541–6546, 2015.

[128] I. F. Akyildiz and E. P. Stuntebeck, "Wireless underground sensor networks: Research challenges," *Ad Hoc Networks*, vol. 4, no. 6, pp. 669–686, 2006.

[129] X. Yu, P. Wu, W. Han, and Z. Zhang, "A survey on wireless sensor network infrastructure for agriculture," *Computer Standards and Interfaces*, vol. 35, no. 1, pp. 59–64, 2013.

[130] Aqeel-Ur-Rehman, A. Z. Abbasi, N. Islam, and Z. A. Shaikh, "A review of wireless sensors and networks' applications in agriculture," *Computer Standards and Interfaces*, vol. 36, no. 2, pp. 263–270, 2014.

[131] A. Salam and M. C. Vuran, "Wireless underground channel diversity reception with multiple antennas for internet of underground things," in *2017 IEEE International Conference on Communications (ICC)*, pp. 1–7, 2017.

[132] X. Jiang, J. Polastre, and D. Culler, "Perpetual environmentally powered sensor networks," *2005 4th International Symposium on Information Processing in Sensor Networks, IPSN 2005*, vol. 2005, pp. 463–468, 2005.

[133] T. Voigt, H. Ritter, and J. Schiller, "Utilizing solar power in wireless sensor networks," *Proceedings - Conference on Local Computer Networks, LCN*, vol. 2003-January, no. November 2003, pp. 416–422, 2003.

[134] J. Pan, B. Xue, and Y. Inoue, "A Self-Powered Sensor Module Using Vibration-Based," in *2005 6th International Conference on ASIC*, pp. 443–446, 2005.

[135] S. Roundy, P. K. Wright, and J. Rabaey, "A study of low level vibrations as a power source for wireless sensor nodes," *Computer Communications*, vol. 26, no. 11, pp. 1131–1144, 2003.

[136] J. Burrell, T. Brooke, and R. Beckwith, "Vineyard Computing: Sensor Networks in Agricultural Production," *IEEE Pervasive Computing*, vol. 3, no. 1, pp. 38–45, 2004.

[137] I. F. Akyildiz and M. C. Vuran, "Wireless Underground Sensor Networks," *Wireless Sensor Networks*, vol. 10, no. 12, pp. 4334–4344, 2011.

[138] S. Kisseleff, I. F. Akyildiz, and W. H. Gerstacker, "Survey on Advances in Magnetic Induction based Wireless Underground Sensor Networks," *IEEE Internet of Things Journal*, vol. 5, no. 6, pp. 4843–4856, 2018.

[139] K. Roth, R. Schulin, H. Flühler, and W. Attinger, "Calibration of time domain reflectometry for water content measurement using a composite dielectric approach," *Water Resources Research*, vol. 26, no. 10, pp. 2267–2273, 1990.

[140] P. Lorrain, D. R. Corson, and F. Lorrain, *Electromagnetic fields and waves : including electric circuits*. Freeman, 1988.

[141] N. Chaamwe, W. Liu, and H. Jiang, "Wave propagation communication models for Wireless Underground Sensor Networks," in *(ICCT), 2010 12th IEEE International Conference on Communication Technology*, pp. 9–12, 2010.

[142] A. M. Sadeghioon, D. N. Chapman, N. Metje, and C. J. Anthony, "A New Approach to Estimating the Path Loss in Underground Wireless Sensor Networks," *Journal of Sensor and Actuator Networks*, vol. 6, no. 3, p. 18, 2017.

[143] J. O. Curtis, C. A. Weiss Jr., and J. B. Everett, "Effect of Soil Composition on Complex Dielectric Properties," Tech. Rep. Dec, Army Engineer Waterways Experiment Station Vicksburg Ms Environmental Lab, 1995.

[144] Z. Sun, I. F. Akyildiz, and G. P. Hancke, "Dynamic connectivity in wireless underground sensor networks," *IEEE Transactions on Wireless Communications*, vol. 10, no. 12, pp. 4334–4344, 2011.

[145] A. Salam and M. C. Vuran, "EM-Based Wireless Underground Sensor Networks," in *Underground Sensing: Monitoring and Hazard Detection for Environment and Infrastructure*, ch. 5, pp. 247–285, Elsevier Inc., 1 ed., 2017.

[146] S. Kisseleff, W. Gerstacker, R. Schober, Z. Sun, and I. F. Akyildiz, "Channel capacity of magnetic induction based Wireless Underground Sensor Networks under practical constraints," *IEEE Wireless Communications and Networking Conference, WCNC*, pp. 2603–2608, 2013.

[147] D. Du, H. Zhang, J. Yang, and P. Yang, "Propagation Characteristics of the Underground-to-Aboveground Communication Link about 2 . 4GHz and 433MHz Radio Wave : An Empirical Study in the Pine Forest of Guizhou Province," in *2017 3rd IEEE International Conference on Computer and Communications (ICCC)*, pp. 1041–1045, IEEE, 2017.

[148] H. Zemmour, G. Baudoin, and A. Diet, "Soil Effects on the Underground-To-Aboveground Communication Link in Ultrawideband Wireless Underground Sensor Networks," *IEEE Antennas and Wireless Propagation Letters*, vol. 16, no. c, pp. 218–221, 2017.

[149] V. L. Mironov and S. V. Fomin, "Temperature and Mineralogy Dependable Model for Microwave Dielectric Spectra of Moist Soils," *PIERS Online*, vol. 5, no. 5, pp. 411–415, 2009.

[150] V. L. Mironov, M. C. Dobson, V. H. Kaupp, S. A. Komarov, and V. N. Kleshchenko, "Generalized Refractive Mixing Dielectric Model for Moist Soils," *IEEE Transactions on Geoscience and Remote Sensing*, vol. 42, no. 4, pp. 773–785, 2004.

[151] "UCAD - Le jardin botanique: Le poumon vert du campus," [Online]. Available: https://www.biologievegetale.sn/index.php/actualite/117-ucad-le-jardin-botanique-le-poumon-vert-du-campus. [Accessed: 04-Jul-2020].

[152] I. Zaman, N. Jain, and A. Förster, "Artificial Neural Network based Soil VWC and Field Capacity Estimation Using Low Cost Sensors," in *2018 IFIP/IEEE International Conference on Performance Evaluation and Modeling in Wired and Wireless Networks (PEMWN)*, vol. 9, (Toulouse), pp. 1–6, IEEE, 2018.

[153] D. Wohwe Sambo, A. Förster, B. O. Yenke, and I. Sarr, "A New Approach for Path Loss Prediction in Wireless Underground Sensor Networks," in *Proceedings - 2019 IEEE 44th Local Computer Networks Symposium on Emerging Topics in Networking, LCN Symposium 2019*, (Osnabrück), pp. 50–57, IEEE, 2019.

[154] I. Zaman, M. Gelhaar, J. Dede, H. Koehler, and A. Förster, "MoleNet : A New Sensor Node for Underground Monitoring," in *IEEE SenseApp*, 2016.

[155] D. Wohwe Sambo, A. Förster, B. O. Yenke, I. Sarr, B. Gueye, and P. Dayang, "Wireless Underground Sensor Networks Path Loss Model for Precision Agriculture (WUSN-PLM)," *IEEE Sensors Journal*, vol. 20, no. 10, pp. 5298–5313, 2020.

[156] "Fuzzy Inference Process - MATLAB; Simulink - MathWorks," [Online]. Available: https://fr.mathworks.com/help/fuzzy/fuzzy-inference-process.html. [Accessed: 04-Jul-2020].

[157] "Defuzzification Methods - MATLAB; Simulink - MathWorks," [Online]. Available: https://fr.mathworks.com/help/fuzzy/defuzzification-methods.html. [Accessed: 04-Jul-2020].

[158] F. Cavallaro, "A Takagi-Sugeno Fuzzy Inference System for Developing a Sustainability Index of Biomass," *Sustainability*, vol. 7, no. 9, pp. 12359–12371, 2015.

[159] "Foundations of Fuzzy Logic - MATLAB; Simulink - MathWorks," [Online]. Available: https://fr.mathworks.com/help/fuzzy/foundations-of-fuzzy-logic.html. [Accessed: 04-Jul-2020].

[160] T. Takagi and M. Sugeno, "Fuzzy identification of systems and its applications to modeling and control," *IEEE Transactions on Systems, Man, and Cybernetics*, vol. 15, no. 1, pp. 116–132, 1985.

Appendix A

Results and comparison of existing path loss models and the proposed WUSN-PLM

A.1 Dry soil

Table A.1: Excerpt of observations in dry soil configuration for UG2UG communication.

Distances and communication			Conventional Modified Friis		N.C. Modified Friis		Proposed WUSN-PLM	
			Sandy clay#1	Sandy clay#2	Sandy clay#1	Sandy clay#2	Sandy clay#1	Sandy clay#2
5m	Top	15 -> 15	TP	TP	TP	TP	TP	TP
		15 -> 20	TP	TP	TP	TP	TP	TP
		15 -> 30	TP	TP	TP	TP	TP	TP
		20 -> 15	TP	TP	TP	TP	TP	TP
		20 -> 20	TP	TP	TP	TP	TP	TP
		20 -> 30	TP	TP	TP	TP	TP	TP
		30 -> 15	TP	TP	TP	TP	TP	TP
		30 -> 20	TP	TP	TP	TP	TP	TP
	Sub	30 -> 30	TP	TP	TP	TP	TP	TP
		30 -> 40	TP	TP	TP	TP	TP	TP
		40 -> 30	TP	TP	TP	TP	TP	TP
		40 -> 40	TP	TP	TP	TP	TP	TP
		15 -> 15	TP	TP	TP	TP	TP	TP
		15 -> 20	TP	TP	TP	TP	TP	TP

10m	**Top**	15 -> 30	TP	TP	TP	TP	TP	TP
		20 -> 15	TP	TP	TP	TP	TP	TP
		20 -> 20	TP	TP	TP	TP	TP	TP
		20 -> 30	TP	TP	TP	TP	TP	TP
		30 -> 15	TP	TP	TP	TP	TP	TP
		30 -> 20	TP	TP	TP	TP	TP	TP
	Sub	30 -> 30	TP	TP	TP	TP	TP	TP
		30 -> 40	TP	TP	TP	TP	TP	TP
		40 -> 30	TP	TP	TP	TP	TP	TP
		40 -> 40	TP	TP	TP	TP	TP	TP
15m	**Top**	15 -> 15	TP	TP	TP	TP	TP	TP
		15 -> 20	TP	TP	TP	TP	TP	TP
		15 -> 30	TP	TP	TP	TP	TP	TP
		20 -> 15	TP	TP	TP	TP	TP	TP
		20 -> 20	TP	TP	TP	TP	TP	TP
		20 -> 30	TP	TP	TP	TP	TP	TP
		30 -> 15	TP	TP	TP	TP	TP	TP
		30 -> 20	TP	TP	TP	TP	TP	TP
	Sub	30 -> 30	TP	TP	TP	TP	TP	TP
		30 -> 40	TP	TP	TP	TP	TP	TP
		40 -> 30	TP	TP	TP	TP	TP	TP
		40 -> 40	TP	TP	TP	TP	TP	TP
20m	**Top**	15 -> 15	FP	FP	FP	FP	FP	FP
		15 -> 20	FP	FP	FP	FP	FP	FP
		15 -> 30	FP	FP	FP	FP	FP	FP
		20 -> 15	FP	FP	FP	FP	FP	FP
		20 -> 20	FP	FP	FP	FP	FP	FP
		20 -> 30	FP	FP	FP	FP	FP	FP
		30 -> 15	FP	FP	FP	FP	FP	FP
		30 -> 20	FP	FP	FP	FP	FP	FP
	Sub	30 -> 30	FP	FP	FP	FP	TN	TN
		30 -> 40	FP	FP	FP	FP	TN	TN
		40 -> 30	FP	FP	FP	FP	TN	TN
		40 -> 40	FP	FP	FP	FP	TN	TN

A.2 Moist soil

Table A.2: Excerpt of observations in dry soil configuration for UG2AG communication.

Distances and communication		Zhi Sun Model		Xin Dong Model		Proposed WUSN-PLM	
		Sandy clay#1	Sandy clay#2	Sandy clay#1	Sandy clay#2	Sandy clay#1	Sandy clay#2
5m	15 -> 0	TP	TP	TP	TP	TP	TP
	20 -> 0	TP	TP	TP	TP	TP	TP
	30 -> 0	TP	TP	TP	TP	TP	TP
	40 -> 0	TP	TP	TP	TP	TP	TP
10m	15 -> 0	TP	TP	TP	TP	TP	TP
	20 -> 0	TP	TP	TP	TP	TP	TP
	30 -> 0	TP	TP	TP	TP	TP	TP
	40 -> 0	TP	TP	TP	TP	TP	TP
15m	15 -> 0	TP	TP	TP	TP	TP	TP
	20 -> 0	TP	TP	TP	TP	TP	TP
	30 -> 0	TP	TP	TP	TP	TP	TP
	40 -> 0	TP	TP	TP	TP	TP	TP
20m	15 -> 0	TP	TP	TP	TP	TP	TP
	20 -> 0	TP	TP	TP	TP	TP	TP
	30 -> 0	TP	TP	TP	TP	TP	TP
	40 -> 0	TP	TP	TP	TP	TP	TP

Table A.3: Excerpt of observations in dry soil configuration for AG2UG communication.

Distances and communication		Zhi Sun Model		Xin Dong Model		Proposed WUSN-PLM	
		Sandy clay#1	Sandy clay#2	Sandy clay#1	Sandy clay#2	Sandy clay#1	Sandy clay#2
5m	0 -> 15	TP	TP	TP	TP	TP	TP
	0 -> 20	TP	TP	TP	TP	TP	TP
	0 -> 30	TP	TP	TP	TP	TP	TP
	0 -> 40	TP	TP	TP	TP	TP	TP
10m	0 -> 15	TP	TP	TP	TP	TP	TP
	0 -> 20	TP	TP	TP	TP	TP	TP
	0 -> 30	TP	TP	TP	TP	TP	TP
	0 -> 40	TP	TP	TP	TP	TP	TP
15m	0 -> 15	TP	TP	TP	TP	TP	TP
	0 -> 20	TP	TP	TP	TP	TP	TP
	0 -> 30	TP	TP	TP	TP	TP	TP
	0 -> 40	TP	TP	TP	TP	TP	TP
20m	0 -> 15	TP	TP	TP	TP	TP	TP
	0 -> 20	TP	TP	TP	TP	TP	TP
	0 -> 30	TP	TP	TP	TP	TP	TP
	0 -> 40	TP	TP	TP	TP	TP	TP

Table A.4: Excerpt of observations in moist soil configuration for UG2UG communication.

Distances and communication			Moist. (%)	Conventional Modified Friis		N.C. Modified Friis		Proposed WUSN-PLM	
				Sandy clay#1	Sandy clay#2	Sandy clay#1	Sandy clay#2	Sandy clay#1	Sandy clay#2
5m	**Top**	15 -> 15	40	FN	TP	TP	TP	FN	FN
		15 -> 20	11	TP	TP	TP	TP	TP	TP
		15 -> 30	41	FN	TP	TP	TP	FN	FN
		20 -> 15	46	FN	TP	FP	TP	FN	FN
		20 -> 20	48	TN	FP	FP	FP	TN	TN
		20 -> 30	47	FN	TP	TP	TP	FN	FN
		30 -> 15	72	FN	TP	FN	TP	FN	FN
		30 -> 20	25	TP	TP	TP	TP	FN	FN
	Sub	30 -> 30	18	FP	FP	FP	FP	TN	TN
10m	**Top**	15 -> 15	57	TN	TN	TN	TN	TN	TN
		15 -> 20	75	TN	TN	TN	TN	TN	TN
		15 -> 30	30	TN	FP	TN	FP	TN	TN
		20 -> 15	54	FN	FN	FN	FN	FN	FN
		20 -> 20	39	TN	FP	TN	FP	TN	TN
		20 -> 30	77	TN	TN	TN	TN	TN	TN
		30 -> 15	70	TN	TN	TN	TN	TN	TN
		30 -> 20	48	TN	TN	TN	TN	TN	TN
	Sub	30 -> 30	63	TN	TN	TN	TN	TN	TN
15m	**Top**	15 -> 15	56	TN	TN	TN	TN	TN	TN
		15 -> 20	75	TN	TN	TN	TN	TN	TN
		15 -> 30	21	TN	TN	TN	FP	TN	TN
		20 -> 15	58	TN	TN	TN	TN	TN	TN
		20 -> 20	32	TN	TN	TN	TN	TN	TN
		20 -> 30	76	TN	TN	TN	TN	TN	TN
		30 -> 15	14	TN	FP	TN	FP	TN	TN
		30 -> 20	80	TN	TN	TN	TN	TN	TN
	Sub	30 -> 30	74	TN	TN	TN	TN	TN	TN
20m	**Top**	15 -> 15	74	TN	TN	TN	TN	TN	TN
		15 -> 20	53	TN	TN	TN	TN	TN	TN
		15 -> 30	37	TN	TN	TN	TN	TN	TN
		20 -> 15	66	FN	FN	FN	FN	FN	FN
		20 -> 20	44	TN	TN	TN	TN	TN	TN
		20 -> 30	66	TN	TN	TN	TN	TN	TN
		30 -> 15	72	TN	TN	TN	TN	TN	TN
		30 -> 20	25	TN	TN	TN	TN	TN	TN
	Sub	30 -> 30	18	TN	TN	TN	TN	TN	TN

Table A.5: Excerpt of observations in moist soil configuration for UG2AG communication.

Distances and communication		Moisture (%)	Zhi Sun Model		Xin Dong Model		Proposed WUSN-PLM	
			Sandy clay#1	Sandy clay#2	Sandy clay#1	Sandy clay#2	Sandy clay#1	Sandy clay#2
5m	15 -> 0	29	TP	TP	TP	TP	TP	TP
	20 -> 0	48	TP	TP	TP	TP	TP	TP
	30 -> 0	90	TP	TP	TP	TP	TP	TP
10m	15 -> 0	72	TP	TP	TP	TP	FP	FP
	20 -> 0	22	FP	FP	FP	FP	TP	TP
	30 -> 0	68	TP	TP	TP	TP	FP	FP
15m	15 -> 0	20	FP	FP	FP	FP	FP	FP
	20 -> 0	66	TP	TP	TP	TP	TP	TP
	30 -> 0	58	FP	FP	FP	FP	FP	FP
20m	15 -> 0	17	TP	TP	TP	TP	TP	TP
	20 -> 0	81	TP	TP	TP	TP	TP	TP
	30 -> 0	39	TP	TP	TP	TP	TP	TP

Table A.6: Excerpt of observations in moist soil configuration for AG2UG communication.

Distances and communication		Moisture (%)	Zhi Sun Model		Xin Dong Model		Proposed WUSN-PLM	
			Sandy clay#1	Sandy clay#2	Sandy clay#1	Sandy clay#2	Sandy clay#1	Sandy clay#2
5m	0 -> 15	91	TP	TP	TP	TP	TP	TP
	0 -> 20	40	TP	TP	TP	TP	TP	TP
	0 -> 30	66	TP	TP	TP	TP	TP	TP
10m	0 -> 15	50	TP	TP	TP	TP	TP	TP
	0 -> 20	66	TP	TP	FP	FP	TP	TP
	0 -> 30	65	TP	TP	TP	TP	TP	TP
15m	0 -> 15	67	TP	TP	TP	TP	TP	TP
	0 -> 20	71	TP	TP	TP	TP	TP	TP
	0 -> 30	73	FP	FP	FP	FP	TN	TN
20m	0 -> 15	95	TP	TP	TP	TP	TP	TP
	0 -> 20	41	TP	TP	TP	TP	TP	TP
	0 -> 30	64	FP	FP	FP	FP	TN	TN

Appendix B

Results of the Fuzzy Logic approach for reliable wireless underground communications

B.1 Dry soil

B.2 Moist soil

Table B.1: Excerpt of observations for 5 m linear distance in dry soil configuration (MST=0%).

Inputs		**Outputs**	**Observations**
BD (cm)	NBD (cm)	Reliability	
0	15	0.9	Received
	20	0.9	Received
	30	0.9	Received
	40	0.9	Received
15	0	0.9	Received
	15	0.9	Received
	20	0.9	Received
	30	0.9	Received
20	0	0.9	Received
	15	0.9	Received
	20	0.9	Received
	30	0.9	Received
30	0	0.9	Received
	15	0.9	Received
	20	0.9	Received
	30	0.9	Received
40	0	0.9	Received
	15	0.9	Received
	20	0.9	Received
	30	0.9	Received
Total	20 TP 0 FP	0 TN 0 FN	20 Observations

Table B.2: Excerpt of observations for 10 m linear distance in dry soil configuration (MST=0%).

Inputs		**Outputs**	**Observations**
BD (cm)	NBD (cm)	Reliability	
0	15	0.833	Received
	20	0.7	Received
	30	0.7	Received
	40	0.7	Received
15	0	0.9	Received
	15	0.811	Received
	20	0.633	Received
	30	0.633	Received
20	0	0.9	Received
	15	0.767	Received
	20	0.5	Received
	30	0.5	Received
30	0	0.9	Received
	15	0.767	Received
	20	0.5	Received
	30	0.5	Received
40	0	0.9	Received
	15	0.5	Received
	20	0.5	Received
	30	0.5	Received
Total	20 TP 0 FP	0 TN 0 FN	20 Observations

Table B.3: Excerpt of observations for 15 m linear distance in dry soil configuration (MST=0%).

Inputs		**Outputs**	**Observations**
BD (cm)	NBD (cm)	Reliability	
0	15	0.833	Received
	20	0.7	Received
	30	0.7	Received
	40	0.7	Received
15	0	0.9	Received
	15	0.811	Received
	20	0.633	Received
	30	0.633	Received
20	0	0.9	Received
	15	0.767	Received
	20	0.5	Received
	30	0.5	Received
30	0	0.9	Received
	15	0.767	Received
	20	0.5	Received
	30	0.5	Received
40	0	0.9	Received
	15	0.5	Received
	20	0.5	Received
	30	0.5	Received
Total	20 TP 0 FP	0 TN 0 FN	20 Observations

Table B.4: Excerpt of observations for 20 m linear distance in dry soil configuration (MST=0%).

Inputs		**Outputs**	**Observations**
BD (cm)	NBD (cm)	Reliability	
0	15	0.5	Received
	20	0.5	Received
	30	0.5	Received
	40	0.5	Received
15	0	0.5	Received
	15	0.478	Not received
	20	0.433	Not received
	30	0.433	Not received
20	0	0.5	Received
	15	0.433	Not received
	20	0.3	Not received
	30	0.3	Not received
30	0	0.5	Received
	15	0.433	Not received
	20	0.3	Not received
	30	0.3	Not received
40	0	0.5	Received
	15	0.433	Not received
	20	0.3	Not received
	30	0.3	Not received
Total	8 TP 0 FP	12 TN 0 FN	20 Observations

Table B.5: Excerpt of observations for transmitter node fixed at the ground surface (BD=0) in moist soil (MST≠0%)

Inputs				**Output**	**Observations**
BD (cm)	MST (%)	LD (m)	NBD (cm)	Reliability	
0	91	5	15	0.7	Received
	40		20	0.7	Received
	66		30	0.7	Received
	50	10	15	0.633	Received
	66		20	0.5	Received
	65		30	0.5	Received
	67	15	15	0.633	Received
	71		20	0.5	Received
	73		30	0.5	Not received
	95	20	15	0.433	Received
	41		20	0.686	Received
	64		30	0.3	Not received
Total			9 TP 1 FP	1 TN 1 FN	12 Observations

Table B.6: Excerpt of observations for transmitter node fixed at 15cm depth in moist soil (MST≠0%)

Inputs				Output	Observations
BD (cm)	MST (%)	LD (m)	NBD (cm)	Reliability	
15	29	5	0	0.9	Received
	40		15	0.811	Received
	11		20	0.858	Received
	41		30	0.633	Received
	72	10	0	0.633	Received
	57		15	0.567	Not received
	75		20	0.433	Not received
	30		30	0.433	Not received
	20	15	0	0.567	Not received
	56		15	0.567	Not received
	75		20	0.433	Not received
	21		30	0.433	Not received
	17	20	0	0.633	Received
	74		15	0.411	Not received
	53		20	0.233	Not received
	37		30	0.433	Not received
	Total		6 TP	7 TN	16
			3 FP	0 FN	Observations

Table B.7: Excerpt of observations for transmitter node fixed at 20cm depth in moist soil (MST≠0%)

Inputs				Output	Observations
BD (cm)	MST (%)	LD (m)	NBD (cm)	Reliability	
20	48	5	0	0.786	Received
	46		15	0.722	Received
	48		20	0.5	Not received
	47		30	0.5	Received
	22	10	0	0.7	Not received
	54		15	0.567	Not received
	39		20	0.3	Not received
	77		30	0.3	Not received
	66	15	0	0.5	Received
	58		15	0.433	Not received
	32		20	0.3	Not received
	76		30	0.3	Not received
	81	20	0	0.5	Received
	66		15	0.367	Received
	44		20	0.264	Not received
	66		30	0.1	Not received
	Total		5 TP	7 TN	16
			3 FP	1 FN	Observations

Table B.8: Excerpt of observations for transmitter node fixed at 30cm depth in moist soil (MST≠0%)

Inputs				Output	Observations
BD (cm)	MST (%)	LD (m)	NBD (cm)	Reliability	
30	90	5	0	0.7	Received
	72		15	0.633	Received
	25		20	0.5	Received
	18		30	0.5	Not received
	68	10	0	0.5	Received
	70		15	0.433	Not received
	48		20	0.3	Not received
	63		30	0.3	Not received
	58	15	0	0.5	Not received
	14		15	0.617	Not received
	89		20	0.3	Not received
	74		30	0.3	Not received
	39	20	0	0.5	Received
	72		15	0.367	Not received
	25		20	0.3	Not received
	18		30	0.3	Not received
Total			5 TP	8 TN	16
			3 FP	0 FN	Observations